LBL-16141
UC-94cb c.2

Lawrence Berkeley Laboratory

UNIVERSITY OF CALIFORNIA

ENERGY & ENVIRONMENT DIVISION

RECEIVED
LAWRENCE
BERKELEY LABORATORY

JUL 21 1983

LIBRARY AND
DOCUMENTS SECTION

TEMPERATURE LIMITATION OF PRIMARY AND SECONDARY ALKALINE BATTERY ELECTRODES

M.C.H. McKubre

May 1983

TWO-WEEK LOAN COPY

This is a Library Circulating Copy which may be borrowed for two weeks. For a personal retention copy, call Tech. Info. Division, Ext. 6782.

ENERGY
AND ENVIRONMENT
DIVISION

Prepared for the U.S. Department of Energy under Contract DE-AC03-76SF00098

LBL-16141 c.2

DISCLAIMER

This document was prepared as an account of work sponsored by the United States Government. While this document is believed to contain correct information, neither the United States Government nor any agency thereof, nor the Regents of the University of California, nor any of their employees, makes any warranty, express or implied, or assumes any legal responsibility for the accuracy, completeness, or usefulness of any information, apparatus, product, or process disclosed, or represents that its use would not infringe privately owned rights. Reference herein to any specific commercial product, process, or service by its trade name, trademark, manufacturer, or otherwise, does not necessarily constitute or imply its endorsement, recommendation, or favoring by the United States Government or any agency thereof, or the Regents of the University of California. The views and opinions of authors expressed herein do not necessarily state or reflect those of the United States Government or any agency thereof or the Regents of the University of California.

LBL-16141

TEMPERATURE LIMITATION OF PRIMARY AND SECONDARY ALKALINE BATTERY ELECTRODES

M.C.H. McKubre
Materials Research Laboratory
SRI International
Menlo Park, California 94025

May 1983

Final Report
to
Energy and Environment Division
Lawrence Berkeley Laboratory
University of California
Berkeley, California 94720

Subcontract No. 4510610

This work was supported by the Assistant Secretary for Conservation and Renewable Energy, Office of Energy Systems Research, Division of Energy Storage, U.S. Department of Energy under Contract Number DE-AC03-76SF00098.

ABSTRACT

When used in electric vehicles, alkaline batteries may be subjected to ambient temperatures below 0°C, and temperatures in excess of 100°C may be reached within the cells by IR heating under conditions of rapid charge or discharge. The purpose of this project was to determine what failure mechanisms or operating limitations will be imposed on Ni/Fe and Ni/Zn battery operation due to thermodynamic or kinetic effects at Ni, Fe, and Zn electrodes in the temperature range 0° to 100°C.

This report contains the results of studies of the mechanisms of dissolution and passivation of Fe and Zn electrodes in concentrated KOH, as these processes effect the charge/discharge characteristics of alkaline batteries. The experimental techniques principally employed were: potentiodynamic sweep voltammetry and coulometry, rotating disk and rotating ring disk electrode studies under constant velocity and constant acceleration rotation conditions, and AC impedance studies.

The results obtained on Fe electrodes have enabled us to postulate a detailed mechanism for the formation and discharge of an oxide film on iron via a number of dissolved intermediate species. The mechanisms are different at high and low temperatures, but at all temperatures pathways via dissolved phase intermediates result in substantial dissolution of metal and oxide. At 75°C dissolution processes account for more than 7.5% of the total charge stored per cycle.

AC impedance measurements were used to characterize the nature of the oxide film, and to determine an effective exchange current density for the Fe/Fe(II) Redox process. It is apparent from the measured values of i_0 that the kinetic constraints for the charge/discharge process are reduced with increasing temperature. However, the principal kinetic limitations of charge and discharge originate within the oxide film, not with the interfacial charge-transfer reaction process.

Experiments were performed to study the influence of convection and zincate concentration on the discharge (dissolution and passivation) kinetics of zinc electrodes in concentrated KOH. AC impedance and rotating ring disk studies were performed to determine the mechanism of dissolution, and the nature of the dissolved product. The model proposed for the discharge of zinc electrodes in KOH, taking into account a number of unusual and seemingly contradictory observations briefly is as follows. Dissolution proceeds via two subsequent one electron transfer processes, via a Zn^+ adsorbed species. The initial discharge product is $Zn(OH)_2$ which is porous and loosely adherent. We postulate that, at potentials below the passivation potential, $Zn(OH)_2$ sloughs from the electrode as a colloid, and is in chemical equilibrium with the Zincate ion. This equilibrium is determined by the local concentration of OH^- ions. Dissolution is catalyzed by the final product (zincate) and the rate is controlled by the diffusion of the zincate ion <u>to</u> the electrode. Discharge is thus autocatalytic with respect to the zincate concentration, which is confirmed by the presence of inductive loops in the impedance locus plots. The autocatalytic nature of discharge provides a plausible mechanism for "shape change" of zinc electrodes.

CONTENTS

ABSTRACT iii

1 INTRODUCTION 1

1.1 Background 1

1.2 Summary of NaOH Results 3

Nickel 3

Iron 5

Zinc 8

1.3 Conclusions from NaOH Studies 11

1.4 Report Organization 14

2 EXPERIMENTAL METHODS 15

2.1 Introduction 15

2.2 Electrolyte Preparation, Electrode and Cell Construction 16

2.3 Instrumentation 19

2.4 Measurement Techniques 23

3 MEASUREMENTS ON IRON 33

3.1 Introduction 33

3.2 Potentiodynamic Studies of Iron 34

3.3 RRDE Collection Efficiency Calibration 47

3.4 RRDE Studies of Iron 49

3.5 AC Impedance Studies of Iron 61

3.6 Conclusions 65

4 MEASUREMENTS ON ZINC 77

4.1 Introduction 77

4.2 Potentiodynamic Studies of Zinc 78

4.3 Rotating Ring Disc Studies of Zinc 83

4.4 The Influence of Zincate Concentration 96

4.5 AC Impedance Results 107

5 SUMMARY AND CONCLUSIONS 125

5.1 Introduction 125

5.2 Observations of Iron Electrodes 125

5.3 Observations of Zinc Electrodes..... 127
5.4 A Model for the Dissolution and Passivation of Zinc..... 129
5.5 Conclusions..... 135
5.6 Suggestions for Further Work..... 138
5.7 Comment..... 139
REFERENCES 141

LIST OF ILLUSTRATIONS

Figure		
1	Cyclic Voltammogram for nickel as a function of Cathodic Hold Time	4
2	The Influence of Temperature on Ring and Disk Currents on Iron Electrode	6
3	Potential Versus Log m_{NaOH}/mol kg^{-1} Diagrams for Iron in Concentrated Sodium Hydroxide Solution as a Function of Temperature	9
4	Measured Passivation Onset Potentials and Calculated Reversible Potentials Versus Temperature, for Zinc in 28 wt% NaOH	10
5	RRDE Potential Step Experiment for Zinc in 18 wt% NaOH at 22.5°C	12
6	Region of Current Instability for Zn in 25 wt% NaOH Under Quiescent Conditions	13
7	Bipotentiostat and Motor and Slip Ring Assemblies	17
8	Schematic Diagram of RRDE Construction and Contact Assembly	18
9	AC Impedance Measurement System	20
10	Transfer Function and Phase Versus Log (Frequency) for FRA/Potentiostat Interface Unit	24
11	The Equivalent Circuit and Expected Impedance Response for a Simple Electrochemical Interface	26
12	The Influence of Cathodic Potential Limit on the Repetitive Sweep Voltammogram for an Iron Disk Rotated at 10 Hz in 30 wt% KOH at 75°C	35
13	The Influence of Anodic Potential Limit on the Repetitive Sweep Voltammogram for an Iron Disk Rotated at 10 Hz in 30 wt% KOH at 75°C	36
14	The Influence of Sweep Rates on the Potentiodynamic Charge/Discharge Curves for an Iron Disk Electrode Rotated at 10 Hz in 30 wt% KOH at 75°C	38

15 The Influence of Sweep Rate on the Potentiodynamic Charge/Discharge Curves for an Iron Disk Electrode at 10 Hz in 30 wt% KOH at 0°C..... 40

16 RRDE Measurements of Iron in 30 wt% KOH at 75°C..... 50

17 RRDE Measurements of Iron in 30 wt% KOH at 50°C..... 54

18 RRDE Measurements of Iron in 30 wt% KOH at 25°C..... 56

19 AC Impedance Response of An Iron Rotating Disk Electrode in 30 wt% KOH with a rotation Speed of 10 Hz.... 63

20 Thermodynamically Favored Reaction Pathways Showing the Calculated Equilibrium Potentials for Fe in 8 Molal NaOH.. 69

21 Simplified High- and Low-Temperature Reaction Sequences for Iron in 30 wt% KOH..... 74

22 Potentiodynamic Discharge of Zinc in 30 wt% KOH at 78°C, as a Function of Disk Rotation Speed..... 79

23 Programmed Rotation Speed RRDE Experiments for Zinc in 35.5 wt% KOH at 25°C..... 85

24 Collection Efficiency Versus Angular Rotation Speed for a Zinc/Vitreous Carbon RRDE in 35.5 wt% KOH at 25°C..... 90

25 The results of Potentiodynamic Sweep Experiments for a Zinc Electrode in Initially Zincate-Free 30 wt% KOH at 25°C, as a Function of Electrode Rotation Speed..... 97

26 The results of Potential-Step Experiments for a Zinc Electrode in Initially Zincate-Free 30 wt% KOH at 25°C, as a Function of Potential-Step Amplitude..... 100

27 The Influence of Dissolved-Zinc Concentration on the Potentiodynamic Dissolution Rate of Zinc in 30 wt% KOH at 25°C..... 103

28 The Passivation Potential of Zinc Versus Electrode Rotation Speed in 30 wt% KOH at 20°C, as a Function of Zincate Concentration..... 105

29 Impedance Locus Showing Inductive Loops for Zn in 35.5% KOH..... 108

30 Equivalent Circuit for the Impedance of a Zinc Electrode Undergoing Discharge at Moderate Anodic Overpotentials..... 110

31 The Influence of Rotation Speed on the Dissolution Kinetics for a Zinc Disk Held at + 75 mV Versus Zn/Zn^{++}, in 36 wt% KOH at 25°C..... 111

32 The Influence of Zincate ion Concentration on the Impedance Locus in 30 wt% KOH, at 25°C..... 113

33 The Real Component of Impedance Versus $\omega^{-1/2}$, as a Function of Zincate Concentration..... 116

34 The Influence of Temperature on the Impedance Locus in Zincate-Free 35.5 wt% KOH..... 120

35 σ/T Versus T Measured in Zincate-Free 35.5 25% KOH, at 0 and +50 mV Anodic Overpotential..... 123

36 Reactions and Diffusion Profiles for the Proposed Mechanism of the Electrocatalytic Dissolution of Zinc under Mass Transport Control..... 133

LIST OF TABLES

Tables

1a Peak Height in Milli-Volts as a Function of Temperature and Sweep Rate for the Potentiodynamic Charge/Disharge of an Iron Disk Rotated at 10 Hz in 30 wt%..... 43

1b Peak Position in Milli-Volts Versus Zn/Zn (II) as a Function of Temperature and Sweep Rate for the Potentiodynamic Charge/Discharge of an Iron Disk Rotated at 10 Hz at in 30 wt%..... 44

2 Regression of Data Obtained for Peak R2 to the Equation $V_{PR2} = {}^{o}V_{R2} + R_{Film}\ I_{PR2}$..... 45

3 Iron RRDE Calibration Results in 0.1 M $K_3Fe(CN)_6$ with T = 25°C and ω = 10.0 Hz..... 48

4 Peak Areas Measured from the Potentiodynamic Data presented in Figure 16..... 53

5 Percent Dissolution Taken from Data in Table 4..... 59

6 Peak Areas Measured From the Potentiodynamic Sweep Data at 0°, 25°, 50°, and 75°C..... 60

7 Percent of Disk Dissolution..... 61

8 Electrochemical Parameters Calculated from the Impedance Dispersion..... 65

9 Calculated Equilibrium Potentials for Iron and Iron Oxide.. 66

10 Slope and Intercepts of the Linear IV Discharge Region of a zinc RDE, as a Function of Temperature, Rotation Speed, and Electrolyte Concentration..... 88

11 The Regression of Data in Table 10 to Equation (25)..... 82

12 The regression of Data in Table 11 to Equation (36)..... 83

13 Programmed rotation speed results for zinc in 35 wt% KOH at 25°C..... 80

14 Collection efficiency as a function of Rotation Speed: Regressing of Ring and Disk Current Data in Table 13 Equation (37) 91

15 Summary of the Influence of Zincate In Concentration on the Measured Potentiodynamic Discharge Parameters in 30 wt% KOH 101

16 The Warburg Diffusion Coefficient Calculated from the Impedance Measured in 35.5 wt% KOH 122

1 INTRODUCTION

1.1 Background

There has been a renewed interest in iron/nickel oxide and zinc/nickel oxide rechargeable alkaline batteries, particularly for electric vehicle applications.[1] The interest is due primarily to the low cost, high mechanical strength and availability of iron and zinc.

When used in electric vehicles, however, these cells may be subjected to ambient temperatures below 0°C, and temperatures in excess of 100°C may be reached by IR heating under conditions of high current flow (e.g., under conditions of rapid charge or discharge). Nearly all previous results of electrode performance in alkaline systems have been reported for the relatively narrow temperature range of 0°C to 50°C. Data from those studies are not sufficient for prediction of possible modes of battery failure at extremes of temperature.

The electrochemical features that may influence battery electrode performance can be summarized as follows:

(1) Specific Energy--The potentials at which charge storage processes occur, the extent to which active material is utilized, and the specific volume resistivity of the electrolyte all are critically dependent on temperature.

(2) Specific Power--The kinetics of charge-discharge processes are influenced by temperature.

(3) Electrode Life, Charge Acceptance, and Charge Retention--Electrode life and the electrode's ability to store charge efficiently are determined primarily by the extent to which electrochemical processes occur that are completely reversible within the times involved in charging or discharging.

Several such processes, each of which is to some degree temperature dependent, are listed below:

- Dissolution of electrode material.
- Sloughing of formed oxide or hydroxide into regions inaccessible to electrochemical reduction.
- Slow (kinetically hindered) oxidation or reduction processes that require potentials outside the normal range of electrode operation to proceed at a meaningful rate.
- Secondary reactions that evolve gases (specifically hydrolysis producing O_2 and H_2).
- Transport of active material away from its original location (shape change).

In the previous year (DOE contract EM-78-C-015159)[2,3] and current year (DOE/LBL subcontract 450561) of funding, SRI has focused attention on both possible kinetic[2] and thermodynamic[3] limitations of Ni, Fe, and Zn electrodes in NaOH and KOH electrolytes.

Electrochemical kinetic studies are being conducted using "pure" metal rotating disk electrodes (RDE) and rotating ring-disk electrodes (RRDE) under potentiostatic control. The principal methods used are:

- AC impedance measurements to determine rate-limiting processes and reaction mechanisms (Ni, Fe, Zn).
- Measurements of ring collection current at programmed electrode rotation speeds to determine the nature and extent of electrode dissolution (Fe and Zn) and the mechanism of passivation (Zn).
- Potential-sweep (Ni, Fe, Zn) and potential-step (Fe, Zn) voltammetry and coulometry to determine the position of charge-storage electrode processes.

Thermodynamic calculations for the equilibrium potential/electrolyte concentration diagrams in this study are derived using the Criss-Cobble extrapolation for ionic entropies to elevated temperatures. We take into account the variation of pH and of the activity of water, a_W, with temperature and electrolyte concentration.

The methods used for both the kinetic and thermodynamic aspects of this study have been described extensively in previous publications.[2-8]

1.2 Summary of NaOH Results

A comprehensive survey of the electrochemistry of Ni, Fe, and Zn in 20, 24, and 28 wt% NaOH was made in the temperature range -20° to 120°C during the first year of this study. A number of specific observed features relating to the use of Ni, Fe, and Zn as alkaline battery electrodes, and these were of sufficient importance to merit further study.

Nickel: Two principal sources of irreversibility were found to contribute significantly to the coulombic inefficiency of the Ni charge/discharge process.

- Within the temperature range -20° to 120°C, the calculated equilibrium potential for oxygen evolution from electrolyte hydrolysis is negative with respect to the Ni(II)/Ni(III) equilibrium. The thermodynamic parameters of these competing processes are similar, although at room temperature and below the processes occur at very different rates. Thus, a high coulombic efficiency is achieved at this electrode only because a large overvoltage is required for oxygen evolution. With increasing temperature, the kinetic constraints are removed and we observe that exchange current density for oxygen evolution on a nickel surface increases markedly, resulting in decreased charge capacity and coulombic efficiency.

- Irreversibility is observed to be associated with deep or prolonged discharge, particularly at elevated temperatures. When a passivated $Ni(OH)_2$ electrode is cycled potentio-dynamically from complete discharge just into the oxygen evolution region, the shape of the anodic peak changes substantially, and the peak moves to more negative potentials (associated with a decrease in capacity), until a steady, reproducible trace is achieved after several tens of cycles. During this transition, the cathodic peak shape and charge remain relatively unchanged. This phenomenon can also be demonstrated by varying the extent of discharge. Figure 1 shows the effect of arresting a potentiodynamic sweep at its negative limit (+200 mV versus Hg/HgO) for

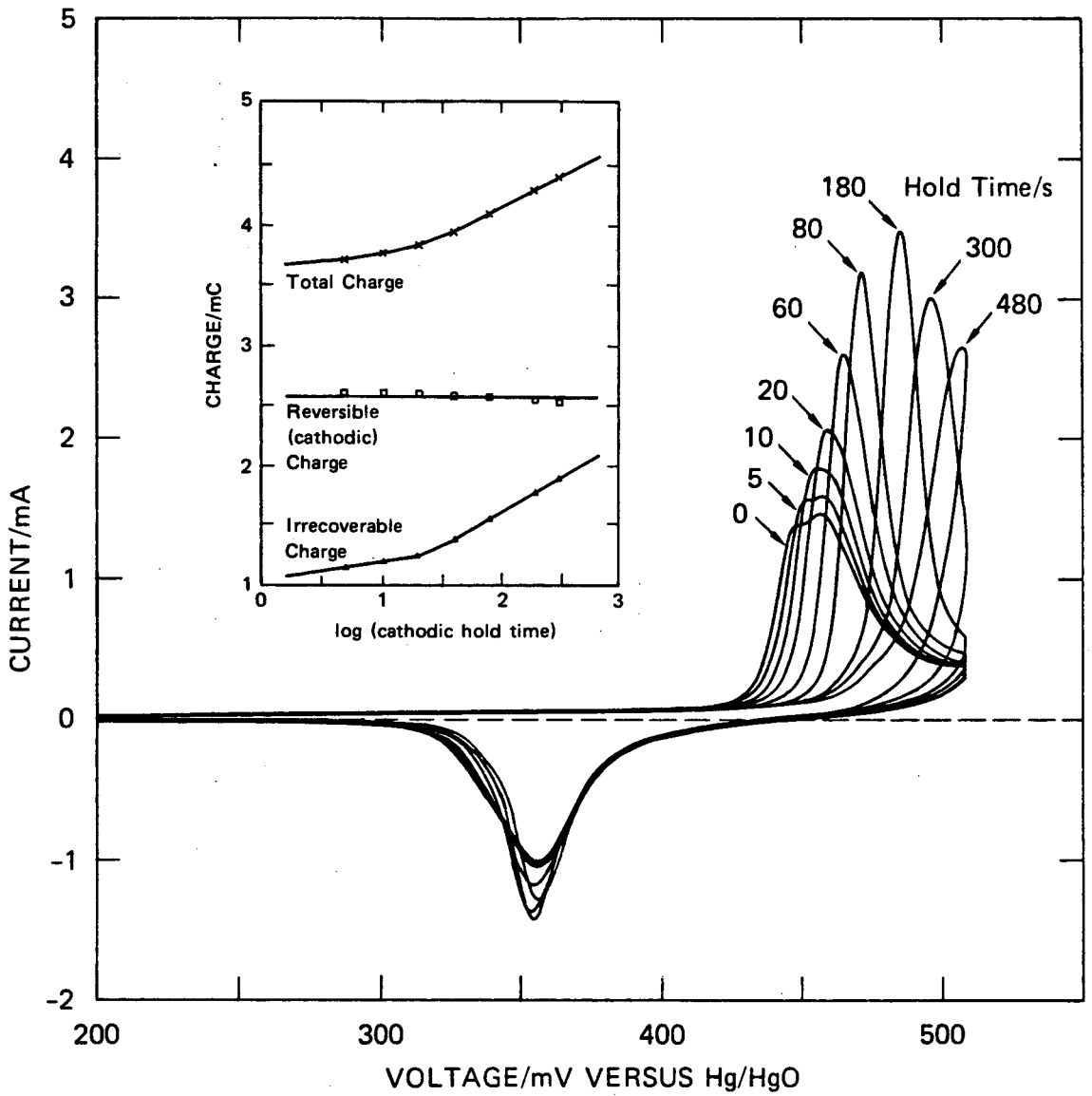

FIGURE 1 CYCLIC VOLTAMMOGRAM FOR NICKEL AS A FUNCTION OF CATHODIC HOLD TIME

20 wt% NaOH, 80°C, sweep rate 20 mV s^{-1}. Cathodic hold potential = 200 mV versus Hg/HgO.

various times after a steady repetitive sweep previously has been established. It is apparent that both the components of charge and the current profiles are strongly influenced by the hold time, τ_c, even though no charge-consuming processes occur at a significant rate at the cathodic limit potential. The anodic process requires a higher potential and consumes a greater charge at longer τ_c. In contrast to the anodic behavior, the cathodic process has a constant charge and occurs at effectively the same potential, independent of τ_c.

Iron:--High-temperature limitations of the iron negative electrode are associated with metal dissolution and with the coevolution of hydrogen at high states of charge. We have identified three distinct dissolution processes of iron and iron oxide in concentrated NaOH that may significantly reduce the cycle life and coulombic efficiency of iron alkaline battery electrodes operating at elevated temperatures. The presence of dissolved species also is of fundamental importance in interpreting the reaction mechanism. Figure 2 shows the results of slow-potentiodynamic-sweep RRDE studies in Fe and 28 wt% NaOH. For the experiments shown, the ring is held at a potential sufficiently positive to oxidize Fe(II) to Fe(III). The ring currents thus reflect the presence of dissolved Fe(II) species within defined regions of disk potential. At temperatures up to 40°C, a reductive dissolution process, D3, is seen to occur in association with disk charging peak V. D3 increases with temperature, and at 40°C accounts for 15% of the current associated with disk peak V. The genesis of an oxidative dissolution peak, D1, also is observed at 40°C. Both D1 and D3 increase at 80°C relative to the disk charge and discharge currents. At 112°C oxidative dissolution is observed during both disk discharge and charge, and the reductive dissolution process accounts for

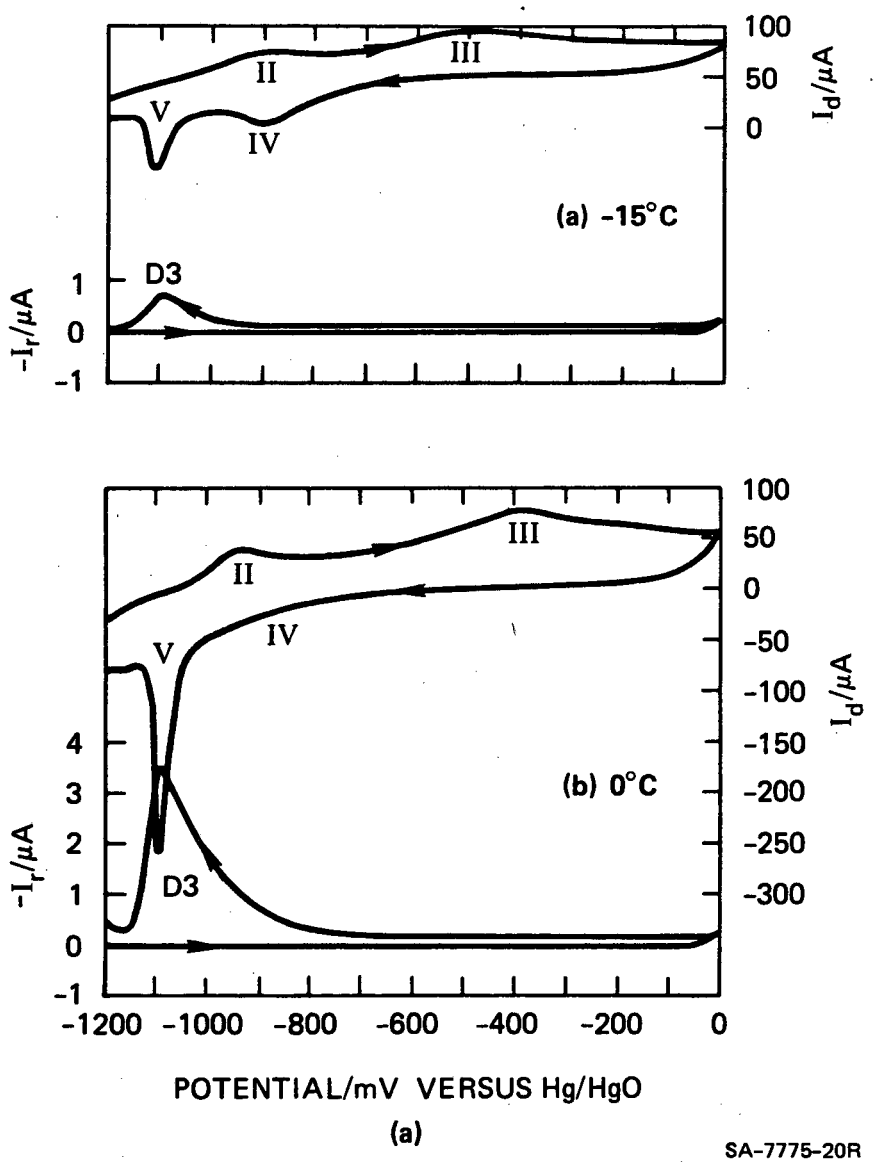

FIGURE 2 THE INFLUENCE OF TEMPERATURE ON RING AND DISK CURRENTS ON IRON ELECTRODE

Disk sweep rate = 10 mV s^{-1}, ring-500 mV versus Hg/HgO. Electrolyte concentration = 28 wt% NaOH, rotation speed = 1200 RPM.

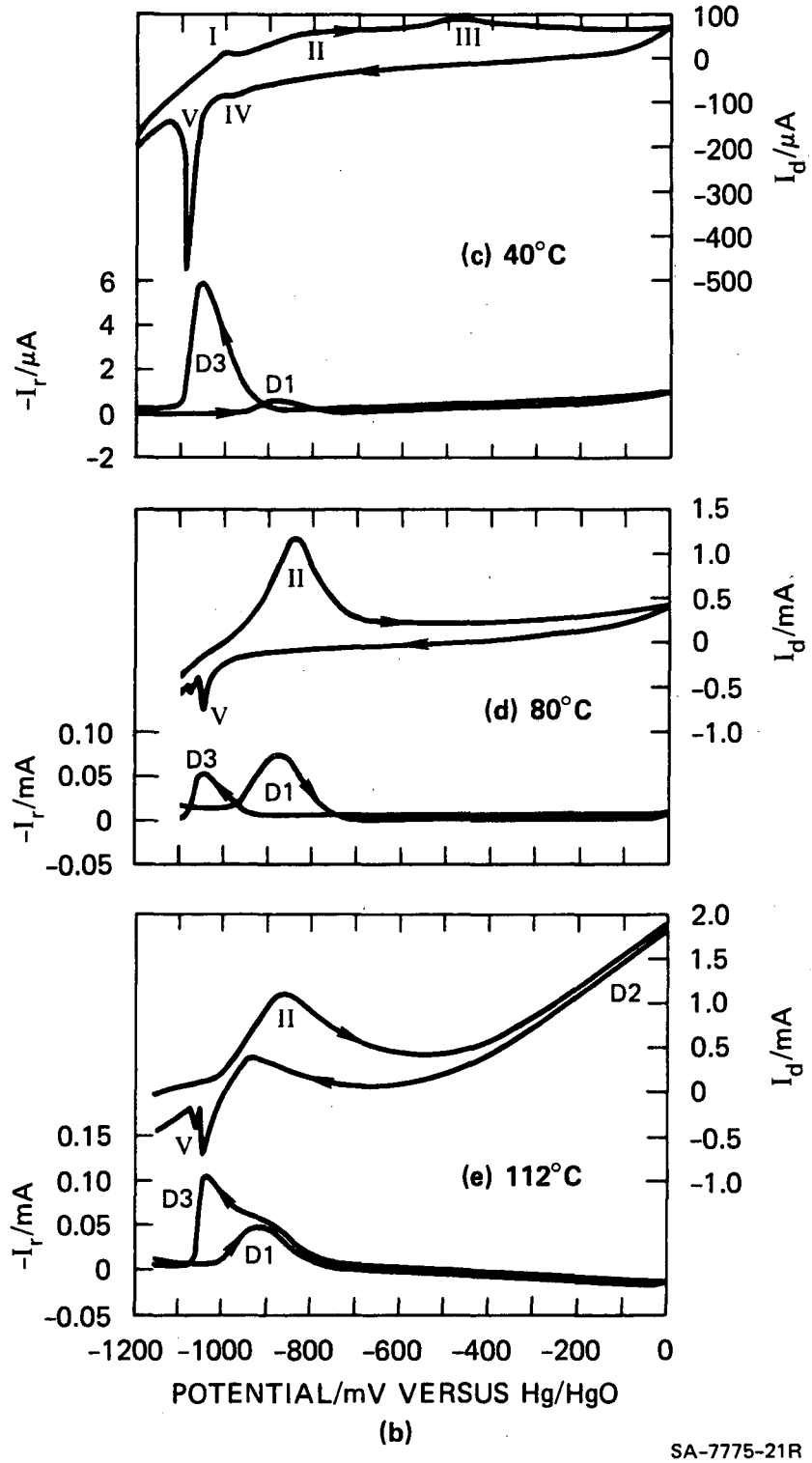

FIGURE 2 THE INFLUENCE OF TEMPERATURE ON RING AND DISK CURRENTS ON IRON ELECTRODE (Concluded)

Disk sweep rate = 10 mV s^{-1}, ring-500 mV versus Hg/HgO. Electrolyte concentration = 28 wt% NaOH, rotation speed = 1200 RPM

about 30% of the charge under disk peak V. At a state of high discharge, dissolution occurs over a wide potential range, producing Fe(III).

The origins of these dissolved species can be found for in the calculated equilibrium properties summarized in Figure 3. The predicted stability regions for the anions FeO_2^{2-} and $HFeO_2^-$ appear as closed loops in E versus log m_{NaOH} space; this suggests that above a certain OH^- ion concentration, irreversibility and coulombic inefficiency due to electrode dissolution may be reduced. Note also that the anion stability domains are predicted to decrease in size with increasing temperature, while the measured dissolution rate increases.

Zinc:--The principal temperature limitations of zinc negative electrodes are associated with the interrelated processes of dissolution, passivation, and current oscillation. We observe that the form of the repetitive sweep voltammogram for zinc in initially zincate-free NaOH depends critically on both electrode rotation speed and electrolyte temperature, with the discharge rate increasing with increasing electrolyte convection and temperature. Figure 4 shows the influence of disk rotation speed and temperature on the passivation onset potential for Zn in 28 wt% NaOH, compared with the reversible potential profiles calculated for redox reactions. It is apparent that the strong temperature dependence of zinc dissolution kinetics, and the more rapid onset of passivation at low temperatures, may sharply decrease the rate and extent of electrode discharge.

Under potentiostatic or slow potentiodynamic sweep conditions, we have observed zinc electrodes to undergo an oscillatory activation/

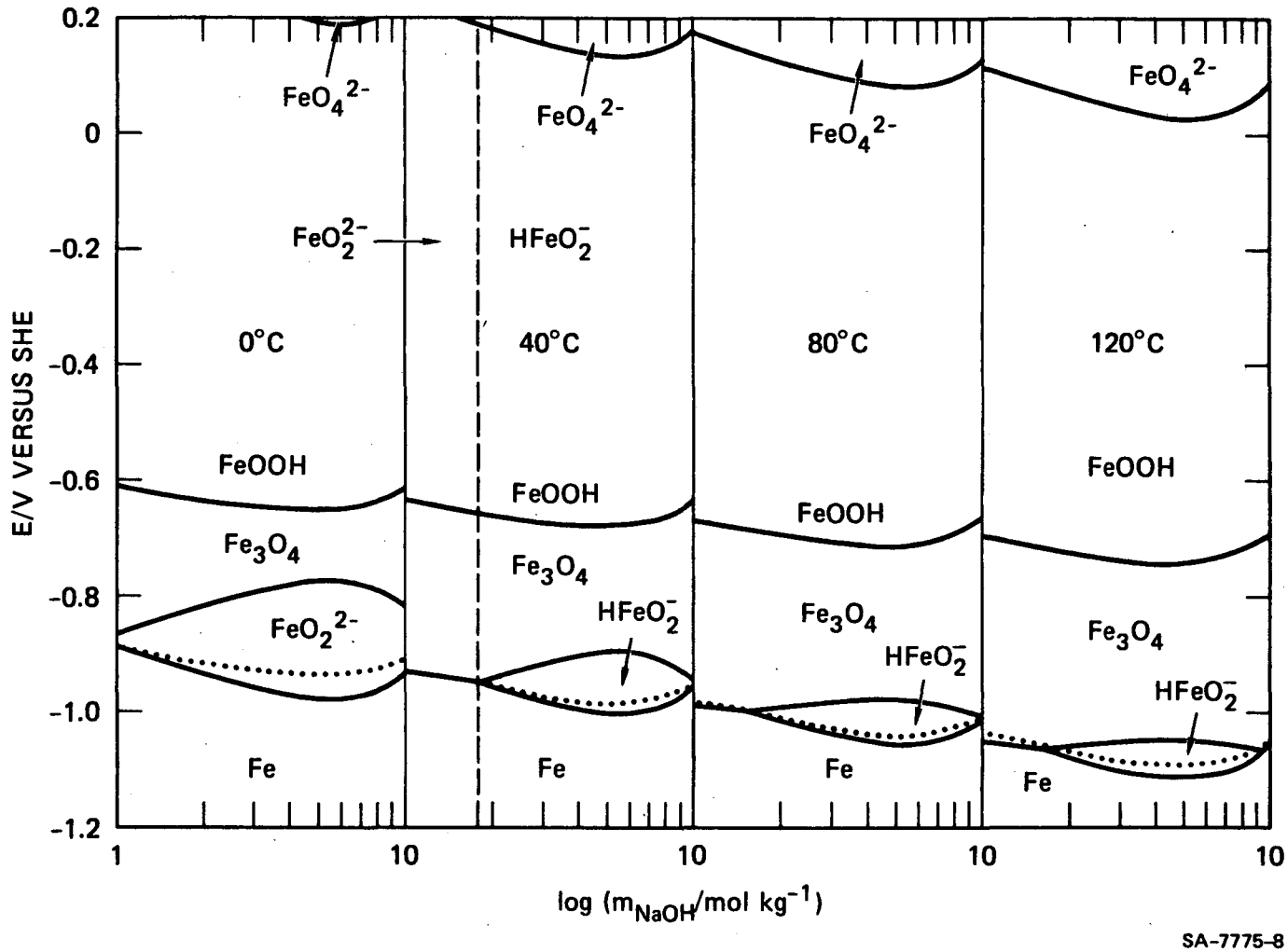

FIGURE 3 POTENTIAL VERSUS LOG m_{NaOH} DIAGRAMS FOR IRON IN CONCENTRATED SODIUM HYDROXIDE SOLUTION AS A FUNCTION OF TEMPERATURE

The line ····· refers to the equilibrium potentials for the Fe/Fe $(OH)_2$ couple.

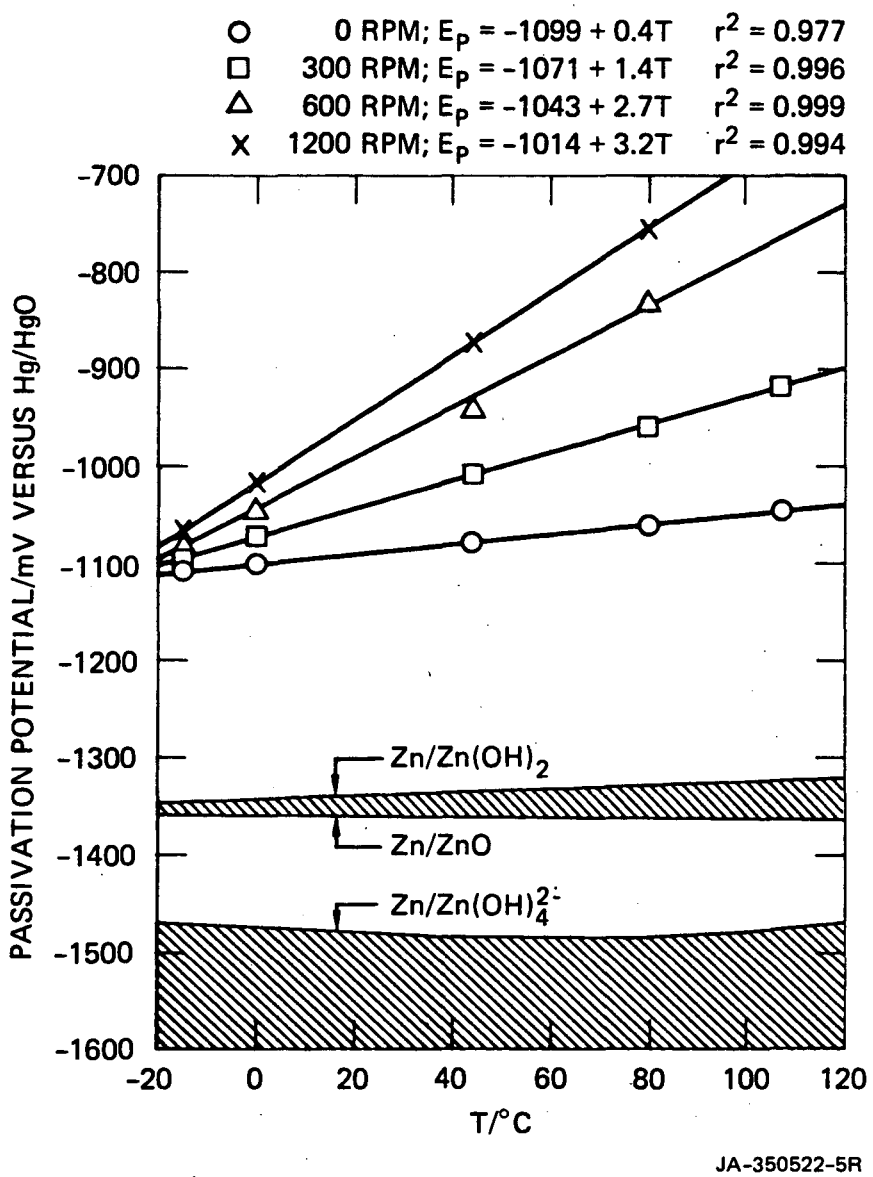

FIGURE 4 MEASURED PASSIVATION ONSET POTENTIALS AND CALCULATED REVERSIBLE POTENTIALS VERSUS TEMPERATURE, FOR ZINC IN 28 wt% NaOH

passivation process within a defined region of potential, which may result in current fluctuations of several orders of magnitude. These are shown in Figure 5 for a rotating zinc disk and vitreous carbon ring electrode, following a potential step from the reversible potential, at an electrode rotation speed of 5.0 Hz. Oscillations appear in quiescent as well as convected electrolyte, and under controlled hydrodynamic conditions appear to be sustainable indefinitely. However, both the oscillation amplitude and period are markedly influenced by step potential, temperature, rotation speed, and zincate concentration. Figure 6 shows the limits of potential over which oscillation occurs in a quiescent system, as a function of temperature.

1.3 Conclusions from NaOH Studies

Nickel appears well suited as a positive battery electrode material operating at extremes of temperature. We find no evidence for metal or oxide dissolution within the normal operating range of potential. Provided this electrode is not completely discharged, high-temperature limitation is imposed only by the competition from oxygen evolution at high charge. This effect may be minimized by control of electrolyte concentration.

In common with the other two metals studied, the decreased rate and extent of charge/discharge processes for nickel at low temperature may well impair battery performance under high-rate charge or discharge conditions at low ambient temperatures.

Both zinc and iron suffer degradation in performance at temperature extremes, which may well limit their use, particularly under high current

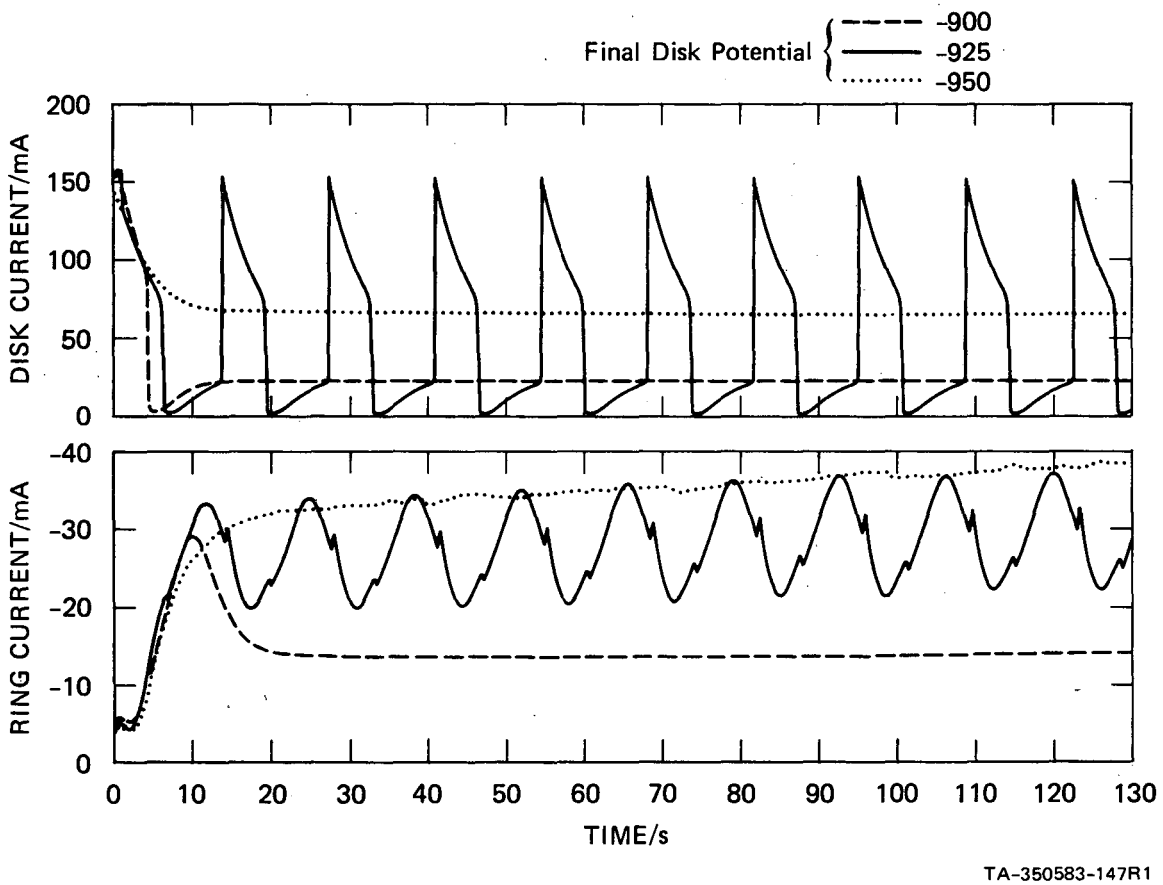

FIGURE 5 RRDE POTENTIAL STEP EXPERIMENT FOR ZINC IN 28 wt% NaOH AT 22.5°C

Ring potential and initial disk potential -1500 mV versus Hg/HgO. Rotation speed 300 RPM.

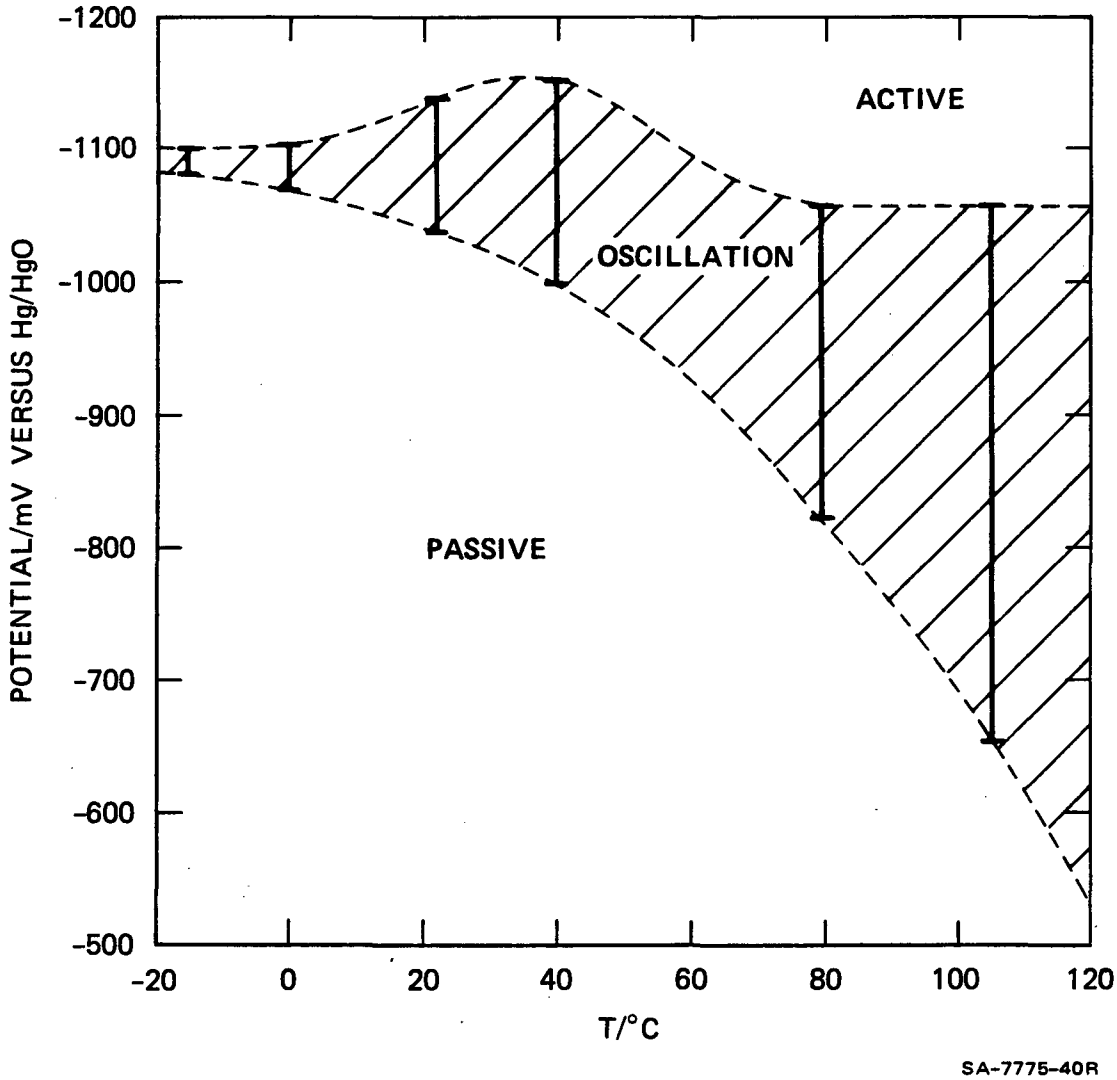

FIGURE 6 REGION OF CURRENT INSTABILITY FOR Zn IN 28 wt% NaOH UNDER QUIESCENT CONDITIONS

conditions where electrolyte IR heating is severe. The increased dissolution rate of zinc with temperature causes wide regions of current oscillation, loss of reactant, irreversibility, and internal short circuit; it may also promote electrode shape change and the growth of dendrites.

The low overpotential for hydrogen evolution on iron and the increase of i_o for this process with temperature severely restrict the operating potential range of iron and may result in substantial coulombic inefficiency. Both oxidative and reductive iron dissolution may lead to coulombic inefficiency and electrode degradation at elevated temperatures. Since these processes occur within narrow regions of potential, however, it is probable that the effects of dissolution can be minimized by appropriate potential control--that is, by using potentiostatic rather than constant-current charging.

1.4 Report Organization

Parts I and II of this report describe the results and conclusions obtained in kinetic[2] and thermodynamic[3] studies of Ni, Fe, and Zn electrodes in concentrated aqueous NaOH electrolytes, Parts III and IV have been organized slightly differently. The present volume (Part III) contains results and conclusions relating to the charge/discharge characteristics of the negative electrode materials, Fe and Zn, in concentrated KOH. Part IV will contain the results of studies of Ni electrodes in KOH, with particular emphasis placed on the role of LiOH in stabilizing the Nickel Oxide positive electrode.

2 EXPERIMENTAL METHODS

2.1 Introduction

Within the current year of funding, SRI has sought to use the "high information" electrochemical methods previously applied to understanding temperature limitations of Ni, Fe, and Zn electrodes in NaOH, and to extend these measurements to KOH solutions. Some refinement of techniques has been undertaken, particularly in the construction of a closed-loop, digital- feedback, variable-speed RRDE motor assembly. Considerable attention also has been paid to the development of stepped-frequency AC impedance measurements under minicomputer control for use as a quantitative tool to obtain mechanistic information in battery electrode studies.

Particular emphasis has been given to the phenomena identified in the work to date. These are:

(1) Determining the mechanisms of irreversibility of Ni associated with deep or prolonged discharge at elevated temperatures.

(2) Quantifying the extent of Fe(II) and Fe(III) dissolution at elevated temperatures, and determining the influence of KOH concentration on dissolution kinetics.

(3) Quantifying the dissolution and studying passivation and oscillation phenomena of Zn as a function of KOH and $Zn(OH)_4^{2-}$ concentration.

Five temperatures at 25°C intervals in the range 0° to 100°C were used. Two electrolyte concentrations (30 and 35 wt%) were chosen as being typical of alkaline battery electrolyte concentrations and are close to the composition for maximum electrolyte conductivity at all temperatures.

2.2 Electrolyte Preparation; Electrode and Cell Construction

An all-Teflon electrochemical cell was used, containing a four-electrode rotating ring-disk electrode (RRDE) assembly. This apparatus is similar to that described previously;[2,3] it differs in the following features:

- A mercury slip ring assembly (Omega Model SR-2) replaces the Ag/Hg/Cu brushes previously used for RRDE contacts.
- A Digital Systems Division Model MC141A motor control unit provides increased speed range (50 to 3000 RPM), increased stability (± 0.25%), and programmable rotation-speed sweep capability.
- A Pine Model RDE-3 bipotentiostat improves current handling-capability for RRDE studies.

The bipotentiostat and motor and mercury slip ring assemblies are shown in Figure 7.

For nickel, only a rotating disk electrode (RDE) was used. The dissolution of Ni has been shown to be negligible[2,4] at all temperatures studied within the normal range of operating potential of the nickel positive electrode. The RRDE used in studies of the dissolution of iron and zinc employed a PTFE insulating spacer and a vitreous carbon* ring. Details of the RRDE construction are presented in Figure 8.

Electrolytes were prepared in polyethylene containers by diluting "Baker Analyzed" reagent-grade 45 wt% KOH to the desired concentration with doubly distilled deionized water. The second distillation was performed under high-purity N_2 gas immediately before use to exclude

---

*Vitreous carbon was generously supplied by Dr. A. Norris, Fluorocarbon Corporation, Anaheim, California.

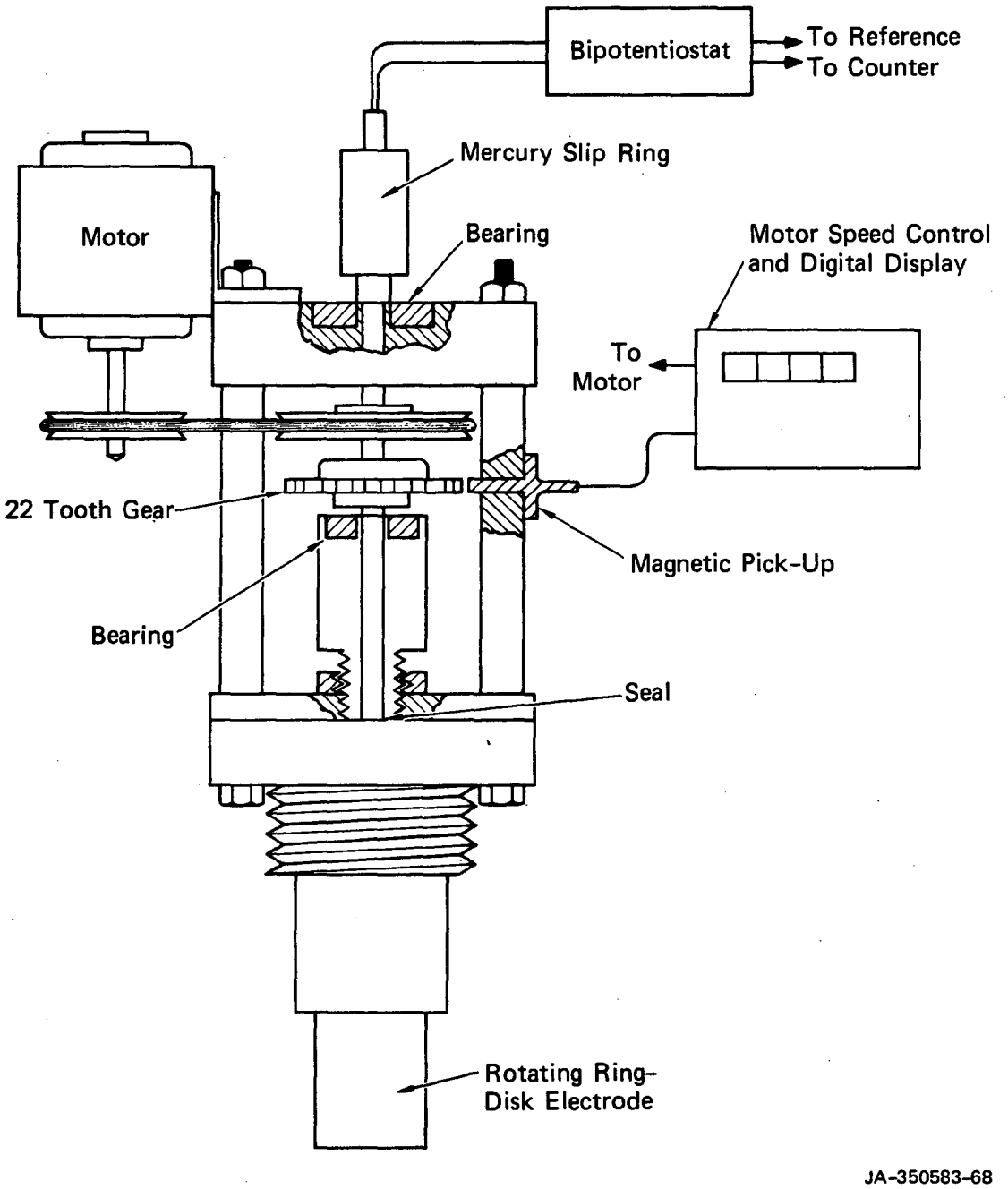

FIGURE 7 BIPOTENTIOSTAT AND MOTOR AND SLIP RING ASSEMBLIES

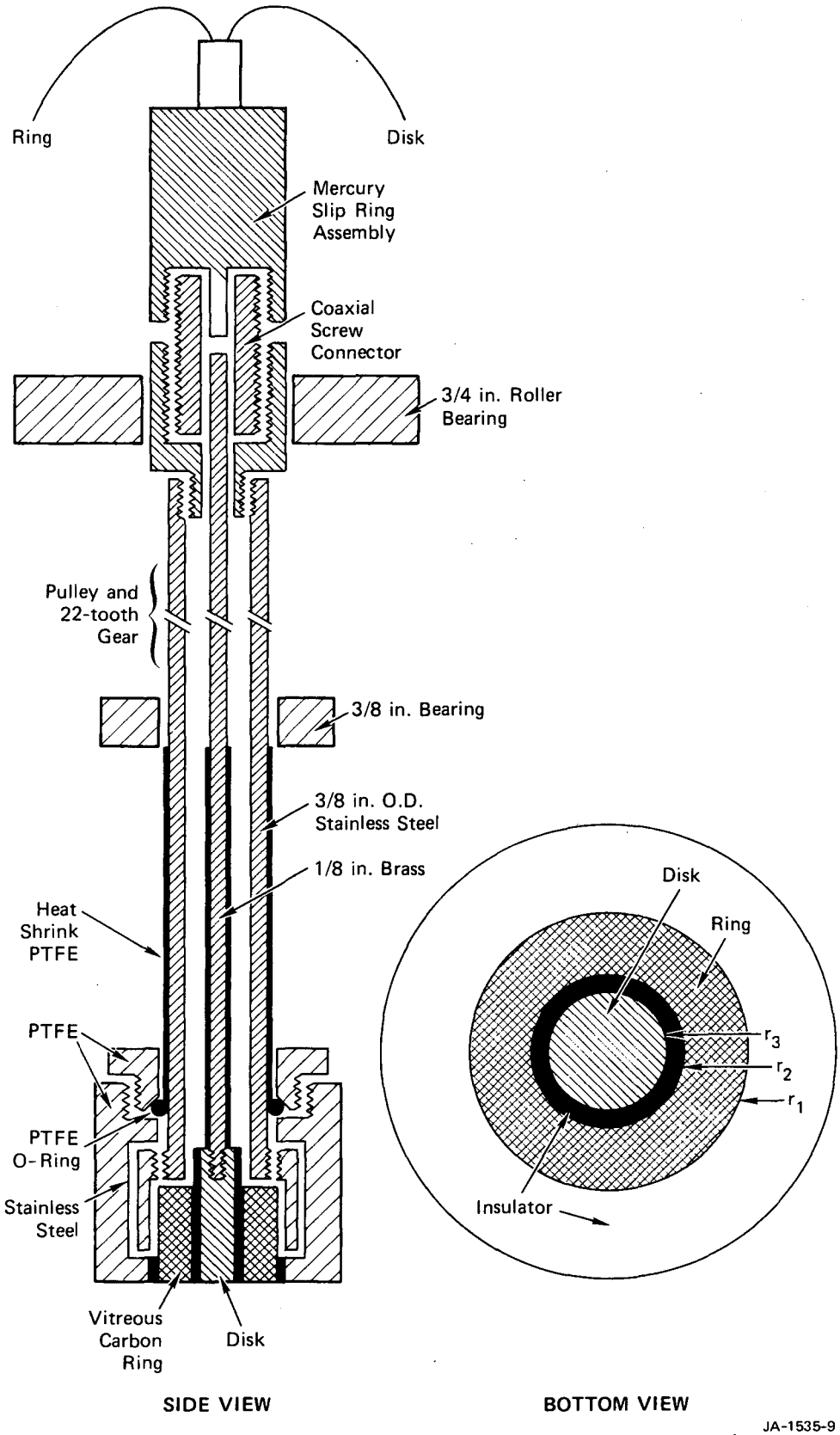

FIGURE 8 SCHEMATIC DIAGRAM OF RRDE CONSTRUCTION AND CONTACT ASSEMBLY

CO_2. The concentrations of hydroxide and carbonate were determined by acid titration, using the method described in Reference 10.

2.3 Instrumentation

The principal electrochemical techniques used in the present study were:

- Linear sweep voltammetry and coulometry
- Programmed rotation speed rotating ring-disk studies
- Potential-step transient analysis
- AC impedance studies.

The methodology for the experiments has been described previously.[2-8] Reference 2 contains a detailed description of the apparatus and experimental methods for the first three techniques.

AC impedance studies were performed using the experimental configuration shown schematically in Figure 9. Briefly, a Solartron model 1172/1183C/1185 Frequency Response Analyzer (FRA) was used in conjunction with an Apple II microcomputer to automatically perform RDE AC impedance measurements over a range of frequencies and applied DC potentials. The data are displayed on the video monitor as either a Nyquist or Bode plot. Data can be saved on disk for subsequent analysis.

The use of this apparatus required the development of IEEE-488 bus communication between computer and FRA, and the design and construction of an appropriate FRA/potentiostat interface unit. The software necessary to make impedance measurements under computer control and to display, record, and analyze the results is presented in Appendix I. The interface unit was intended to address two specific problems in the use of the Solartron model 1172 to make electrochemical impedance measurements:

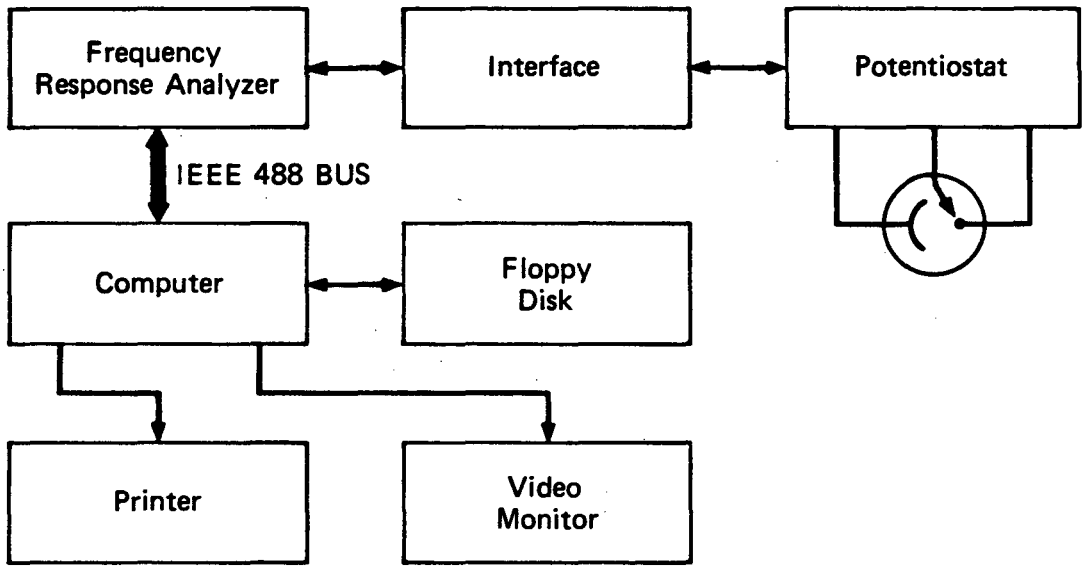

(a) SCHEMATIC DIAGRAM OF INSTRUMENTATION

JA-350583-51A

FIGURE 9 AC IMPEDANCE MEASUREMENT SYSTEM

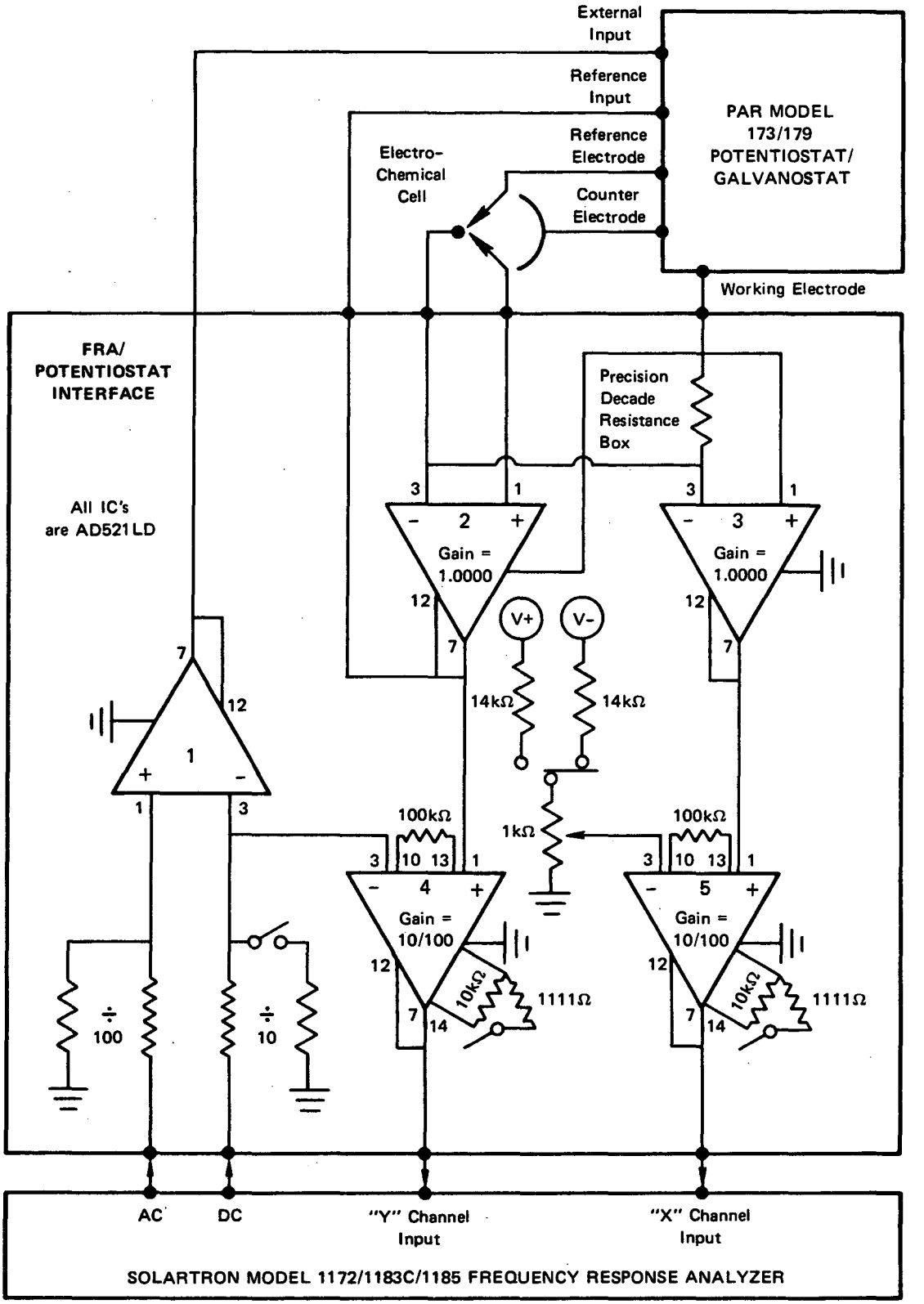

(b) FRA/POTENTIOSTAT INTERFACE UNIT CIRCUITRY

JA-1535-10

FIGURE 9 AC IMPEDANCE MEASUREMENT SYSTEM (Concluded)

(1) The minimum output AC voltage amplitude from the FRA is 10 mV, but the maximum electrode perturbation allowable while preserving a linear current/voltage response is of the order of 5 mV.

(2) The reference/working electrode potential typically comprises an AC component of magnitude < 5 mV, superimposed on a DC level of hundreds of thousands of mV. A large fraction of the DC voltage must be removed before amplification to allow the Solartron to operate on its most sensitive input range.

Requirement 1 is accomplished by attenuating the AC output from the Solartron before combining it with the DC output in instrumentation amplifier 1. The combined output is provided to the potentiostat "external" input and applied to the cell. A precision, decade-adjustable resistor is placed in series with the cell counter* electrode. The voltage drops across the resistor, and between the reference and working electrodes, are determined by instrumentation amplifiers 2 and 3. The output of amplifier 3 provides the negative feedback return path to the potentiostat.

The outputs from amplifiers 2 and 3 are amplified by instrumentation amplifiers 4 and 5 and are provided to the "Y" and "X" channels of the Solartron for analysis. In order to accomplish requirement 2, a DC level is substracted from each signal before amplification. For the current signal (output "X"), this DC backoff is accomplished manually using a 10-turn potentiometer. The backoff signal for the cell voltage (output "Y") is obtained from the DC input to amplifier 1. The potentiostat functions nearly ideally with regard to the DC component of the applied voltage,[8]

---

*This resistor also has been placed in series with the working electrode. Since the signal fed back to the potentiostat is determined differentially between the reference and working electrodes, the potentiostat can be induced to operate with the working electrode floating.

and the gain function for the instrumentation amplifiers can be expressed as[11,12]

$$V_{out} = (V_+ - V_-)G - V_{ref} \quad , \tag{1}$$

where V_+ and V_- are the inverting and noninverting input voltages, G is the amplifier closed loop gain and V_{ref} is the reference terminal voltage. Thus, amplifier 5 serves to reduce the DC component of the cell voltage to a very low level (0 ± 2 mV), independent of the gain of the AC component.

The bandwidth of this device is of critical importance in determining the high-frequency AC impedance. Accordingly, measurements were made of the impedance of a nonreactive dummy cell (of nominal impedance 999.0 Ω). The results shown in (Figure 10) indicate that the measurement system is accurate to within ± 0.1% at frequencies up to 2 kHz, and within ± 0.5% up to 6 kHz.

2.4 Measurement Techniques

The methods employed for cyclic voltammetry, rotating ring-disk, and coulometry studies are detailed in Reference 2, Section 3. Additional methods used in the present study were as follows.

Measurements of the electrochemical impedance of rotating disk electrodes were made as a function of electrode speed, electrolyte concentration, temperature, and applied DC potential. The response to a small-amplitude ($\lesssim$ 5 mV) sinusoidal perturbation in the frequency range

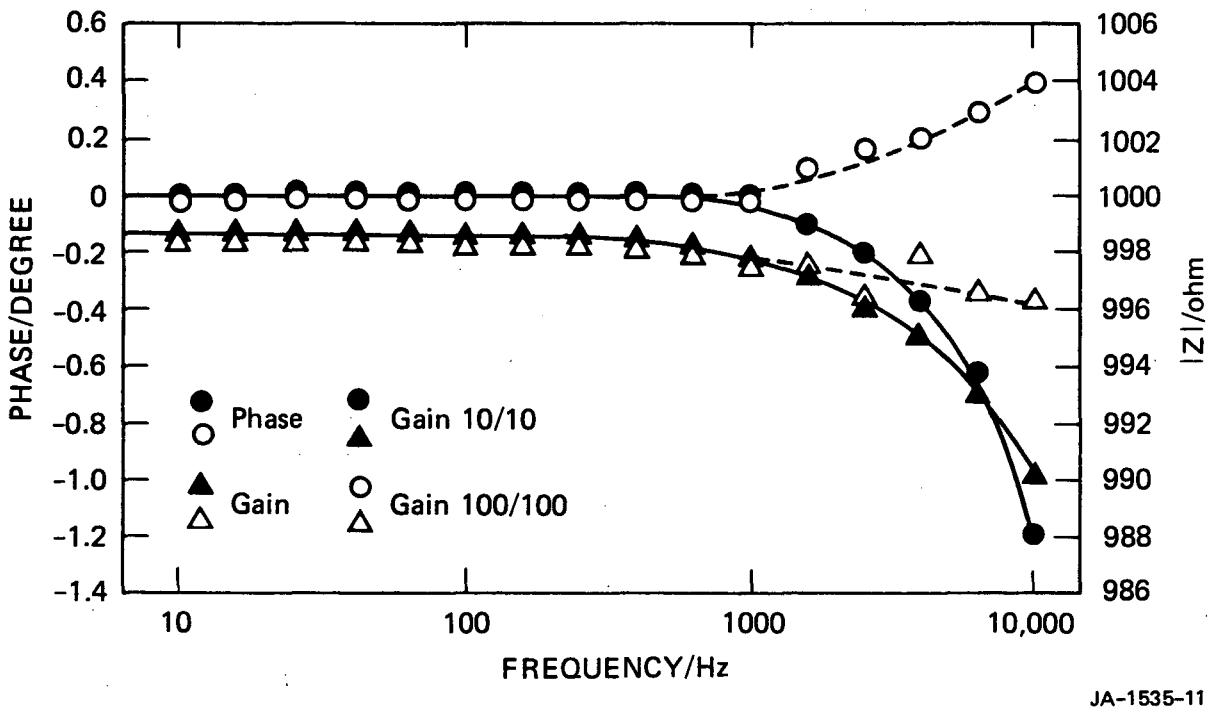

FIGURE 10 TRANSFER FUNCTION AND PHASE VERSUS LOG (FREQUENCY) FOR FRA/POTENTIOSTAT INTERFACE UNIT

$10^{-3} \leq f \leq 10^{4}$ Hz was analyzed to provide information on the reaction mechanisms, interfacial reaction rates and the mass transport parameters. The nature of the analysis and the assumptions implied have been described previously.[8]

By way of a brief review, a smooth plane-parallel electrode can be represented by the equivalent circuit shown in Figure 11(a). The uncompensated electrolyte resistance (RO) reflects the resistance of the volume of electrolyte between the reference probe (tip of Luggin capillary) and the plane of the working electrode, and the double-layer capacitance provides a measure of the distribution of charge in the fixed and diffuse electrical double layers. The measured capacitance is a function of voltage[8] and may contain low-frequency contributions from surface-adsorbed species. This parameter generally is not of great interest in battery studies.

The interfacial reaction (charge/discharge) rate is determined by the series combination of two terms that reflect the mass transport of reactant to or product away from the interface and the intrinsic kinetics of the reaction process. An expression for the interfacial reaction resistance for simple electrode processes can be obtained by linearizing the Butler-Volmer equation

$$I = i_o[\exp(\vec{\beta}V) - \exp(\overleftarrow{\beta}V)] \quad , \tag{2}$$

where

$$\vec{\beta} = \alpha nF/RT \tag{3}$$

$$\overleftarrow{\beta} = (1 - \alpha)nF/RT \ . \tag{4}$$

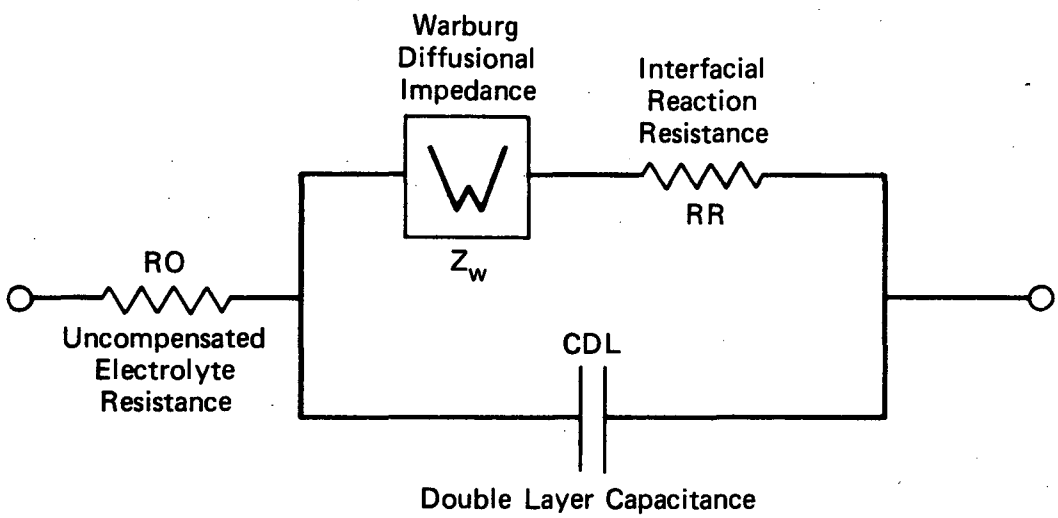

(a) RANDLES CIRCUIT FOR THE ELECTRODE/ ELECTROLYTE INTERFACE

JA-1535-12

FIGURE 11 THE EQUIVALENT CIRCUIT AND EXPECTED IMPEDANCE RESPONSE FOR A SIMPLE ELECTROCHEMICAL INTERFACE

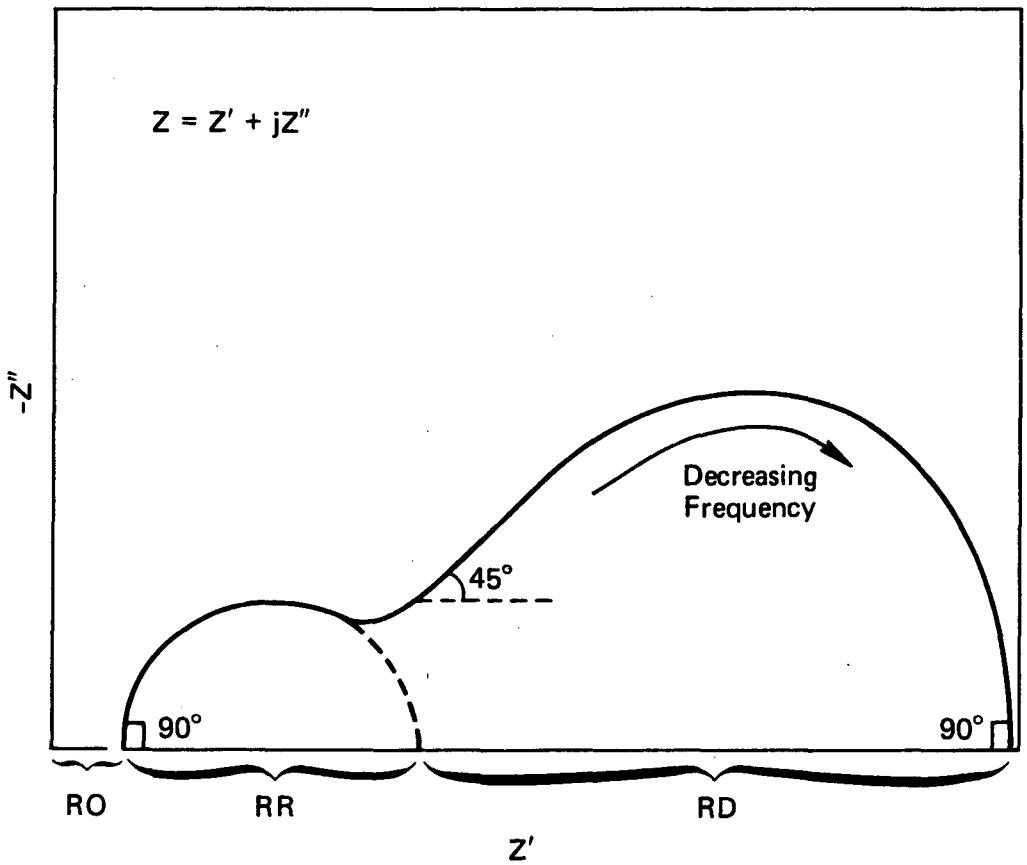

(b) Expected frequency response for an electrochemical interface undergoing a single, uncoupled charge transfer process, under mass transport control in a well-convected system

JA-1535-13

FIGURE 11 THE EQUIVALENT CIRCUIT AND EXPECTED IMPEDANCE RESPONSE FOR A SIMPLE ELECTROCHEMICAL INTERFACE (Concluded)

For a sinusoidal perturbation superimposed on a steady DC level, V can be expressed as

$$V = {}_oV + v \sin(\omega t) \tag{5}$$

where ${}_oV$ is the difference between the applied DC level and the reversible electrode potential.

Substituting (5) into (2) one obtains

$$I = i_o \left[\exp(\vec{\beta}_o V) \exp(\vec{\beta} v \sin [\omega t]) - \exp(\overleftarrow{\beta}_o V) \exp(\overleftarrow{\beta} v \sin[\omega t])\right] . \tag{6}$$

We can expand exp(x) as

$$e^x = 1 + \frac{x}{1} + \frac{x^2}{2} + \frac{x^3}{6} + \ldots + \frac{x^n}{n!} \quad . \tag{7}$$

The nonlinear form of equation (6) results in a series of harmonic terms in the AC response.[13-16] The first three terms of the DC and fundamental AC responses are given by:[13,15]

DC:

$$\begin{aligned} {}_oI = {} & i_o[\exp(\vec{\beta}_o V) - \exp(\overleftarrow{\beta}_o V)] \\ & + \frac{i_o v^2}{4} [\vec{\beta}^2 \exp(\vec{\beta}_o V) - \overleftarrow{\beta}^2 \exp(\overleftarrow{\beta}_o V)] \\ & + \frac{i_o v^4}{64} [\vec{\beta}^4 \exp(\vec{\beta}_o V) - \overleftarrow{\beta}^4 \exp(\overleftarrow{\beta}_o V)] \end{aligned} \tag{8}$$

Fundamental: $$i = \frac{i_o v}{1} \vec{\beta} \exp(\vec{\beta}_o V) - \overleftarrow{\beta} \exp(\overleftarrow{\beta}_o V)]$$

$$+ \frac{i_o v^3}{8} [\vec{\beta}^3 \exp(\vec{\beta}_o V) - \overleftarrow{\beta}^3 \exp(\overleftarrow{\beta}_o V)]$$

$$+ \frac{i_o v^5}{192} [\vec{\beta}^5 \exp(\vec{\beta}_o V) - \overleftarrow{\beta}^5 \exp(\overleftarrow{\beta}_o V)] \quad . \tag{9}$$

For small applied AC amplitudes ($v \ll 1$), the DC response simplifies to its expected Butler-Volmer form,

$$_oI = i_o \, [\exp(\vec{\beta}_o V) - \exp(\overleftarrow{\beta}_o V)] \quad , \tag{10}$$

and the reaction resistance is given by

$$\frac{1}{RR} = \frac{i}{v} = i_o[\vec{\beta} \exp(\vec{\beta}_o V) - \overleftarrow{\beta} \exp(\overleftarrow{\beta}_o V)] \quad . \tag{11}$$

Under the simplifying conditions of a symmetric reaction ($\alpha = 0.5 : \vec{\beta} = -\overleftarrow{\beta} = \beta$),

$$\frac{1}{RR} = 2i_o\beta \exp(\beta_o V) = \frac{i_o nF}{RT} \exp\,(0.5\ nF\ _oV/RT) \quad . \tag{12}$$

Thus, we define a voltage-dependent resistance that is inversely proportional to the exchange-current density in combination with other (generally known) electrochemical parameters.

The Warburg diffusional impedance in Figure 11(a) reflects the limitation on the reaction rate that is imposed by the mass transport of reactant to and product from the electrode. A sinusoidal voltage perturbation at the electrode results in a damped concentration wave, symmetric about the bulk concentration of reactant (or product), that propagates toward the electrolyte bulk. This concentration wave has a period equal to the imposed electrical perturbation, but is 45° out of phase. At high frequencies the wave is effectively damped out within the Nernst diffusion layer, and the diffusional impedance is given by

$$Z_w = \sigma(1 - j)\omega^{-\frac{1}{2}} \quad , \tag{13}$$

where

$$\sigma = RT/[n^2F^2(2\bar{D})^{\frac{1}{2}}\,\bar{c}] \quad , \tag{14}$$

$\bar{D}$ and $\bar{c}$ are the mean diffusion coefficient and mean concentration of reactant (or product), and ω is the frequency in radians s^{-1}. At lower frequencies the concentration wave interacts with the diffusion layer, at which point the concentration is considered to be damped rapidly to its mean value by natural convection processes in the electrolyte bulk. The diffusional impedance in this slightly more complicated case is given by

$$Z_w = [\frac{RT}{nF(i - i_\ell)}]\ [\frac{\tanh(ju)^{1/2}}{(ju)^{1/2}}] \quad , \tag{15}$$

where

$$u = \omega\delta^2/\bar{D} \tag{16}$$

and δ is the diffusion layer thickness, i is the DC current density, and i_ℓ is the limiting current density. At high frequencies equation (15) reduces to equation (13). At the limit of low frequency ($\omega \rightarrow 0$), equation (15) defines the diffusional resistance,

$$RD = \sigma\delta/(\bar{D}/2)^{1/2} \quad . \tag{17}$$

The characteristic impedance plane response (Nyquist plot) of the equivalent circuit shown in Figure 11(a) is given in Figure 11(b). Under ideal conditions the three principal resistances--RO, RR, and RD--are clearly resolvable, and the region determined by equation (13) appears as a straight line of slope 45°. For a perfectly smooth electrode with surface everywhere perpendicular to the applied field gradient (i.e. current flux normal to the surface), the intercept of the impedance locus at limiting high and low frequencies, occurs at 90°.

In battery studies we are particularly interested in i_o. To obtain this parameter with precision from the high-frequency AC response, we have developed a regression technique to fit the measured impedance data to a series/parallel equivalent circuit comprising RO, RR, and CDL. Details of the regression technique, and the computer program employed are included as Appendix II.

Programmed-rotation-speed ring-disk voltammetry was also used in the current study. In this method, the ring and disk are held at constant potential, and the respective currents are monitored as a function of a continuously varying rotation speed. The rotation speed variation is

"programmed" by applying an external voltage at the reference input of the motor speed controller shown in Figure 7. The shaft rotation speed is tightly controlled by the digital feedback loop and the angular momentum of the rotating assembly is low in comparison with the motor power (Bodine, 1/50 HP). Thus, the electrode rotation follows the program voltage variation closely, to high slew rates. Rotation speed information is taken directly from the magnetic pickup induced by the 22-tooth gear. In this way the rotation speed can be updated 22 times per revolution.

We have used two principal rotation speed perturbation schemes. Linear cycling of the rotation-speed from low to high rotation and return, has been used to measure the rotating speed dependence of the measured RRDE collection efficiency. In this case the rate of rotation speed change was calculated to be sufficiently low to maintain hydrodynamic equilibrium[17] at the electrode surface. The second method was to impose a small sinusoidal perturbation of rotation about a fixed (DC) rotation speed. Measurements of the dependence of disk current on the modulation frequency provide a very effective means of distinguishing convective-diffusion processes from interfacial electrode reactions that are not governed by mass transport.[17-21]

The advantages of programmed speed control of rotating disk and rotating ring-disk electrodes have been well reviewed in the pioneering study of Miller et al.[17]

3 MEASUREMENTS ON IRON

3.1 Introduction

Experiments were performed using a rotating 99.9985% purity Fe disk and vitreous carbon ring electrode. A single electrolyte concentration (30 wt% KOH) was studied at temperatures of 0°, 25°, 50°, and 75°C. Experiments at 100°C resulted in severe corrosion and degradation of the Fe disk electrode, and no useful results were obtained at that temperature.

The experiments performed may be divided into three categories. Potentiodynamic studies comprising rotating disk electrode voltammetry and coulometry were used to examine possible kinetic limitations of the iron/iron oxide redox processes, and to measure the rate of hydrogen evolution under high-charge conditions. Rotating ring-disk studies were performed to quantify the rate of dissolution of iron and iron oxide species. AC impedance measurements were made to investigate the nature of the oxide films. Results of these measurements are presented in Sections 3.2 to 3.5.

A considerable insight into the mechanisms of dissolution and passivation is contained in the results. The implications are discussed in Section 3.6.

3.2 Potentiodynamic Studies of Iron

The discharge of an iron electrode in concentrated alkali proceeds via three sequential oxidation processes; each of these is manifest as a peak on a potentiodynamic discharge curve. On reversal of the potential sweep direction, three consecutive reduction peaks are resolvable.

Figures 12 and 13 show the influence of the anodic and cathodic reversal potentials on the repetitive-sweep voltammogram for Fe at 75°C and a rotation speed of 10 Hz, with a potentiodynamic sweep rate of 50 mV s^{-1}. It is clear from these results that the peaks designated as O1 and R2 are conjugate processes, and that O3 and R3 are conjugates. That is, the oxidized species formed under peak O1 is reduced at R1, and similarly for O3 and R3.

The dependence of the height and position of peaks O2 and R2 on sweep rate and reversal potential suggests slightly more complex reaction paths. In Figure 12 the reoxidation of a fraction of O2 can be seen to occur for reversal potentials more negative than +500 mV*. A plot of the area under O2 versus cathodic reversal potential is inset in Figure 12, and indicates that the species formed at O2 is reduced continuously (i.e., the reduction process is not characterized by a peak on the potentiodynamic charge curve).

The origin of R2 can be seen most clearly in Figure 13. Peak R2 is absent in all voltammograms except those performed with the two most

---

*Unless otherwise specified, measurements of potential are with respect to a Zn/Zn^{++} reference couple in an electrolyte of the same composition and temperature as the working electrode chamber.

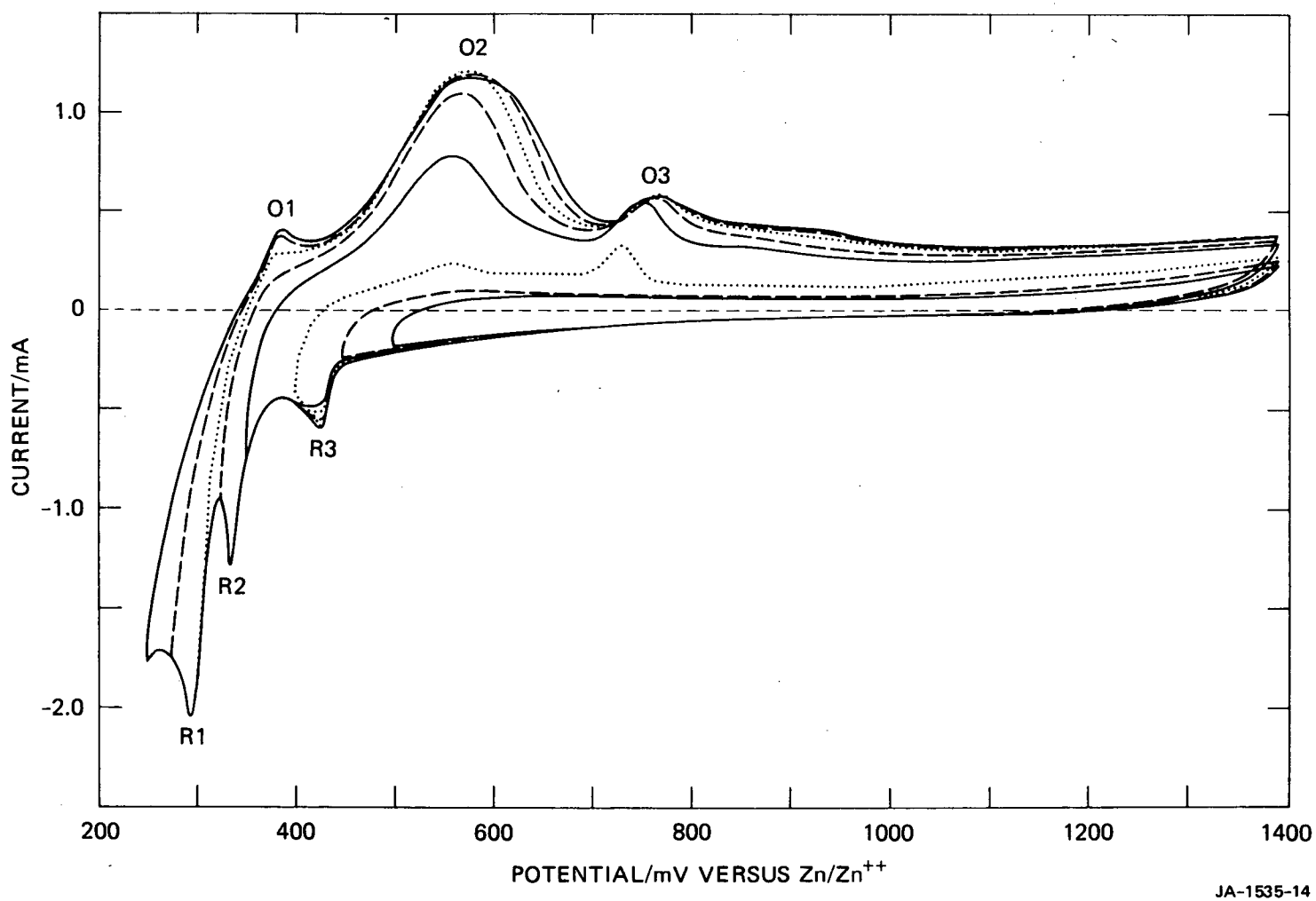

FIGURE 12 THE INFLUENCE OF CATHODIC POTENTIAL LIMIT ON THE REPETITIVE SWEEP VOLTAMMOGRAM FOR AN IRON DISK ROTATED AT 10 Hz IN 30 wt% KOH AT 75°C

Potentiodynamic sweep rate = 50 mV s^{-1}.

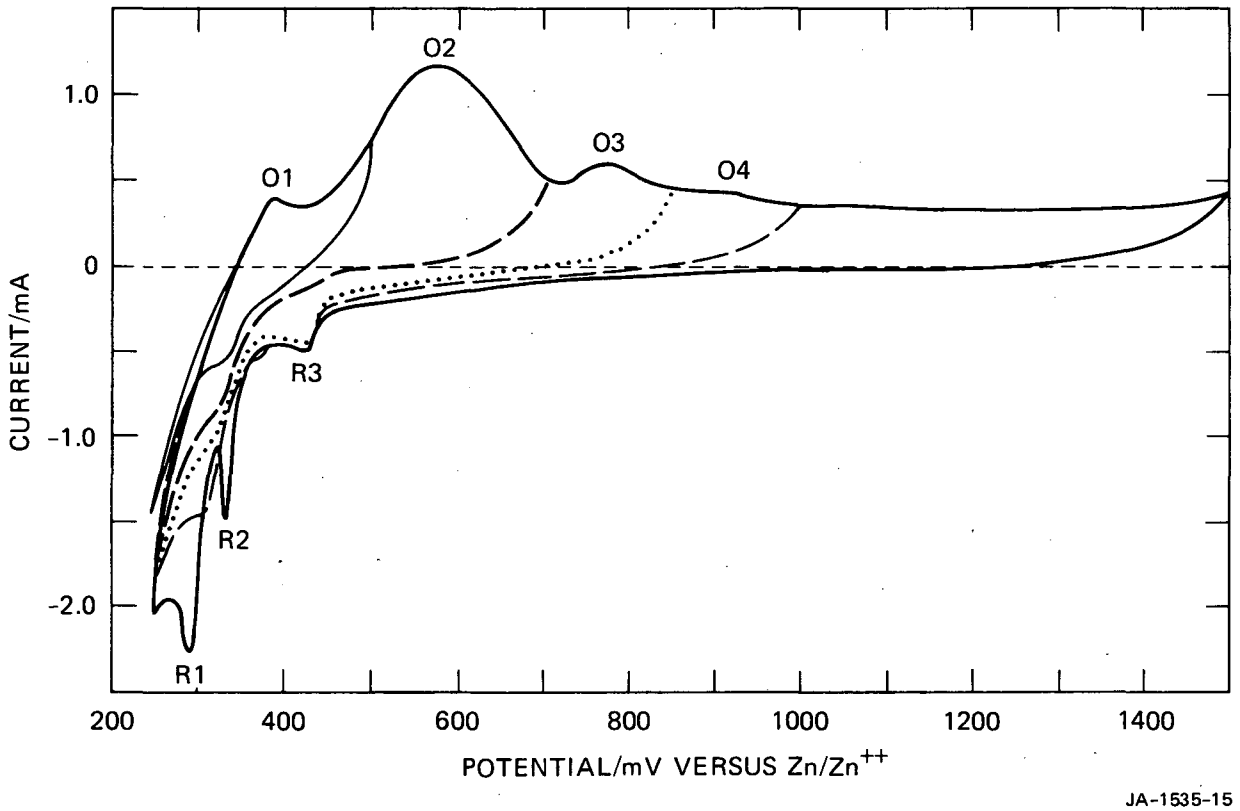

FIGURE 13 THE INFLUENCE OF ANODIC POTENTIAL LIMIT ON THE REPETITIVE SWEEP VOLTAMMOGRAM FOR AN IRON DISK ROTATED AT 10 Hz IN 30 wt % KOH AT 75°C

Potentiodynamic sweep rate = 50 mV s^{-1}.

positive anodic reversal potentials. For V_a = +1000 mV, a shoulder is visible on the cathodic potential sweep between R3 and R1, and for V_a = +1500 mV, R2 is apparent as a well-defined peak. Figure 13 also reinforces the assignment of O3 and R3 as conjugate processes. At anodic reversal potentials more negative than O3, the reduction process that gives rise to R3 is completely absent. For an anodic reversal potential more positive than O3, peak R3 is present, at effectively constant area, independent of V_a.

This latter behavior is not replicated for O1 $\rightleftarrows$ R1. The oxidation process has a constant area, independent of V_a, indicating that the oxide formed is completely reduced at V_c. The area of the reduction peak, however, increases with V_a. An analysis of the potential/charge curves (the integral of the curves in Figure 13) indicates that the majority of product formed by reduction process R2 is the reactant for reduction process R3. The above conclusions will be used in Section 3.5 in conjunction with the results of RRDE and AC impedance studies and our previous thermodynamic analysis, to make a complete identification of the charge and discharge processes for iron in concentrated alkali.

The influence of sweep rate on the potentiodynamic charge/discharge curves is shown in Figure 14 for an iron disk rotated at 10 Hz in 30 wt% KOH at 75°C and in Figure 15 at 0°C. It is immediately apparent from the poor resolution of the peaks at 0°C that kinetic factors limit the charge and discharge processes at the lower temperature. At 0°C peaks O1, O2, O3, R1, R2, and R3 are resolvable only at the lowest potentiodynamic sweep rates ($\leq$ 1 mV s^{-1}).

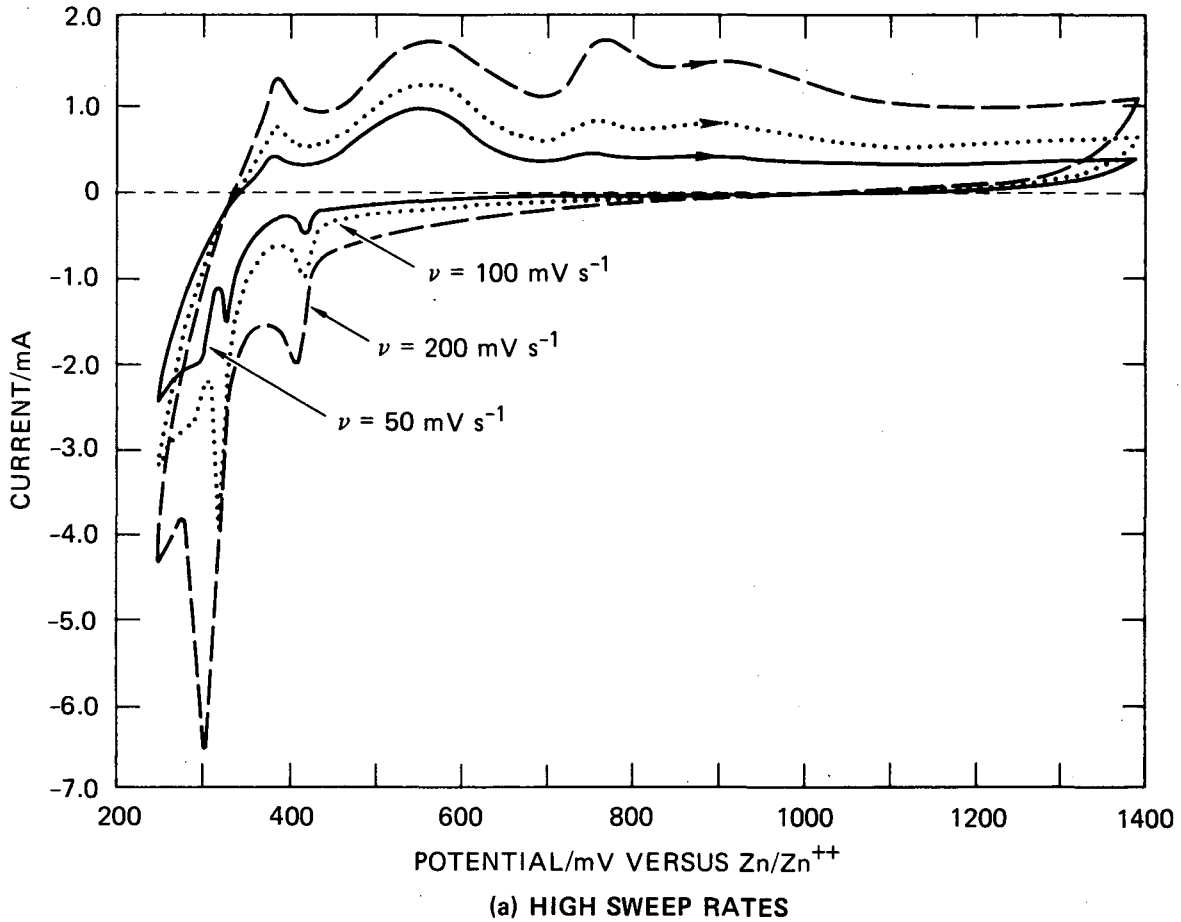

FIGURE 14 THE INFLUENCE OF SWEEP RATE ON THE POTENTIODYNAMIC CHARGE/DISCHARGE CURVES FOR AN IRON DISK ELECTRODE ROTATED AT 10 Hz IN 30 wt% KOH AT 75°C

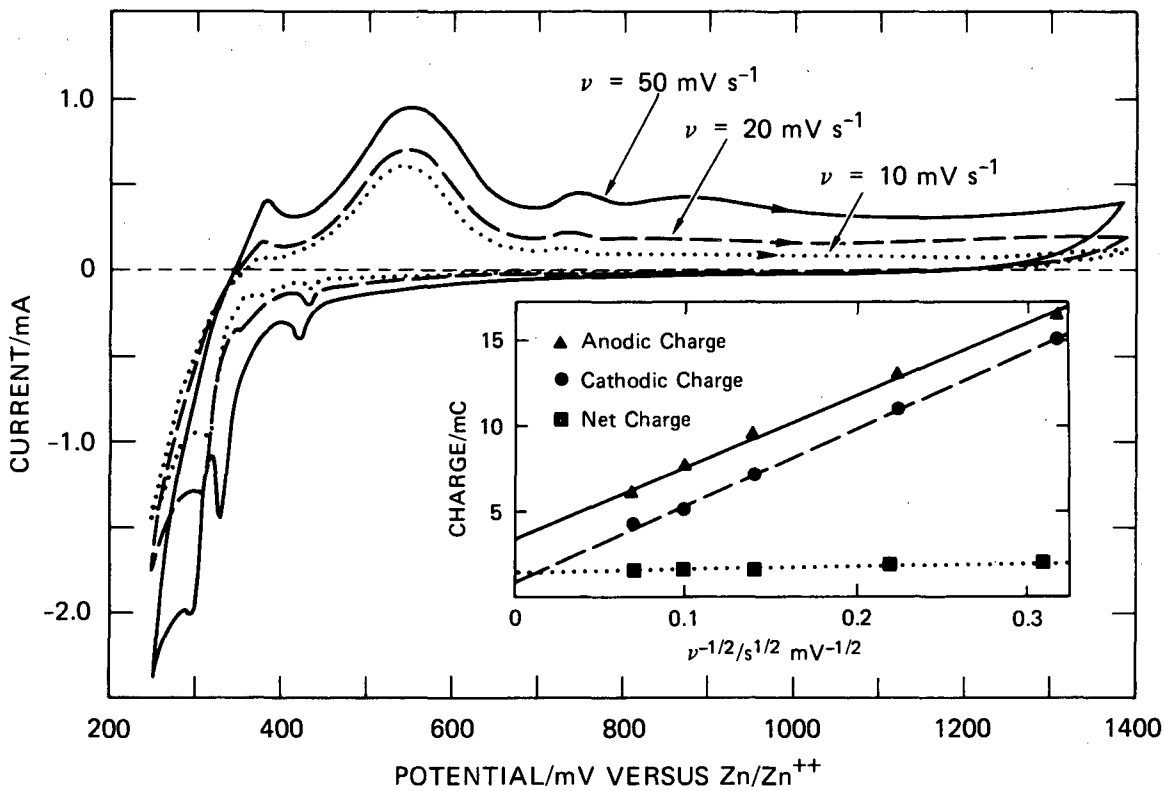

(b) LOW SWEEP RATES

JA-1535-17

FIGURE 14 THE INFLUENCE OF SWEEP RATE ON THE POTENTIODYNAMIC CHARGE/DISCHARGE CURVES FOR AN IRON DISK ELECTRODE ROTATED AT 10 Hz IN 30 wt % KOH AT 75°C (Concluded)

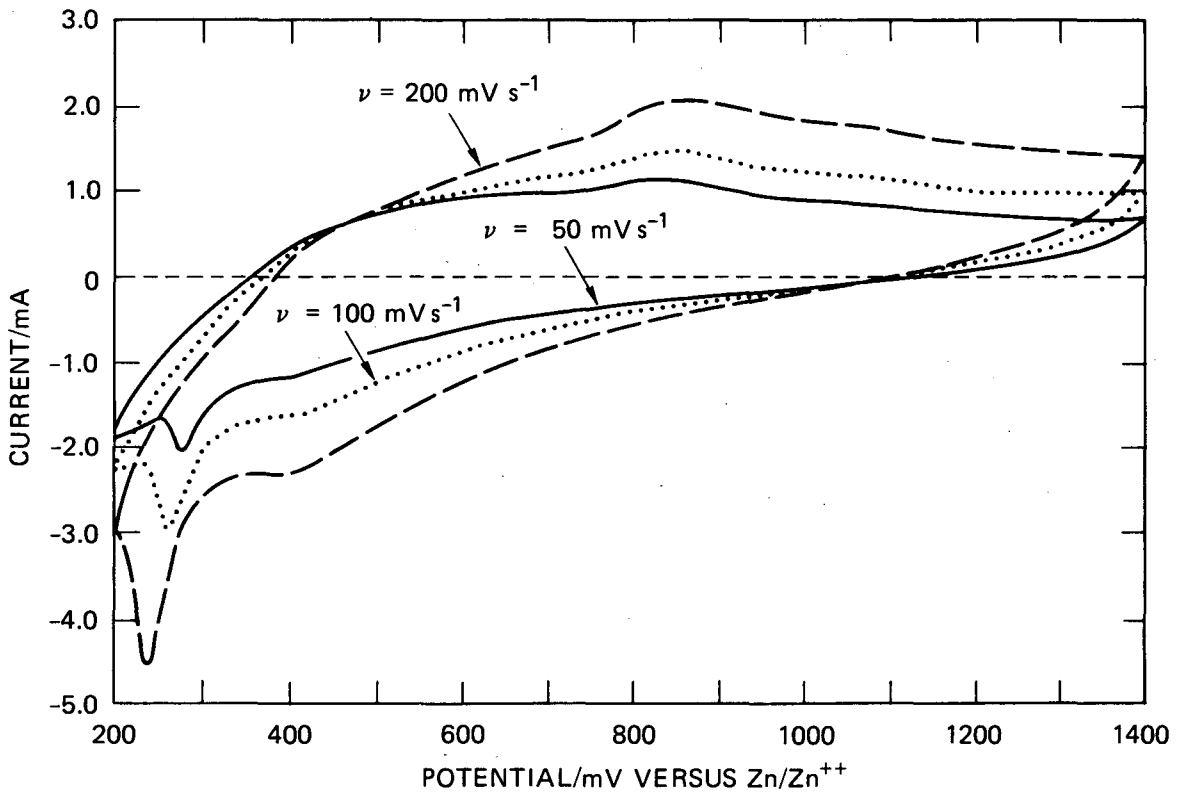

(a) HIGH SWEEP RATES

JA-1535-18

FIGURE 15 THE INFLUENCE OF SWEEP RATE ON THE POTENTIODYNAMIC CHARGE/DISCHARGE CURVES FOR AN IRON DISK ELECTRODE ROTATED AT 10 Hz IN 30 wt% KOH AT 0°C

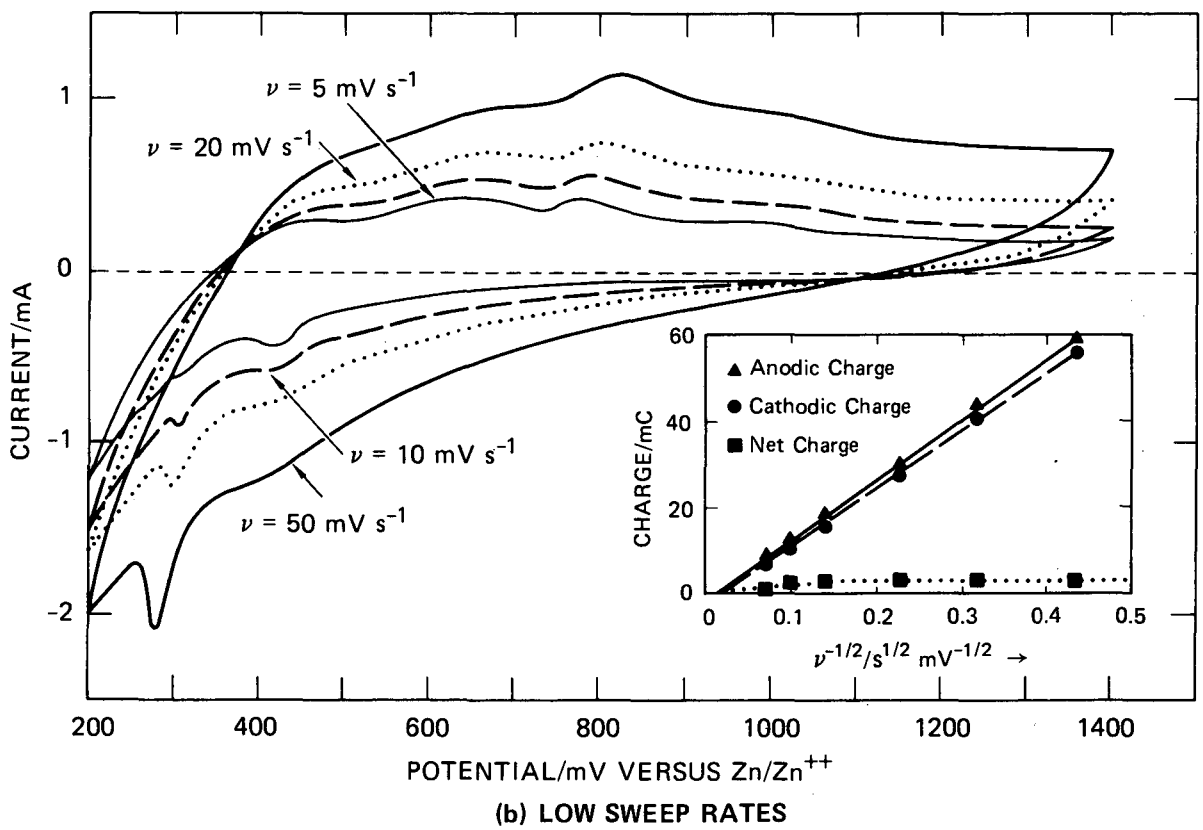

(b) LOW SWEEP RATES

JA-1535-19

FIGURE 15 THE INFLUENCE OF SWEEP RATE ON THE POTENTIODYNAMIC CHARGE/DISCHARGE CURVES FOR AN IRON DISK ELECTRODE ROTATED AT 10 Hz IN 30 wt% KOH AT 0°C (Concluded)

Inset within Figures 14 and 15 are plots of the anodic, cathodic and net (anodic) charge versus the inverse square root of the potentiodynamic sweep rate v. In the previous study a correlation versus $\nu^{-1/3}$ was used. These functional dependences are not significantly different, and either one provides a useful empirical fit against sweep rate that is linear over a wide range of ν. A theoretical interpretation of this observation currently is being considered.

The dependence of peak height and position on the potentiodynamic sweep rate in KOH is essentially identical to that observed previously[2] in NaOH electrolytes. Table 1 gives the peak height and position information for the curves presented in Figures 14 and 15. In all cases, the positions of the oxidation peaks display relatively little dependence on sweep rate, while the reduction peak positions are linearly dependent on peak height. Thus, for R2,

$$T = 0°C: \quad V_{PR2} = 318 + 17.9\ I_{PR2} \ : \ r^2 = .991 \tag{18}$$

$$T = 75°C: \quad V_{PR2} = 338 + 5.4\ I_{PR2} \ : \ r^2 = .991, \tag{19}$$

where r^2 is the regression coefficient.[22]

A linear dependence of peak position on peak height indicates the presence of a resistive surface film,[23] the values of this resistance being the slopes of equations (18) and (19). A similar analysis of potentiodynamic curves obtained at 25° and 50°C yields the results shown in Table 2.

Table 1a

PEAK HEIGHT IN MILLI-VOLTS AS A FUNCTION OF TEMPERATURE AND SWEEP RATE FOR THE POTENTIODYNAMIC CHARGE/DISCHARGE OF AN IRON DISK ROTATED AT 10 Hz IN 30 WT% KOH

ν/mV s^{-1}	T/°C	O1	O2	O3	O4	R1	R2	R3
200	75	1.29	1.74	1.79	1.51	-	-6.52	-1.95
100	75	0.77	1.28	0.88	0.80	-2.81	-3.81	-0.99
50	75	0.41	0.86	0.47	0.43	-2.02	-1.50	-0.46
20	75	0.161	0.710	0.214	0.181	-1.30	-0.359	-0.228
10	75	0.069	0.646	0.122	0.098	-	-0.162	-0.114
5	75	0.022	0.590	0.072	0.056	-	-0.089	-0.061
2	75	-	0.559	-	-	-	-0.023	-0.018
200	25	-	-	2.39	-	-	-4.60	-2.19
100	25	-	-	1.76	-	-	-3.14	-1.58
50	25	0.55	0.92	1.34	-	-	-2.27	-1.27
20	25	0.40	0.68	0.84	0.68	-	-1.32	-0.84
10	25	0.294	0.549	0.567	0.460	-	-0.84	-0.55
5	25	0.181	0.387	0.372	0.294	-	-0.515	-0.367
2	25	0.092	0.254	0.220	0.141	-	-0.382	-0.215
200	0	-	-	2.86	-	-	-4.50	-2.31
100	0	-	-	1.47	-	-	-2.96	-1.60
50	0	-	-	1.13	-	-	-2.05	-1.20
20	0	-	0.70	0.76	-	-	-1.24	-0.76
10	0	0.39	0.56	0.58	-	-	-0.87	-0.56
5	0	0.302	0.422	0.425	0.290	-	-0.600	-0.469
2	0	0.182	0.253	0.239	0.145	-	-	-0.306

Table 1b

PEAK POSITION IN MILLI-VOLTS VERSUS ZN/ZN (II) AS A FUNCTION OF TEMPERATURE AND SWEEP RATE FOR THE POTENTIODYNAMIC CHARGE/DISCHARGE OF AN IRON DISK ROTATED AT 10 Hz AT IN 30 WT5 KOH

ν/mV s^{-1}	T/°C	01	02	03	04	R1	R2	R3
200	75	387	554	768	910	-	302	408
100	75	385	551	754	++	**	319	417
50	75	379	549	743	++	291	328	422
20	75	337	546	732	++	303	349	428
10	75	376	542	722	++	-	367	433
5	75	**	536	711	++	-	380	436
2	75	-	528	-	-	-	400	438
200	25	-	-	875	-	-	288	**
100	25	-	-	851	-	-	299	**
50	25	**	**	835	-	-	307	**
20	25	++	**	825	**	-	311	416
10	25	454	676	852	**	-	316	431
5	25	446	660	841	**	-	328	443
2	25	443	622	803	++	-	340	451
200	0	-	-	863	-	-	239	**
100	0	-	-	842	-	-	265	**
50	0	-	-	829	-	-	279	**
20	0	-	673	806	-	-	297	**
10	0	**	662	791	-	-	305	420
5	0	462	625	775	999	-	315	428
2	0	444	650	784	984	-	**	438

- = Peak not observed.
++ = Plateau.
** = Shoulder.

Table 2

REGRESSION OF DATA OBTAINED FOR PEAK R2 TO THE EQUATION
$V_{PR2} = {}^{o}V_{R2} + R_{Film}\, I_{PR2}$

T/°C	$^{o}V_{R2}$/mV	R_{film}/ Ω	r^2
0	318	17.9	.991
25	326	7.8	.995
50	333	6.2	.989
75	338	5.4	.991

It is apparent that the resistance of the oxide film formed during the discharge of an iron electrode increases monotonically with decreasing temperature. This resistance partially controls the charge rate during the reduction cycle. The potential at limiting low sweep rates increases approximately linearly with increasing temperature.

The dependence of peak current on sweep rate for the oxidation processes is complicated somewhat by the thickening of the oxide film. The regression lines calculated from the data in Table 1 are as follows:

Peak 01

$$T = 0°C: \quad I_{PO1} = 0.22 + 0.118\, \nu^{1/2} \quad : \quad r^2 = .985 \tag{20}$$

$$T = 75°C: \quad I_{PO1} = 0.023 + 0.0066\, \nu \quad : \quad r^2 = .996 \tag{21}$$

Peak O2

$$T = 0°C: \quad I_{PO2} = 0.127 + 0.124\ \nu^{1/2} \quad : \quad r^2 = .983 \tag{22}$$

$$T = 75°C: \quad I_{PO2} = 0.248 + 0.104\ \nu^{1/2} \quad : \quad r^2 = .997 \tag{23}$$

Peak O3

$$T = 0°C: \quad I_{PO3} = 0.103 + 0.141\ \nu^{1/2} \quad : \quad r^2 = .996 \tag{24}$$

$$T = 75°C: \quad I_{PO3} = 0.026 + 0.026\ \nu \quad : \quad r^2 = .9998 \quad . \tag{25}$$

A well-behaved $\nu^{1/2}$ dependence is observed for the principal discharge process, O2. Such a dependence has been interpreted previously[2,23,26] in terms of the pore resistance model, in which the potentiodynamic peak current is determined by the resistance of the electrolyte in pores at the growing oxide film. This model predicts the following functional dependence for I_p and V_p.

$$I_p = (nF\rho\kappa/M)^{1/2}\ A_o(1 - \theta_p)^{1/2}\nu \tag{26}$$

$$V_p = (nF\rho\kappa/M)^{1/2}\ (\ell/\kappa) + R_oA_o(1 - \theta_p)^{1/2}\nu \tag{27}$$

where θ_p is the fractional surface coverage at the peak

ρ is the density of the deposited phase

κ is the specific conductance of the solution

ℓ is the thickness of the film

A_o is the effective surface area

R_o is the uncompensated electrolyte resistance.

The pore resistance model appears to describe oxidation peak O2 adequately at all temperatures, and peaks O1 and O3 at 0°C. However, the form of equations (26) and (27) conveys relatively little information regarding the nature of the oxide film. A more detailed discussion is presented in Reference 2.

At high temperatures, the form of the peak-current dependence for processes O1 and O3 changes from $\nu^{1/2}$ to ν. The significance of this change is not understood.

3.3 RRDE Collection Efficiency Calibration

The radius ratios of the rotating vitreous carbon ring and iron disk electrode (see Figure 8) exceeds those tabulated by Albery et al.[25] and by Pleskov et al.[26] However, the theoretical collection efficiency, N, can be evaluated from the equation[25]

$$N = 1 - f(\alpha/\beta) + \beta^{2/3}[1 - f(\alpha)] - (1 + \alpha + \beta)^{2/3}\{1 - f[(\alpha/\beta)(1 + \alpha + \beta)]\} \quad (28)$$

where

$$\alpha = (r_2/r_1)^3 - 1 \quad (29)$$

$$\beta = (r_3/r_1)^3 - (r_2/r_1)^3$$

and

$$f(\theta) = \frac{3^{1/2}}{4\pi} \ln[\frac{(1 + \theta^{1/3})^3}{1 + \theta}] + \frac{3}{2\pi} \tan^{-1} [\frac{2\theta^{1/3} - 1}{3^{1/2}}] + \frac{1}{4} \quad . \quad (30)$$

Equations (28) to (30) are evaluated using the basic program in Appendix II to yield values of N.

The iron RRDE was calibrated experimentally by using a solution of 0.1 M $K_3Fe(CN)_6$ in 1.0 M KOH supporting electrolyte. The results of this calibration at 25°C and at a rotation speed of 10 Hz are presented in Table 3.

Table 3

IRON RRDE CALIBRATION RESULTS IN 0.1 M $K_3Fe(CN)_6$
WITH T = 25°C AND ω = 10.0 Hz

Disk Potential =	1000 MV	800 MV	700 MV	650 MV	600 MV	550 MV	500 MV
V_{ring} = 1200 mV							
I_{disk}/mA	0.03	0.17	0.71	1.52	2.92	4.79	6.77
I_{ring}/mA	0.46	0.49	0.71	1.04	1.63	2.40	3.21
V_{ring} = 1400 mV							
I_{disk}/mA	0.03	0.16	0.63	1.39	2.73	4.66	6.68
I_{ring}/mA	1.03	1.04	1.21	1.54	2.10	2.92	3.78
V_{ring} = 1500 mV							
I_{disk}/mA	0.03	0.17	0.68	1.52	2.91	4.72	6.69
I_{ring}/mA	1.68	1.67	1.84	2.18	2.74	3.50	4.29

The value of N can be determined from the regression of I_{ring} versus I_{disk}:

$$V_{ring} = 1200 \text{ mV}: I_{ring} = 0.4183 + 0.4129\, I_{disk} \quad : \quad r^2 = 1.0000 \qquad (31)$$

$$V_{ring} = 1400 \text{ mV}: I_{ring} = 0.9553 + 0.4220\, I_{disk} \quad : \quad r^2 = 0.9999 \qquad (32)$$

$$V_{ring} = 1500 \text{ mV}: I_{ring} = 1.5756 + 0.4054\, I_{disk} \quad : \quad r^2 = 0.9998 \quad . \qquad (33)$$

Therefore, over the range of ring potentials indicated, N = 43.3 ± 0.8%. The value of N calculated from equation (28) with r_1 = 0.76,

r_2 = 0.51 and r_3 = 0.32 ± 0.01 cm is N = 41.4% This conformity between experiment and theory provides a good indication that the RRDE is functioning ideally. The experimentally determined value of N = 41.3% will be used in all subsequent discussion.

3.4 RRDE Studies of Iron

As discussed previously for NaOH electrolytes,[2] the dissolution of iron and iron oxide in KOH occurs by several distinguishably different mechanisms within defined regions of electrode potential.

Figure 16 shows the results of RRDE measurements of Fe in 30 wt% KOH at 75°C, with a potentiodynamic sweep of the disk, as a function of ring potential. The various dissolution processes can be seen in Figure 16(a) as oxidative peaks in the ring current at large positive ring potentials and/or as reductive ring current peaks at low ring potentials. This experiment can be used to determine the oxidation number of the dissolved ionic species; with the ring held at +1400 mV, we expect to oxidize any Fe(II) dissolved species to Fe(III). As shown in Figure 16(b), for V_{ring} > 600 mV there are three ring oxidation current peaks and no reduction peaks. Peaks DO1 and DO2 are observed to be associated, respectively, with O1 and O2 on the potentiodynamic discharge cycle, and DO3 is observed to be associated with disk peak R2 during charge.

A ring potential of +400 mV is sufficient to reduce Fe(III) to Fe(II), but not to reduce Fe(II) to Fe(0). Two such reduction processes are shown in Figure 16(b). Dissolution peak DR2 occurs in conjunction with disk oxidation peak O2, and an additional dissolution peak, DR3, is seen at large disk potentials corresponding roughly to the disk peak labeled O4 in Figure 16(a).

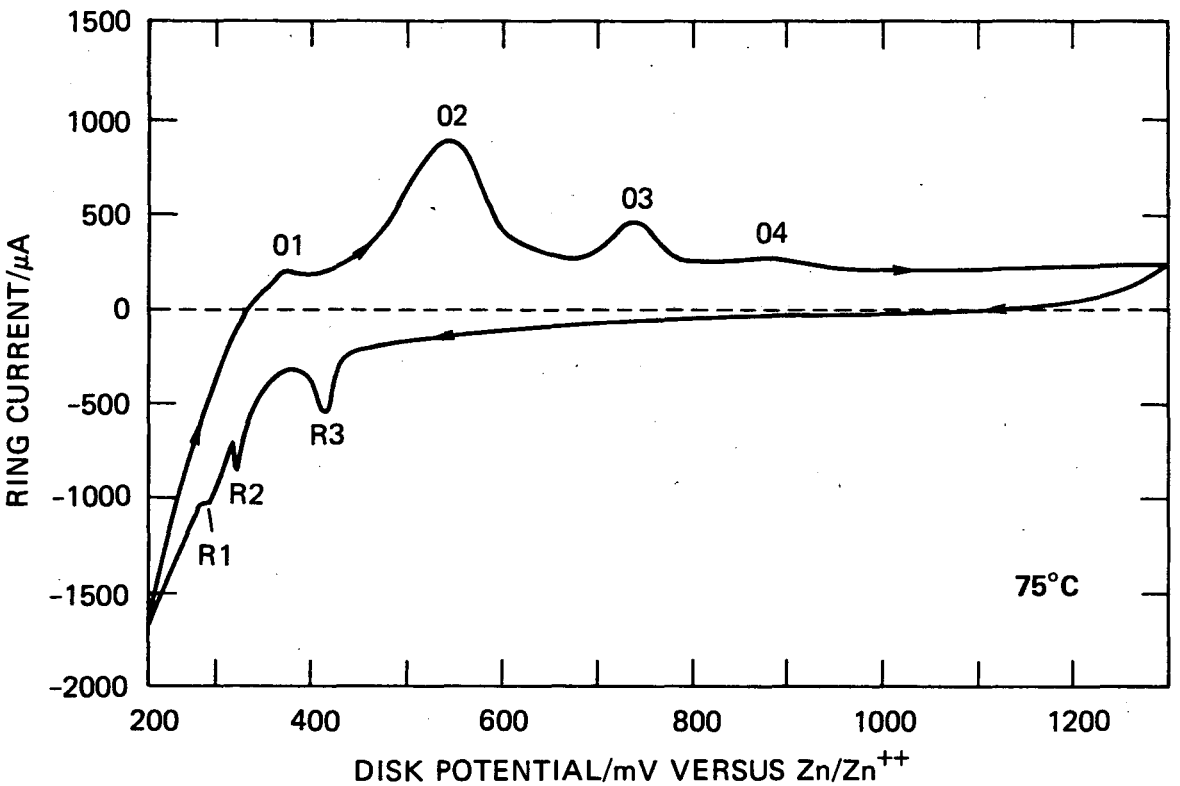

(a) DISK CURRENT VERSUS DISK POTENTIAL

JA-1535-20

FIGURE 16 RRDE MEASUREMENTS OF IRON IN 30 wt% KOH AT 75°C
Disk potentiodynamic sweep rate = 50 mV s^{-1}.

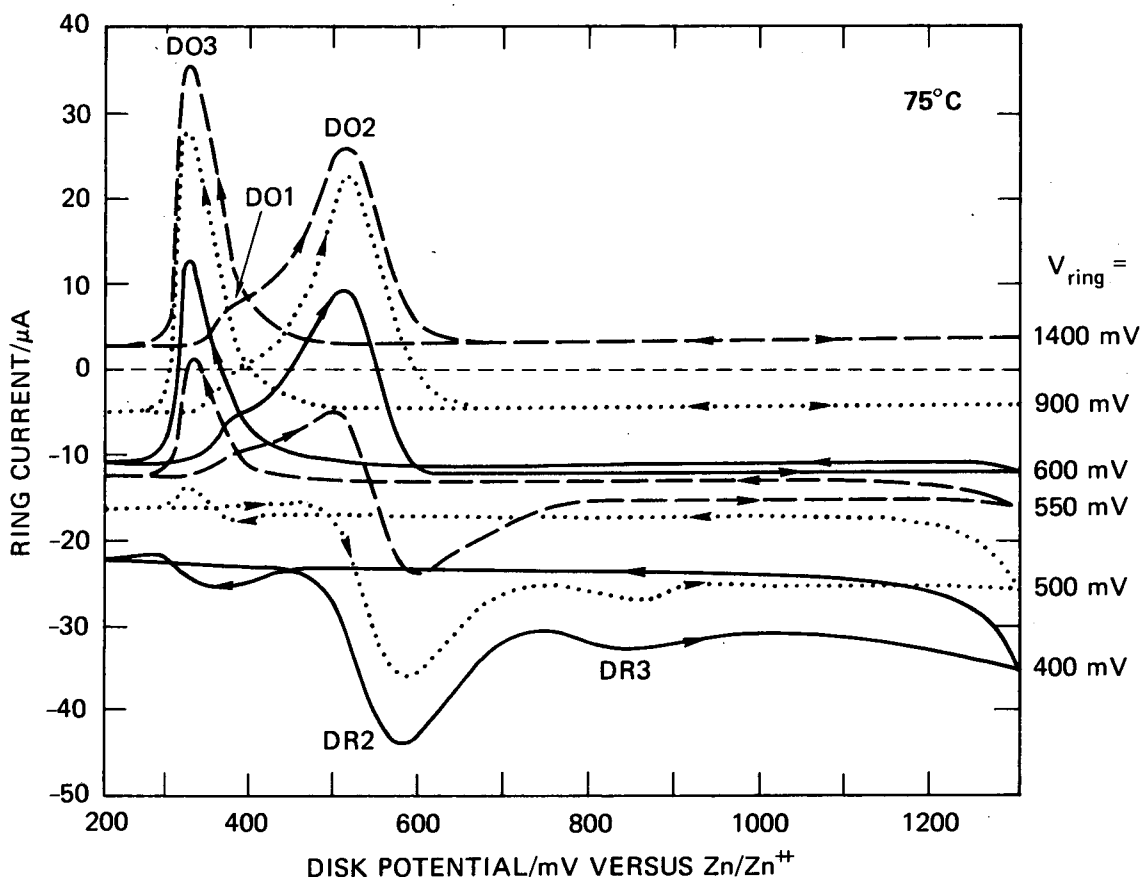

(b) RING CURRENT VERSUS DISK POTENTIAL

JA-1535-21

FIGURE 16 RRDE MEASUREMENTS OF IRON IN 30 wt% KOH AT 75°C (Concluded)
Disk potentiodynamic sweep rate = 50 mV s^{-1}.

At ring potentials more negative than 300 mV (not shown in Figure 16), peak DR2 increases in amplitude, and a dissolution-reduction peak designated as DR1 appears as a complement to DO3. Both processes involve the reduction of Fe(II) to Fe(0) at the ring. These collection processes cannot be quantified because of competition from hydrogen ion reduction at the vitreous carbon ring.

At intermediate ring potentials ($500 < V_{ring} < 600$ mV), reduction and oxidation peaks are observed simultaneously in conjunction with disk oxidation peak O2. Peak O2 already has been observed to be complex,[2] and at very low potentiodynamic discharge rates this peak splits into a roughly symmetric doublet. It is clear, therefore, that O2 conceals two separate oxidation processes. The process occurring at lower potentials involves a dissolved Fe(II) species, presumably as a reaction intermediate in the growth of the oxide film. The higher-potential process yields an Fe(III) ion, the dissolution of which apparently is terminated by disk oxidation process O3.

Table 4 gives peak areas for disk currents and for ring currents at various ring potentials, taken from the potentiodynamic data in Figure 16.

These data indicate that, at 75°C, an appreciable fraction of each of the principal charge and discharge processes involves the formation of soluble ionic species. This is a matter of some concern in battery technology since a dissolved ion may not be fully recovered when the current is reversed, thus resulting in coulombic inefficiency. More importantly, Fe(II) ions will oxidize at the positive electrode, resulting in a chemical "short circuit," and may poison that electrode. Also, continued dissolution of iron may result in shape change.

Table 4

PEAK AREAS MEASURED FROM THE POTENTIODYNAMIC DATA PRESENTED IN FIGURE 16
(μC)

Disk Peak	O1	O2	O3	O4	R2	R3
	821	6605	2380	2011	1174	433
Ring Peak	**DO1**	**DO2**	**DO3**	**DR1**	**DR2**	**DR3**
V_{ring} = +1400 mV	18	144	111	0	0	0
V_{ring} = +600 mV	17	144	77	0	0	0
V_{ring} = +550 mV	11	37	38	0	94	67
V_{ring} = +400 mV	0	0	0	0	194	124

From the data in Table 4 we can calculate the percentage of the disk redox process that results in a soluble species as

$$PD = \frac{100\ Q_r\ n_d}{N\ \ Q_d\ n_r} \tag{34}$$

where Q_r and Q_d are the ring and disk peak areas

n_r and n_d are the number of electrons involved in the redox process

N is the RRDE collection efficiency = 0.413.

In each case n_r = 1, and n_d depends on the assignment of the disk peaks.

Figures 17 and 18 show the results of RRDE experiments at 50°C and 25°C. The peak areas measured from the potentiodynamic data at temperatures from 0° to 75°C are summarized in Table 6.

Figures 16 to 18 indicate qualitatively, and Table 6 shows quantitatively, that there is a progressive change in charge and dissolution processes as temperature is increased. Thus, at low temperatures O3

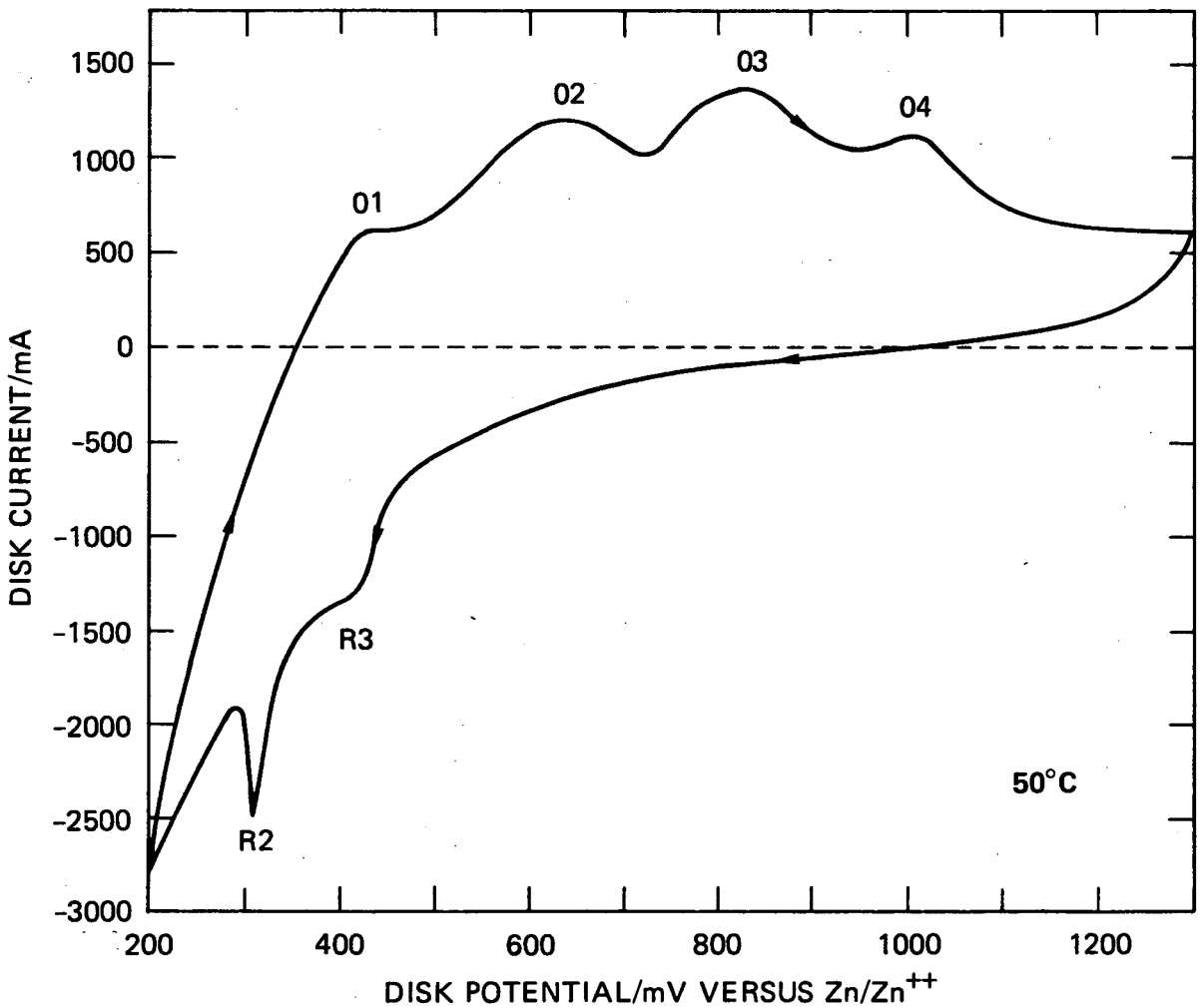

(a) DISK CURRENT VERSUS DISK POTENTIAL

JA-1535-22

FIGURE 17 RRDE MEASUREMENTS OF IRON IN 30 wt% KOH AT 50°C

Potentiodynamic sweep rate = 50 mV s^{-1}.

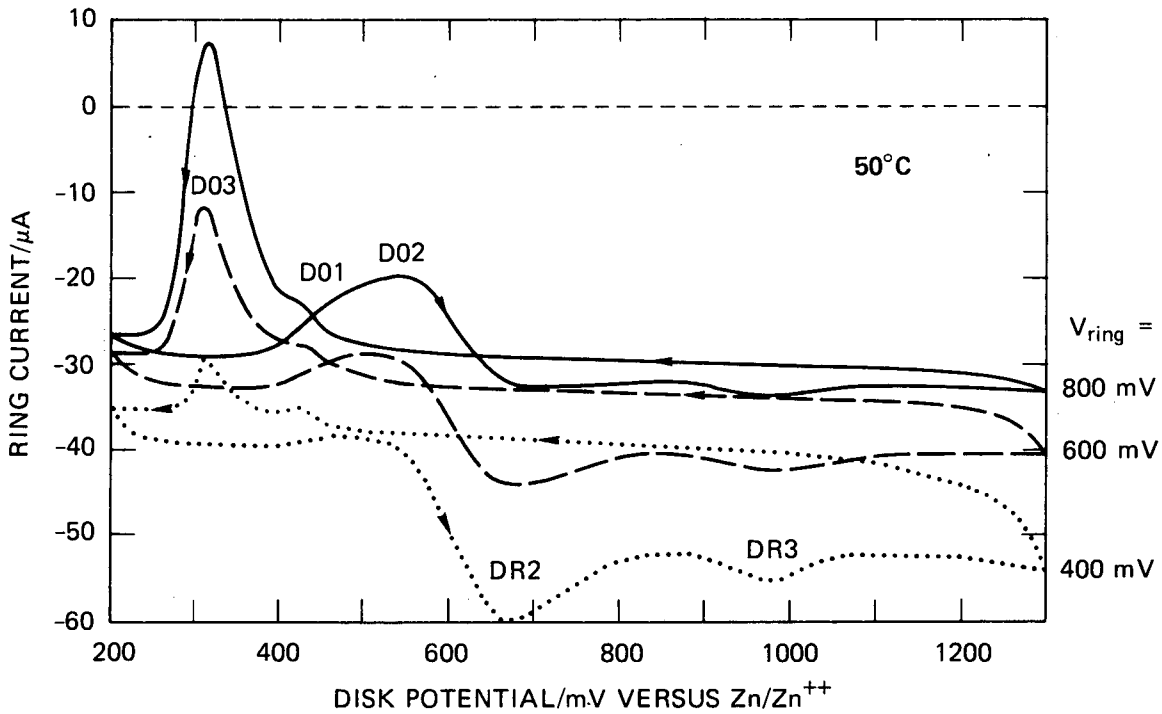

(b) RING CURRENT VERSUS DISK POTENTIAL

JA-1535-23

FIGURE 17 RRDE MEASUREMENTS OF IRON IN 30 wt% KOH AT 50°C (Concluded)
Potentiodynamic sweep rate = 50 mV s^{-1}.

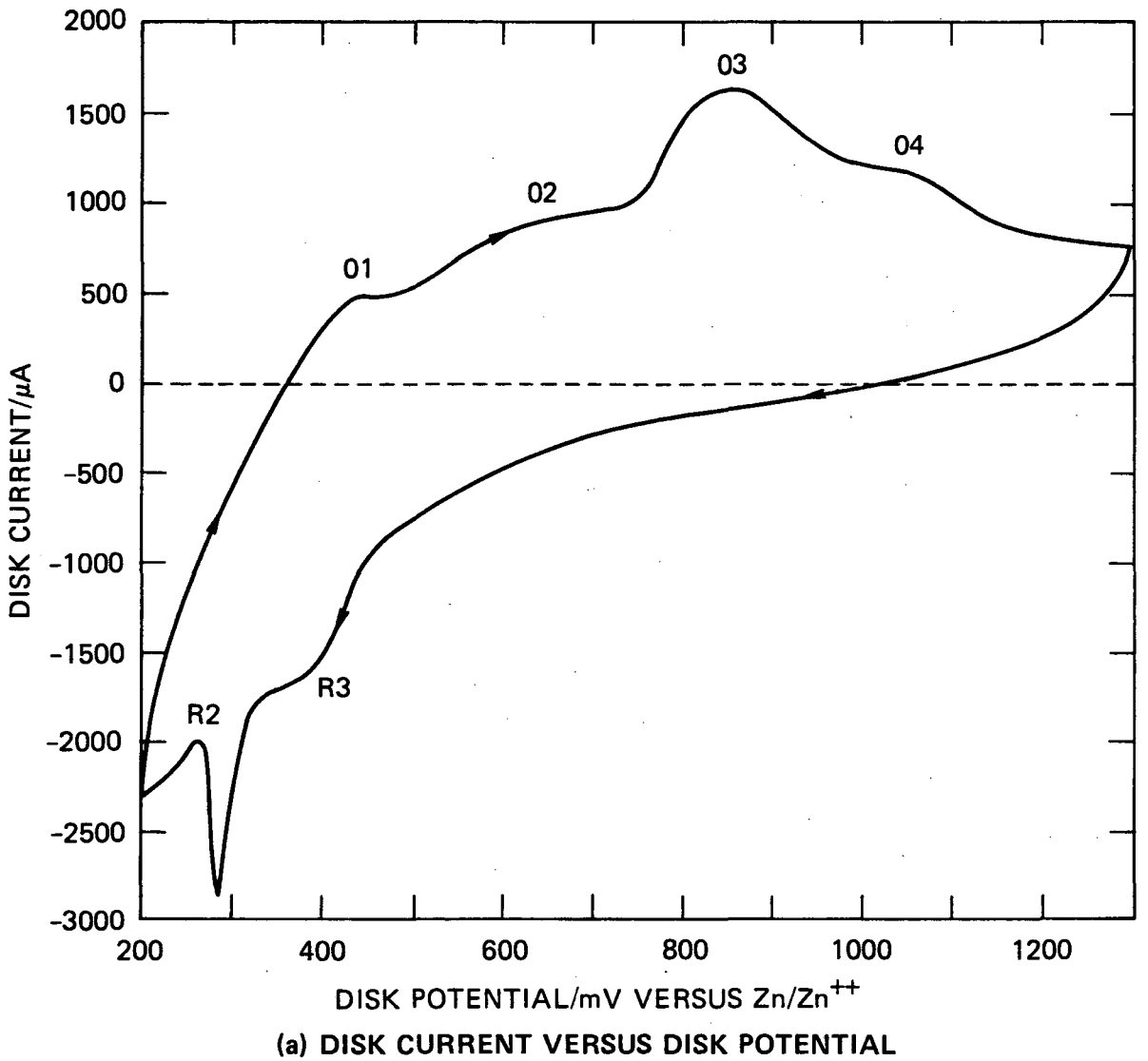

(a) DISK CURRENT VERSUS DISK POTENTIAL

JA-1535-24

FIGURE 18 RRDE MEASUREMENTS OF IRON IN 30 wt% KOH AT 25°C
Potentiodynamic sweep rate = 50 mV s^{-1}.

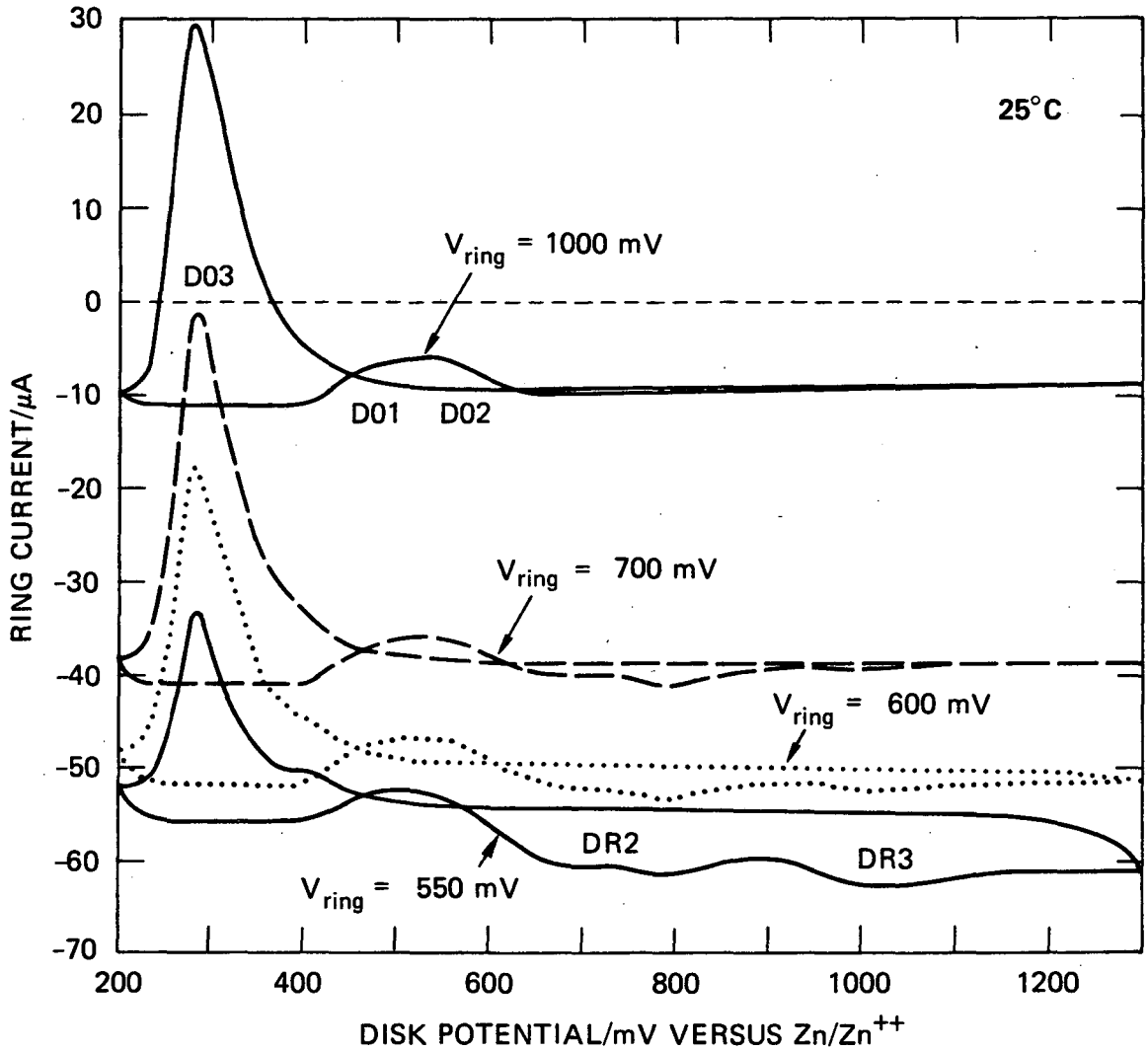

(b) RING CURRENT VERSUS DISK POTENTIAL

JA-1535-25

FIGURE 18 RRDE MEASUREMENTS OF IRON IN 30 wt% KOH AT 25°C (Continued)
Potentiodynamic sweep rate = 50 mV s^{-1}

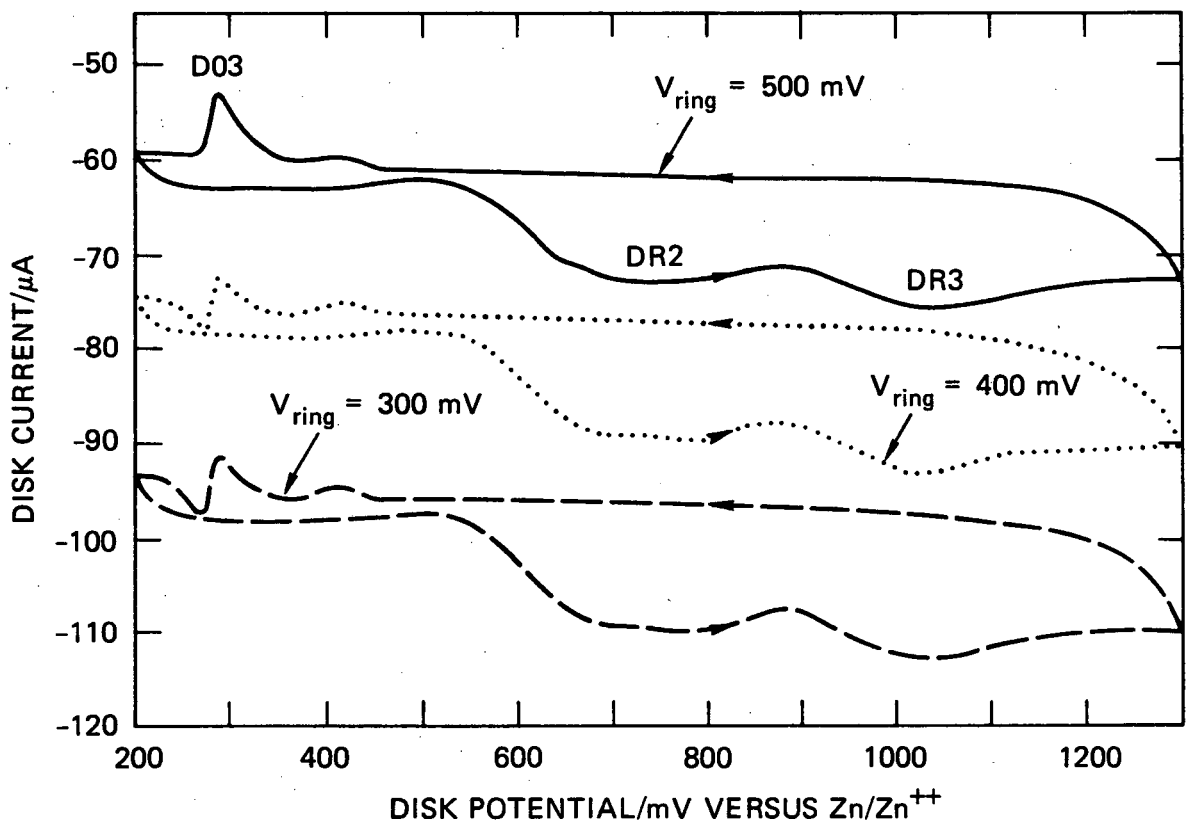

(c) RING CURRENT VERSUS DISK POTENTIAL

JA-1535-26

FIGURE 18 RRDE MEASUREMENTS OF IRON IN 30 wt% KOH AT 25°C (Concluded)
Potentiodynamic sweep rate = 50 mV s^{-1}

Table 5

PERCENT DISSOLUTION TAKEN FROM DATA IN TABLE 4

Dissolution Peak	Dissolved Species	Associated Disk Peak	Dissolution Percentage
DO1	Fe(II)	O1	5.3 n_d
DO2	Fe(II)	O2	5.3 n_d
DO3	Fe(II)	R2	22.9 n_d
DR1	Fe(II)	O1	-
DR2	Fe(III)	O2	7.1 n_d
DR3	Fe(III)	O4	14.9 n_d

constitutes the principal discharge process, while at elevated temperatures peak O2 dominates discharge. Disk peaks O1 and O4 both show a monotonic decrease in area with decreasing temperature. In contrast, the disk charge peak areas show essentially no dependence on temperature.

The extent of dissolution as a percentage of the disk process is presented in Table 7 for all temperatures studied.

Presented in this way the extent of dissolution is seen generally to decline with decreasing temperature until, at 0°C, only DO3 is observed at the ring. Two exceptions are the apparent lack of dependence of DO1/O1 on temperature, and the decrease of DR3/O4 at temperatures above ambient. This latter process, however, occurs at potentials sufficiently positive to be of no interest in battery studies.

It should be noted that the figures presented in Tables 4 to 7 reflect only the extent to which the features of the potentiodynamic charge/discharge curves that can be resolved into separate peaks result in a dissolved product. However, not all of the charge or discharge

Table 6

PEAK AREAS MEASURED FROM THE POTENTIODYNAMIC SWEEP DATA AT 0°, 25°, 50°, AND 75°C
(μC)

T/°C	Disk Peak:	01	02	03	04	R2	R3
75		821	6605	2380	2011	1176	433
50		470	4460	2250	1000	1180	440
25		280	2160	3250	910	1190	410
0		---	1230	4450	---	440	410

T/°C	Ring Peak:	DO1	DO2	DO3	DR1	DR2	DR3
	V_{ring}/mV						
75	1400	18	144	111	0	0	0
75	600	17	144	77	0	0	0
75	550	11	37	38	0	94	67
75	400	0	0	0	0	194	124
50	800	11	19	51	0	0	0
50	600	4	6	21	0	54	41
50	400	0	0	5	0	96	74
25	1000	6	8	66	0	0	0
25	700	7	9	61	0	0	0
25	600	8	9	50	0	0	0
25	550	4	5	26	0	35	37
25	500	0	0	5	0	46	78
25	400	0	0	2	0	54	78
25	300	0	0	0	0	56	81
0	1000	-	-	7	-	-	-

Table 7

PERCENT OF DISK DISSOLUTION

	0°C	25°C	50°C	75°C
D01/01	*	5.2	5.7	5.3
D02/01	*	0.9	1.0	5.3
DR2/02	*	6.3	5.2	7.1
(D02 + DR2)/02	*	7.4	6.2	12.3
D03/R2	3.9	13.4	10.5	22.9
DR3/04	*	21.6	17.9	14.9

*Insufficient precision in peak area determinations.

processes result in a potentiodynamic peak. For example, the principal charge process (the converse of 02) has no associated peak. Thus, the decrease in total coulombic efficiency resulting from metal dissolution is somewhat less than would be indicated by the data in Table 7. The total dissolution relative to the total anodic and cathodic disk charges is as follows:

T/°C	Oxidative Dissolution	Reductive Dissolution
75	5.98%	1.56%
50	2.55%	0.29%
25	3.16%	0.08%
0	0%	0.08%

3.5 AC Impedance Studies of Iron

The impedance locus plots in Figure 19 show the effects of temperature and applied DC potential on the measured AC response of an iron RDE in 30% KOH, at a constant rotation speed of 10 Hz.

The growth of an oxide film can be seen qualitatively in the influence of applied DC bias on the measured impedance dispersion [Figure 19(a)]. Close to the potential of zero current (+250 mV), the impedance response displays the expected Randles form for a smooth, plane-parallel, unfilmed electrode [Figure 11(a)]. That is, at high frequencies the impedance locus has the form of a semicircle with center on the real axis, which is attributable to the parallel combination of the double-layer capacitance and the interfacial reaction resistance.[8] At low frequencies the impedance locus is attributable to diffusion across a stratified Nernst diffusion layer within the electrolyte.[8] At larger applied DC potentials, a large series impedance becomes evident, which is associated with the surface iron oxide film. This series oxide impedance corresponds roughly to the parallel combination of a bulk geometric capacitance, the resistance due to the passage of electrons (or holes) in the oxide phase, and an impedance associated with the diffusion of oxygen and/or metal ions in the oxide phase and hydroxyl ions in the liquid phase. A complete quantitative analysis of these data, and of the results of a number of additional experiments, currently is being prepared and will be included in the next annual report. Qualitatively, the resistance of the oxide film increases monotonically with increasing potential.

The data in Figure 19(b) can be analyzed to determine the influence of temperature on the double-layer capacitance, and exchange-current density i_o, for the iron electrode in the vicinity of the [$Fe \rightleftarrows Fe(OH)_2$] peak (peak O1). These parameters have been obtained by fitting the impedances measured at high frequency to an RC series/parallel equivalent current using the regression program that is included as Appendix III.

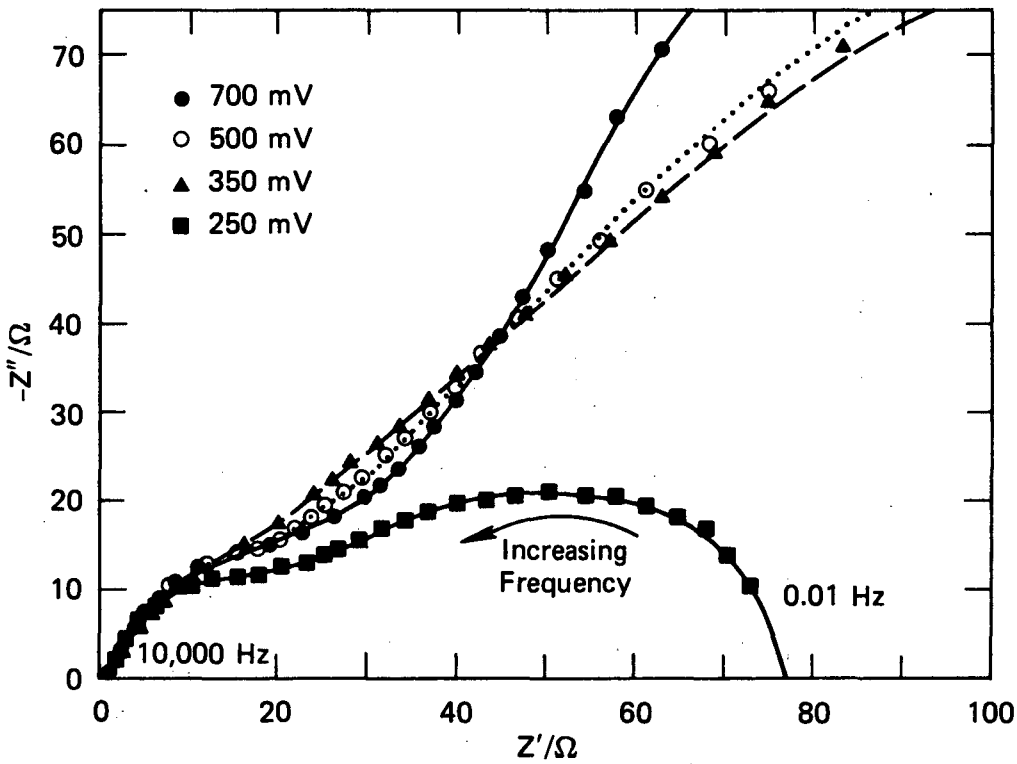

(a) INFLUENCE OF APPLIED DC POTENTIAL AT 25°C

JA-1535-27

FIGURE 19 AC IMPEDANCE RESPONSE OF AN IRON ROTATING DISK ELECTRODE IN 30 wt% KOH WITH A ROTATION SPEED OF 10 Hz

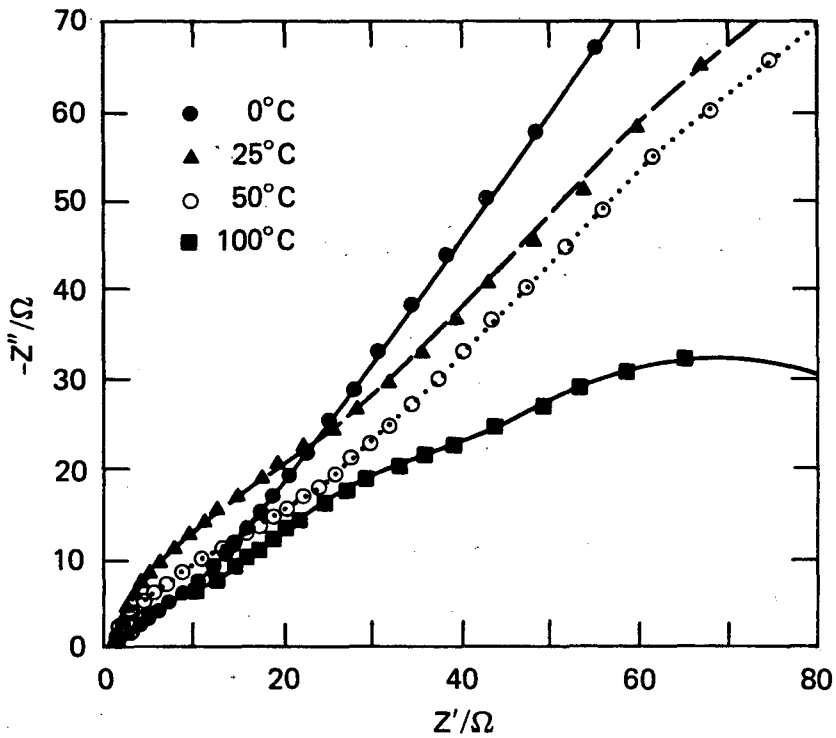

(b) INFLUENCE OF TEMPERATURE AT +350 mV

JA-1535-28

FIGURE 19 AC IMPEDANCE RESPONSE OF AN IRON ROTATING DISK ELECTRODE IN 30 wt% KOH WITH A ROTATION SPEED OF 10 Hz (Concluded)

The results of this regression analysis for the data in Figure 19(b) are presented in Table 8. The values of the, i_o were calculated using equation (12).

It is apparent from the tabulated values of i_o that the kinetic constraints for the $Fe \rightleftarrows Fe(OH)_2$ charge/discharge process are reduced with increasing temperature. However, the principal kinetic limitations of charge and discharge originate within the oxide film, not with the interfacial reaction process.

The values tabulated for C display a maximum at 80°C but are relatively independent of temperature.

Table 8

ELECTROCHEMICAL PARAMETERS CALCULATED FROM THE IMPEDANCE DISPERSION MEASURED FOR AN IRON RDE HELD AT +350 mV in 30 wt% KOH, AT A ROTATION SPEED OF 10 Hz

T/°C	RS/Ω cm^{-2}	RR/Ω cm^{-2}	C/μF cm^{-2}	i_o mA cm^{-2}
0	0.71	3.12	77.4	3.76
25	0.39	2.44	80.8	5.25
50	0.26	2.32	90.1	6.00
75	0.23	1.87	89.2	8.03
100	0.19	1.61	88.0	9.98

3.6 Mechanisms of the Charge/Discharge Reactions of Iron

The equilibrium potentials for all pertinent iron and iron oxide redox processes are presented in Table 9. The tabulated data summarize the results of our thermodynamic calculations for iron in 8 molal (corresponding to 31 wt%) NaOH.

Table 9

CALCULATED EQUILIBRIUM POTENTIALS FOR IRON AND IRON OXIDE REDOX PROCESSES IN 8 MOLAL NaOH

Reaction	Number of e^-	Equilibrium Potential/mV versus Zn/Zn^{++}					
		0°C	20°C	40°C	60°C	80°C	100°C
Metal ⇄ Soluble Ion							
$Fe/HFeO_2^-$	+2	491	488	484	479	474	462
$Fe/FeO_2^=$	+2	429	456	472	493	514	560
$Fe/Fe)OH)_4^-$	+3	547	532	517	549	473	429
Metal Oxide ⇄ Soluble Ion							
$FeOH_2/Fe(OH)_4^-$	+1	690	633	575	507	439	325
$Fe_3O_4/HFeO_2^-$	-2/3	453	480	512	517	524	495
$Fe_3O/FeO_2^=$	-2/3	612	575	546	474	403	200
$Fe_3O_4/Fe(OH)_4^-$	+1/3	1072	905	733	551	368	97
$Fe_2O_3/HFeO_2^-$	-1	1522	1526	1529	1531	1533	1528
$Fe_2O_3/FeO_2^=$	-1	667	645	629	582	536	399
$FeOOH/HFeO_2^-$	-1	558	581	607	615	623	609
$FeOOH/FeO_2^=$	-1	633	644	630	586	542	412
$Fe(OH)_3/HFeO_2^-$	-1	694	726	760	777	796	804
$Fe(OH)_3/FeO_2^=$	-1	800	789	783	748	717	606
Soluble Ion ⇄ Soluble Ion							
$HFeO_2^-/Fe(OH)_4^-$	+1	660	622	585	728	472	362
$FeO_2^=/FE(OH)_4^-$	+1	765	685	609	600	392	165
Metal ⇄ Metal Oxide							
$Fe/Fe(OH)_2$	+2	476	482	489	489	464	481
Fe/Fe_3O_4	+8/3	482	485	490	488	457	470
Metal Oxide ⇄ Metal Oxide							
$Fe(OH)_2/Fe_3O_4$	+2/3	499	496	495	484	436	439
$Fe(OH)_2/Fe(OH)_3$	+1	724	736	749	755	742	765
$Fe(OH)_2/FeOOH$	+1	588	592	596	593	560	572
$Fe(OH)_2/Fe_2O_3$	+1/3	777	786	795	797	776	795

Iron in 8 molal (corresponding to 31 wt%) NaOH.

Table 9 Concluded

Reaction	Number of e^-	Equilibrium potential/mV versus Zn/Zn^{++}					
		0°C	20°C	40°C	60°C	80°C	100°C
Metal ⇄ Soluble Ion							
$Fe/HFeO_2^-$	+2	491	188	486	479	474	462
$Fe/FeO_2^=$	+2	439	456	472	493	514	560
$Fe/Fe(OH)_4^-$	+3	547	532	517	495	473	429
Metal Oxide ⇄ Soluble Ion							
$FeOH_2/Fe(OH)_4$	+1	690	633	575	507	439	325
$Fe_3O_4/HFeO_2^-$	-2/3	453	480	512	517	524	495
$Fe_3O_4/FeO_2^=$	-2/3	612	575	546	474	403	200
$Fe_3O_4/Fe(OH)_4^-$	+1/3	1072	905	733	551	368	97
$Fe_2O_3/HFeO_2^-$	-1	1522	1526	1529	1531	1533	1528
$Fe_2O_3/FeO_2^=$	-1	667	645	629	582	536	399
$FeOOH/HFeO_2^-$	-1	558	581	607	615	623	609
$FeOOH/FeO_2^=$	-1	663	644	630	586	542	412
$Fe(OH)_3/HFeO_2^-$	-1	694	726	760	777	796	804
$Fe(OH)_3/FeO_2^=$	-1	800	789	783	748	717	606
Soluble Ion ⇄ Soluble Ion							
$HFeO_2^-/Fe(OH)_4^-$	+1	660	622	585	728	472	362
$FeO_2^=/Fe(OH)_4^-$	+1	705	685	609	500	392	156
Metal ⇄ Metal Oxide							
$Fe/Fe(OH)_2/$	2	476	482	489	489	464	481
Fe/Fe_3O_4	+8/3	482	485	490	488	457	470
Metal Oxide ⇄ Metal Oxide							
$Fe(OH)_2/Fe_3O_4$	+2/3	499	496	495	484	436	439
$Fe(OH)_2/Fe()H)_3$	+1	724	736	749	755	742	765
$Fe(OH)_2/FeOOH$	+1	588	592	596	593	560	572
$Fe(OH)_2Fe_2O_3$	+1	591	593	595	589	549	558
$Fe_3O_4/FeOOH$	+1/3	766	782	799	810	807	836
Fe_3O_4/Fe_2O_3	+1/3	777	786	795	797	776	795

It should be stressed that the calculations were made for NaOH, while the experiments performed in this study were conducted in KOH. Nevertheless, the cation effect is expected to be sufficiently small that the data in Table 9 reflect the trends of the thermodynamic parameters.

The reaction sequences shown in Figure 20 summarize the data in Table 9; these may be used in conjunction with the potentiodynamic sweep and RRDE results in an attempt to explain the charge, discharge, and dissolution mechanisms of iron in concentrated hydroxide.

Figure 20(a) shows the thermodynamically favored reaction paths at low temperatures ($\lesssim$ 25°C); Figure 20(b) shows the high-temperature ($\gtrsim$ 50°C) mechanisms. In each case the numbers in boxes adjacent to the reversible arrows indicate the calculated equilibrium potentials for the specified processes, taken from Table 9: in Figure 20(a) at 100°C and in Figure 20(b) at 0°C. Heavy arrows indicate thermodynamically most favored pathways, while dotted lines indicate improbable reaction paths.

At high temperatures [Figure 20(a)], discharge occurs initially to form $HFeO_2^-$; this ion then precipitates to form $Fe(OH)_2$ on the electrode surface. Oxidation via this dissolved intermediate is favored by only 20 mV over the direct formation of $Fe(OH_2)$, and the differential rates will be determined by kinetic factors. However, the presence of a dissolved Fe(II) intermediate is clearly indicated by the results of RRDE experiments, shown in Figure 16 (peak D01). With the buildup of an $Fe(OH)_2$ film, the rate of this reaction decreases, and a potentiodynamic peak (O2) is observed. At higher potentials a second discharge peak (O1) conceals three processes: the oxidation of surface-formed $Fe(OH)_2$ to Fe_3O_4 (peak O2, path [a]) the continued dissolution of Fe → $HFeO_2^-$ → $Fe(OH)_2$ →

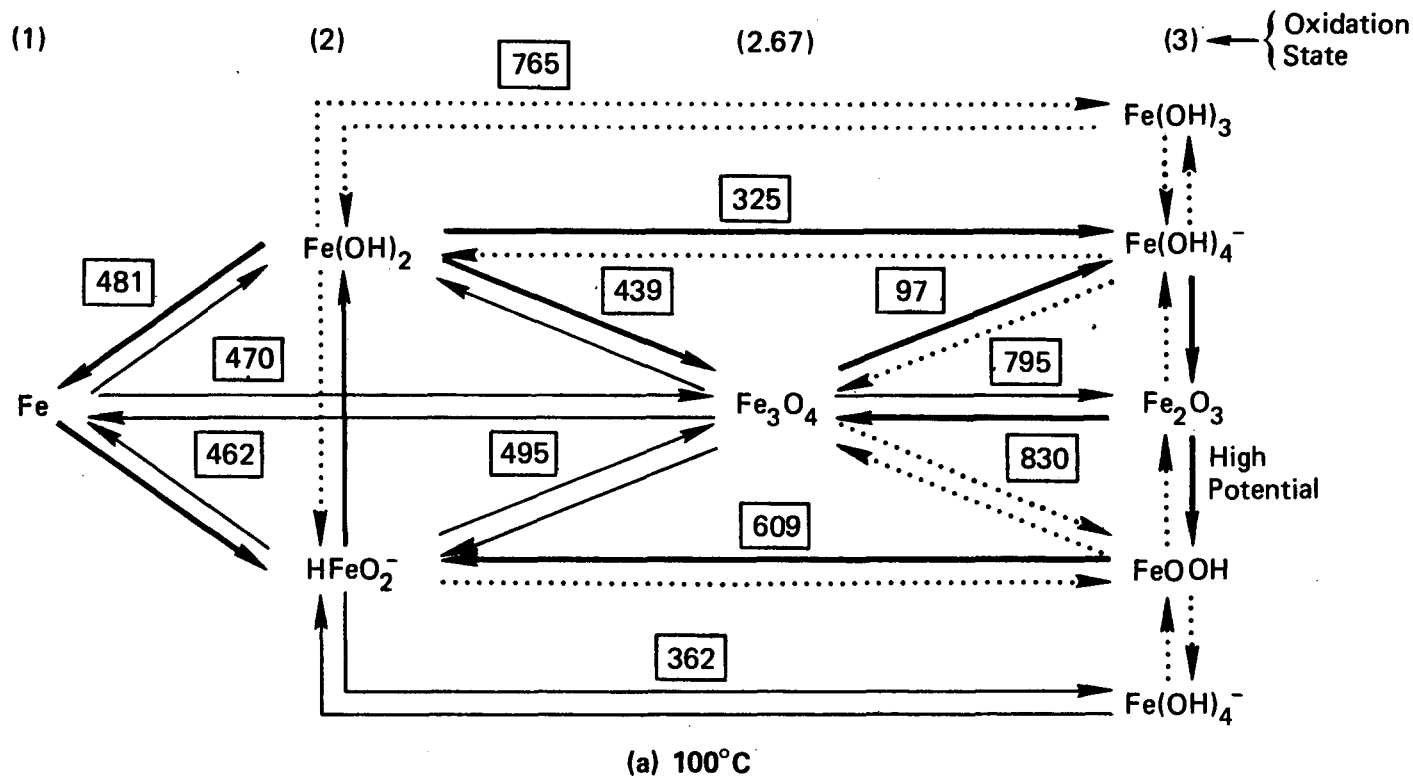

FIGURE 20 THERMODYNAMICALLY FAVORED REACTION PATHWAYS SHOWING THE CALCULATED EQUILIBRIUM POTENTIALS FOR Fe IN 8 MOLAL NaOH

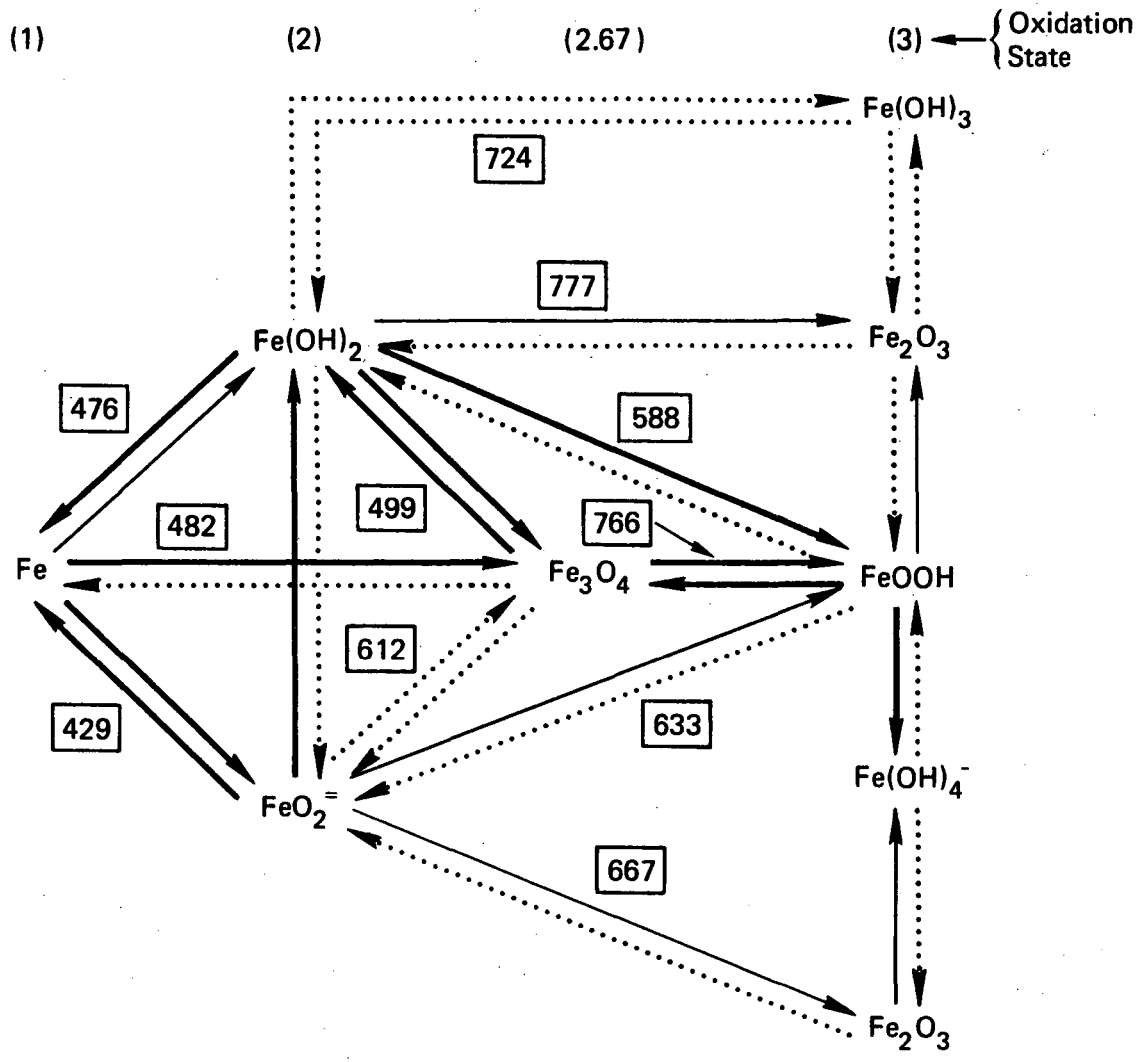

FIGURE 20 THERMODYNAMICALLY FAVORED REACTION PATHWAYS SHOWING THE CALCULATED EQUILIBRIUM POTENTIALS FOR Fe IN 8 MOLAL NaOH (Concluded)

Fe_3O_4 (peak O2, path [b]), and the electrochemical dissolution of magnetite formed by these reactions to produce $Fe(OH)_4^-$. This last process becomes highly favored (thermodynamically) with increasing temperature, and must be restricted kinetically, perhaps by the formation of a "pseudo-passivating" Fe(III) surface oxide film by precipitation. If such a film were not formed, magnetite would dissolve completely to form $Fe(OH)_4^-$ at temperatures $\gtrsim$ 80°C. The RRDE results at 75°C presented in Figure 16 and the data summarized in Table 7 show that both Fe(II) ions (peak DO2, which appears as an intermediate in the formation of magnetite) and Fe(III) ions (peak DR2, resulting from the electrochemical dissolution of magnetite) are observed in conjunction with disk peak O2.

Oxidation peaks O3 and O4 can tentatively be assigned to the oxidation of unreacted $Fe(OH)_2$ directly to Fe_2O_3 and the oxidation of Fe_3O_4 to Fe_2O_3. In each case $Fe(OH)_4^-$ is an intermediate, which is observed as ring reduction process DR3. Since a dissolved Fe(III) species is not observed during the reduction half-cycle, it is clear that the precipitation reaction $Fe(OH)_4^- \rightarrow Fe_2O_3$ proceeds rapidly to the right.

Reduction of the disk surface oxide proceeds as follows. As was noted previously (Section 3.2), disk peaks O3 and R3 are conjugate processes. Thus, R3 is related to the reduction of Fe_2O_3 to Fe_3O_4; in this direction, $Fe(OH)_4^-$ is an intermediate. The results presented in Figures 12 and 13 indicate that the reduction of magnetite (produced by oxidation in peak O2 or reduction in peak R3) to $Fe(OH)_3$ does not result in a reduction peak, but occurs continuously at potentials $\lesssim$ 400 mV.

Reduction peak R2 is observed in conjunction with ring oxidation peak DO3, following oxidation at large positive potentials (see Figure 13). It

is probable that this is a result of the partial transformation of Fe_2O_3 to FeOOH at high potentials. During the reduction half-cycle, FeOOH is reduced to $Fe(OH)_2$, with $HFeO_2^-$ as an intermediate.

The $Fe(OH)_2$ formed by processes O1, R3, and R2 is reduced to Fe(0) under peak R1, without a dissolved Fe(II) intermediate.

The influence of temperature on the thermodynamic and electrochemical kinetic parameters is such that the charge, discharge, and dissolution mechanisms at low temperatures deviate somewhat from the high-temperature scheme described above.

Figure 20(b) summarizes the reaction sequence proposed for temperatures $\lesssim$ 25°C. At low temperatures $FeO_2^=$ becomes the stable Fe(II) dissolved species, and the initial discharge of Fe to $Fe(OH)_2$ proceeds with this ion as an intermediate (peaks O1 and DO1 in Figure 17). As indicated in Table 7, the percentage of Fe(II) that is dissolved in this process is effectively independent of temperature.

Disk oxidation peak O2 again conceals three processes: the oxidation of surface-formed $Fe(OH)_2$ to Fe_3O_4, the direct oxidation of Fe to Fe_2O_3 and the dissolution of $Fe(OH)_2$ to $Fe(OH)_4^-$. The first of these processes is the same as at high temperature, but in this case the direct oxidation from iron to magnetite is favored by nearly 20 mV over a path with $Fe(OH)_2$ as an intermediate. The fact that this path does not involve a dissolved Fe(II) species accounts for the relative decrease at low temperatures of ring dissolution peak DO2 [see Figure 17(b) and Table 7]. At low temperatures, also, the available paths from magnetite to Fe(III) all have relatively high potentials, and it is probable that the Fe(III) dissolution peak (DR2) that appears in conjunction with disk peak O2,

temperatures, is due to the electrochemical dissolution of unreacted $Fe(OH)_2$. The influence of potentiodynamic sweep rate on RRDE results tends to support this hypothesis, since ring peak DR2 is not observed at very low disk potential sweep rates.

At low temperatures oxidation peaks O3 and O4 probably correspond to the oxidation of unreacted $Fe(OH)_2$ and of Fe_3O_4 to Fe(III). In this case, the stable Fe(III) oxide is FeOOH (compared with Fe_2O_3 at high temperatures).

On the reduction half-cycle, disk peak R3 corresponds to the reduction of Fe(III) oxide (Fe_2O_3 or FeOOH) to magnetite. As is observed at high temperatures, subsequent reduction of magnetite to $Fe(OH)_2$ occurs continuously and does not result in a peak.

Reduction peak R2 is observed following large anodic potential excursions and, at low temperatures, is attributable to the reduction sequence $Fe_2O_3 \rightarrow FeO_2^{=} \rightarrow Fe(OH)_2$. The well-defined ring oxidation peak is associated with the $FeO_2^{=}$ that is an intermediate in this disk reduction process.

The final reduction process, R1, that is associated with the reduction of $Fe(OH)_2$ to Fe, is concealed at low temperatures by the reduction of hydrogen ions.

This detailed reaction sequence represents an attempt to correlate the calculated thermodynamic and measured kinetic and dissolution parameters for Fe over a range of temperatures. The proposed mechanism should be treated as not definitive but as a working hypothesis for further experimentation. Simplified versions of the oxidation and reduction reaction sequences at high and low temperatures are presented, together with peak assignments, in Figure 21.

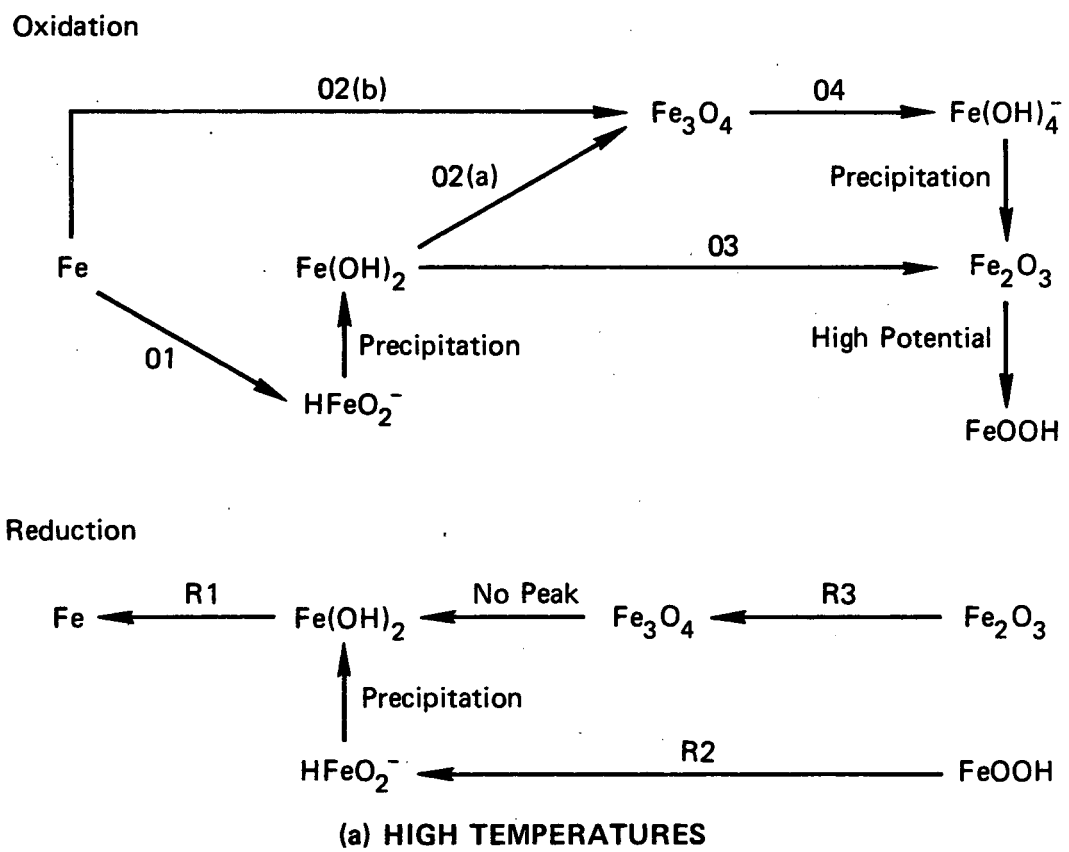

FIGURE 21 SIMPLIFIED HIGH- AND LOW-TEMPERATURE REACTION SEQUENCES FOR IRON IN 30 wt% KOH

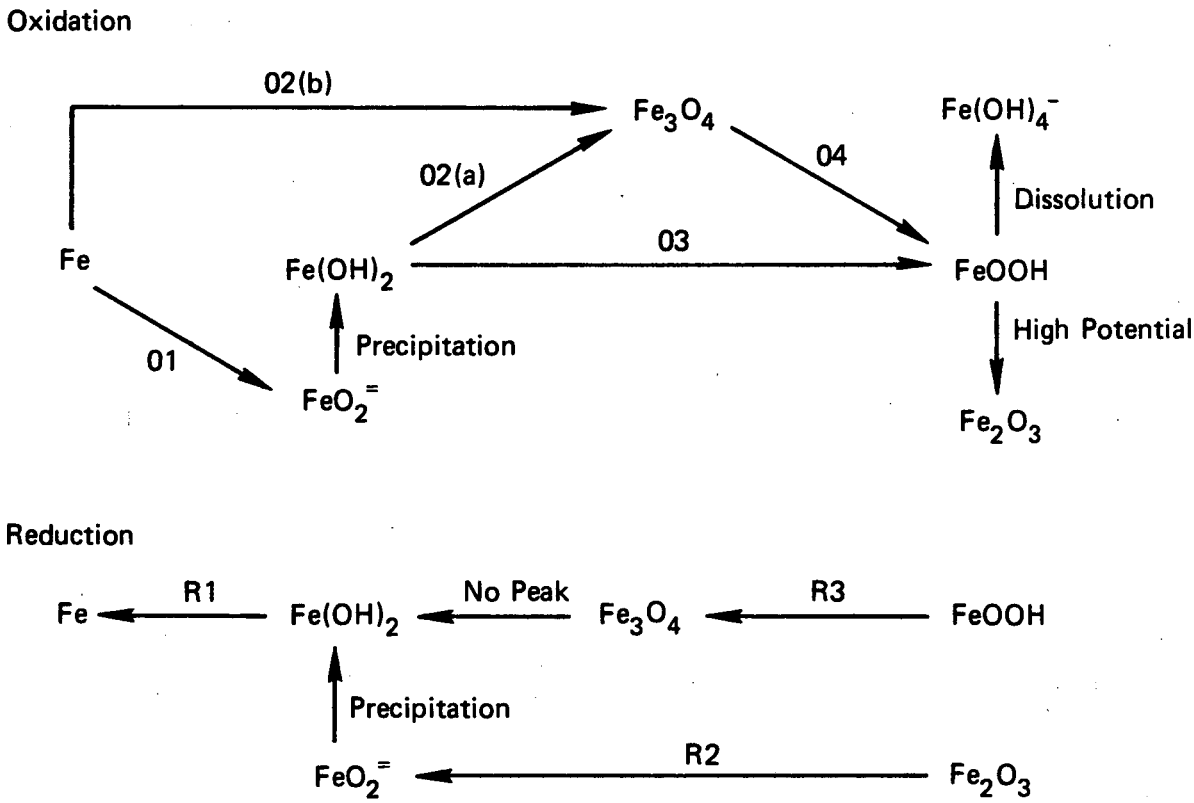

(b) LOW TEMPERATURES

JA-1535-32

FIGURE 21 SIMPLIFIED HIGH- AND LOW-TEMPERATURE REACTION SEQUENCES FOR IRON IN 30 wt% KOH (Concluded)

4 MEASUREMENTS ON ZINC

4.1 Introduction

Measurements were performed using a rotating 99.999% purity Zn disk and vitreous carbon ring electrode. Two electrolyte concentrations containing 30 and 36 wt% KOH were studied at 0°, 25°, 50°, 75°, and 100°C. For selected conditions the solution zincate concentration was varied from effectively zero to supersaturated, by coulometrically dissolving an auxiliary high-purity zinc electrode in the working electrolyte.

In contrast to the iron electrode, where the charge/discharge kinetics are controlled by the electrode/electrolyte interfacial impedance and oxide film resistance, the discharge of Zn prior to passivation is dominated by mass transport processes. Accordingly, potentiodynamic studies of a zinc RDE were performed with rotational speed as the principal independent variable (in contrast to potentiodynamic sweep rate for Fe). In addition to potentiodynamic voltammetry and coulometry, AC impedance experiments were performed as a function of DC potential, electrode rotation speed, KOH and zincate concentration, and temperature to determine the kinetics and mechanism of zinc discharge. RRDE measurements were made as a function of zincate concentration and rotation speed in an attempt to determine the nature of the dissolved product.

4.2 Potentiodynamic Studies of Zinc

The discharge of a zinc electrode in concentrated KOH proceeds qualitatively in the same way as discharge in NaOH.[2,5] For a slow potentiodynamic sweep, an initial exponential dependence of discharge current on potential is followed by a linear region in which the slope is proportional to the inverse square root of rotation speed. Figure 22 shows the influence of electrode rotation speed on the slope of the potentiodynamic discharge curve for zinc in 30 wt% KOH at 78°C. Table 10 contains a complete tabulation of the slopes and intercepts of the linear regions of the dissolution current/voltage curves as a function of angular rotation speed, electrolyte concentration, and temperature. These data were obtained at a potentiodynamic sweep rate of 1 mV s^{-1}. The current/voltage responses display little hysteresis at all nonzero rotation speeds used, and the data tabulated closely reflect steady-state conditions.

The data presented in Table 10 may be fitted to an equation of the form

$$R = R^{\circ} + \alpha\omega^{-1/2} \quad . \tag{35}$$

Thus, over a wide range of potential, the discharge resistance for zinc is the sum of a convection-independent term, and a term proportional to the thickness of the diffusion layer.

Table 11 shows the regression parameters for the fit of all data in Table 10 to equation (35). Both R° and α are seen to decrease

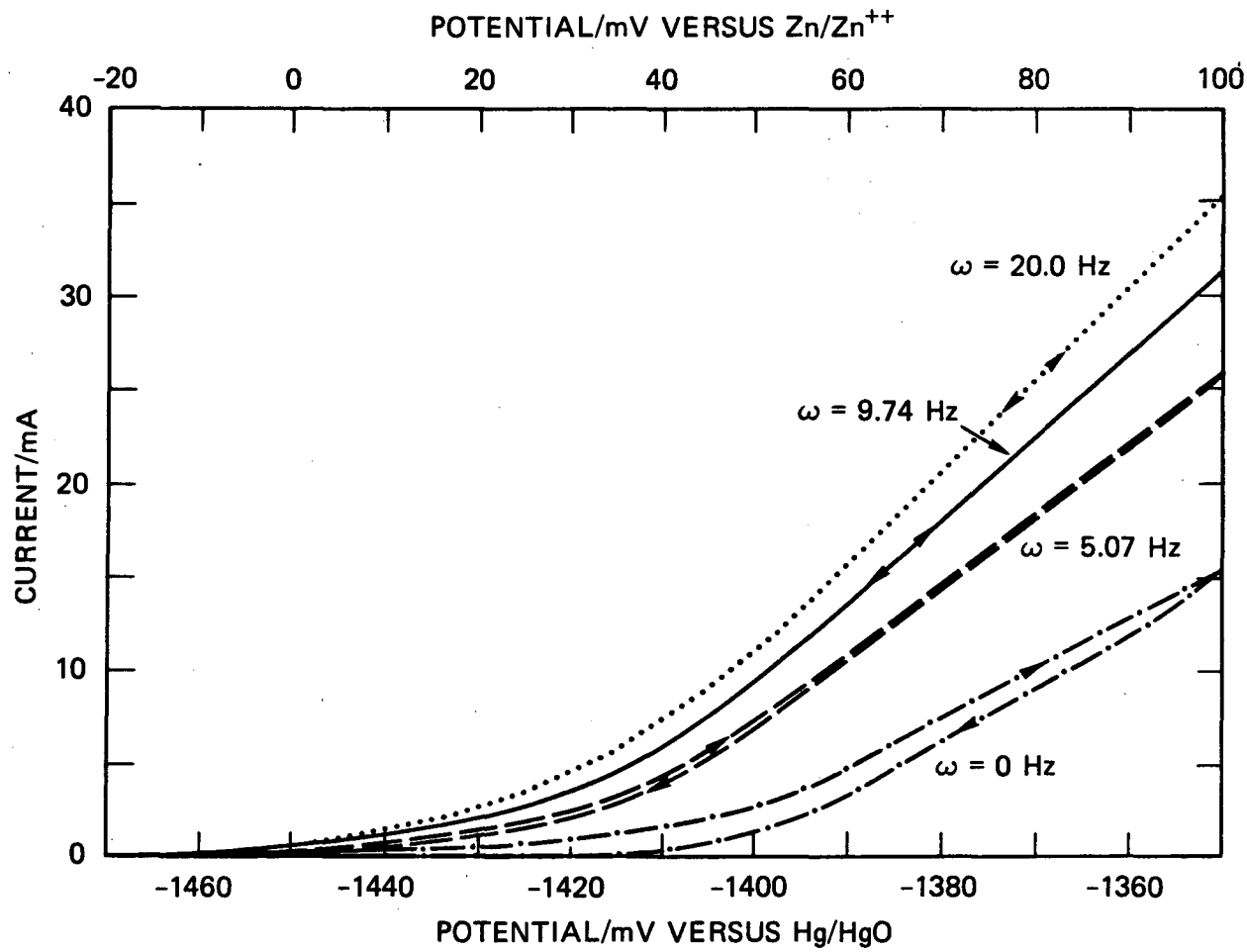

FIGURE 22 POTENTIODYNAMIC DISCHARGE OF ZINC IN 30 wt% KOH AT 78°C, AS A FUNCTION OF DISK ROTATION SPEED

Sweep rate = 1 mV s^{-1}.

Table 10

SLOPE AND INTERCEPTS OF THE LINEAR I-V DISCHARGE REGION OF A ZINC RDE, AS A FUNCTION OF TEMPERATURE, ROTATION SPEED, AND ELECTROLYTE CONCENTRATION

(a) 35 wt% KOH

Electrolyte Temperature /°C	Electrode Diameter /cm	Rotation Velocity /Hz	$\frac{dV}{dI}$/Ω	V_o^R/mV
0	0.640	20.05	4.636	-1381.2
0	0.640	9.95	5.295	-1378.7
0	0.640	5.05	5.626	-1376.5
0	0.640	0.00	6.581	-1373.1
25	0.483	30.00	2.800	-1394.3
25	0.483	19.90	3.039	-1392.8
25	0.483	10.00	3.339	-1389.4
25	0.483	8.05	3.459	-1386.9
25	0.483	5.00	3.831	-1386.6
25	0.483	0.00	4.530	-1376.8
25*	0.405	20.00	3.20	-1375.9
25*	0.405	10.00	3.33	-1371.8
25*	0.405	5.03	3.58	-1370.3
25*	0.405	2.50	3.86	-1369.7
25*	0.405	0.00	4.57	-1365.8
50	0.640	19.93	2.02	-1414.0
50	0.640	9.60	2.21	-1409.6
50	0.640	5.06	2.41	-1403.9
50	0.640	0.00	3.30	-1392.6
75	0.640	20.00	1.79	-1416.2
75	0.640	9.94	1.88	-1411.8
75	0.640	5.07	2.05	-1407.2
75	0.640	0.00	2.57	-1395.8
100	0.640	19.90	1.35	-1416.9
100	0.640	9.93	1.43	-1416.3
100	0.640	4.99	1.55	-1414.8
100	0.640	0.00	2.01	-1405.6

*Saturated with zincate ions.

Table 10 (Concluded)

(b) 30 wt% KOH

Electrolyte Temperature /°C	Electrode Diameter /cm	Rotation Velocity /Hz	$\frac{dV}{dI}/\Omega$	V_o^R/mV
0	0.640	19.99	2.317	-1350.0
0	0.640	10.01	2.410	-1347.6
0	0.640	5.03	2.550	-1346.5
0	0.640	2.50	2.750	-1345.8
0	0.640	0.00	2.882	-1340.6
25	0.640	20.00	1.713	-1351.9
25	0.640	10.00	1.825	-1351.1
25	0.640	5.00	1.948	-1359.1
25	0.640	0.00	2.200	-1339.6
51	0.640	20.00	1.126	-1363.2
51	0.640	10.00	1.152	-1362.8
51	0.640	5.00	1.194	-1359.9
51	0.640	2.50	1.279	-1357.3
51	0.640	0.00	1.377	-1351.1
78	0.640	20.02	1.370	-1414.1
78	0.640	10.01	1.420	-1410.2
78	0.640	5.00	1.609	-1407.6
78	0.640	2.51	1.619	-1405.7
78	0.640	0.00	1.748	-1394.4
100	0.640	20.09	0.997	-1414.3
100	0.640	10.03	1.032	-1411.4
100	0.640	5.00	1.107	-1408.9

Table 11

THE REGRESSION OF DATA IN TABLE 10 TO EQUATION (35)

Electrolyte Concentration /wt%	Electrolyte Temperature /°C	R° /Ω cm^{-2}	α /Ω $s^{-1/2}cm^{-2}$	Regression Coefficient r^2
35	0	11.67	13.54	.925
35	25	7.80	13.71	.994
35*	25	7.85	4.56	.997
35	50	5.07	5.48	.998
35	50	7.85	4.56	.992
35	100	3.57	2.79	1.000
30	0	6.47	3.26	.999
30	25	4.61	3.24	.995
30	51	3.22	3.22	.987
30	78	2.70	2.95	.950
30	100	2.15	1.21	.989

*Solution saturated with zincate.

monotonically with increasing temperature. The convection-independent term, R°, reflects, in part, the presence of an uncompensated electrolyte resistance. The data in Table 11 can be analyzed to determine the activation energy for conduction in 30 and 35 wt% KOH. In the best fit to an Arrhenius equation of the form

$$R^\circ = A_o \exp[E_a/RT], \tag{36}$$

one obtains the regression parameters shown in Table 12. The values of E_a obtained are somewhat larger than those expected for electrolyte phase

Table 12

THE REGRESSION OF DATA IN TABLE 11 TO EQUATION (36)

Electrolyte Concentration/wt%	A_o/Ω	Activation Energy/ kJ mol^{-1}	Regression Coefficient
30	0.110	9.23	.995
35	0.147	9.84	.975

conduction, suggesting the presence of a series term in the oxide film or interface regions.

The variation of the convection-dependent parameter, α, with temperature and electrolyte concentration is of fundamental importance in understanding the discharge kinetics and the mechanisms of dissolution and passivation of zinc. We currently believe that this resistive term is associated with the prepassive film as described previously.[5,28] The rate of dissolution of this film is controlled by the rate of the reprecipitation reaction and by the rate of mass transfer of the dissolved species from the film/electrolyte interface to the bulk solution. Under some circumstances it is possible to predict a film thickness that is inversely proportional to the diffusion layer thickness thickness. We are currently developing a model the describe to observed dependence of the initial discharge of zinc on convection rate, and a potential-step transient technique to verify this model.

4.3 Rotating Ring Disk Studies of Zinc

It has been previously noted[2,5,29] that the percentage of dissolved zinc species that is reducible on the ring declines at high rotation speeds

for an RRDE operated in NaOH. The mechanism for decrease in the apparent collection efficiency at high convection rates has been interpreted[29] as follows. The anodic charge transfer process produces an inactive intermediate that transforms in time to the electrochemically active product by chemical dissolution. It is this final product that is reducible on the ring.

Experiments were performed using a rotating ring-disk electrode with programmed rotation speed to verify that this phenomenon is observable in KOH electrolytes and to shed some light on the dissolution process.

The motor speed controller was programmed using an external DC voltage ramp to increase the electrode rotation speed linearly from a preset minimum to a predetermined maximum angular velocity, and back. Care was taken to keep the speed control function, $d\omega/dt$, low enough to maintain the hydrodynamic equilibrium.[17] Experiments were performed with the ring at a potential sufficiently negative to reduce any soluble reducible zinc species to Zn. Measurements were made as a function of disk potential, in the region of active zinc dissolution. A typical set of results is shown in Figure 23. It is worth mentioning that sweeping the rotation speed provides the only practical and convenient means of obtaining RRDE data for the dissolution of zinc over a wide range of rotation speeds. Because the zinc disk electrode dissolves rapidly at moderate overpotentials, and because the deposit on the ring is mossy or dendritic, the laminar flow condition necessary for a predictable and constant collection efficiency is soon destroyed. Indeed, at elevated temperatures the useful operating life of a zinc RRDE may be only a few minutes, following which the electrode is must to be disassembled and repolished. To increase the acquisition rate

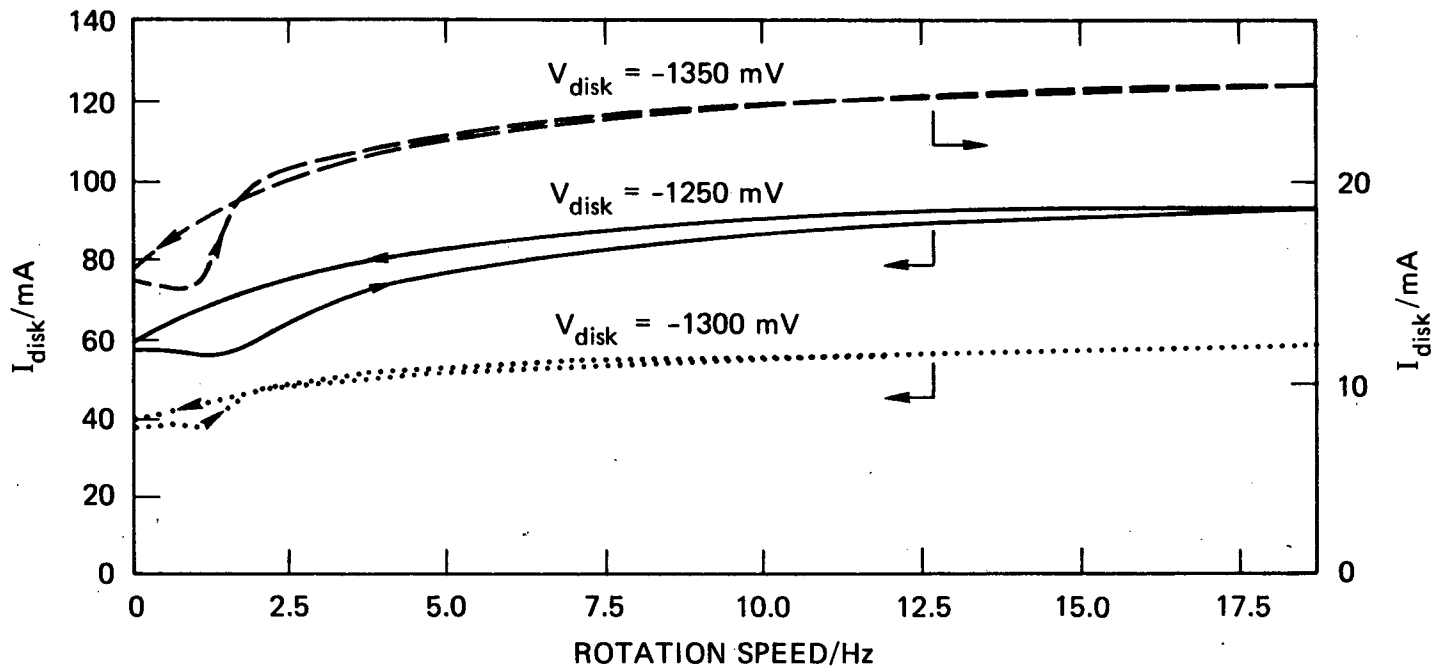

(a) DISK CURRENT VERSUS ROTATION SPEED AS A FUNCTION OF DISK POTENTIAL

JA-1535-36

FIGURE 23 PROGRAMMED ROTATION SPEED RRDE EXPERIMENTS FOR ZINC IN 36 wt% KOH AT 25°C
Disk acceleration = 0.1 Hz s^{-1}.

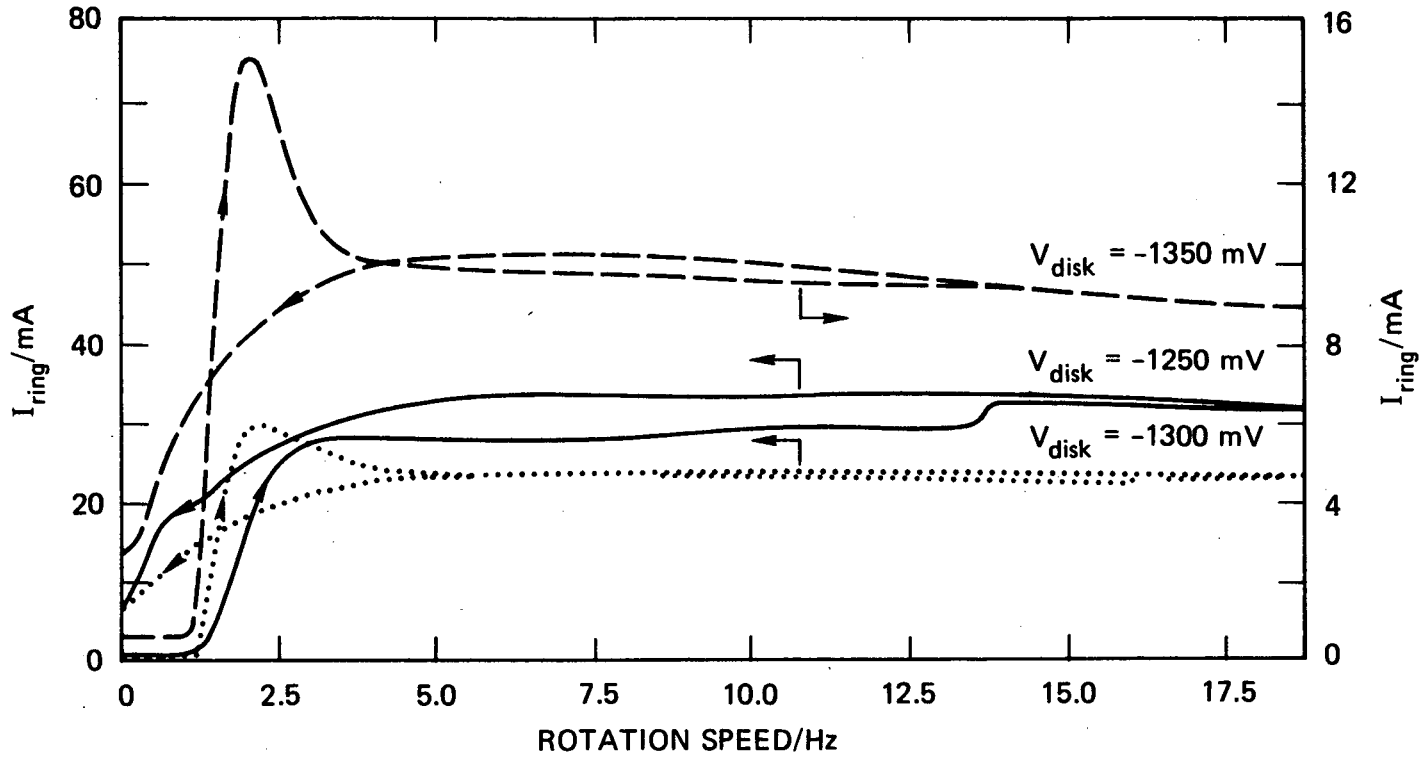

(b) RING CURRENT VERSUS ROTATION SPEED WITH RING POTENTIAL HELD AT -1500 mV VERSUS Hg/HgO

JA-1535-37

FIGURE 23 PROGRAMMED ROTATION SPEED RRDE EXPERIMENTS FOR ZINC IN 36 wt% KOH AT 25°C
Disk acceleration = 0.1 Hz s^{-1} (Concluded).

further while maintaining hydrodynamic equilibrium, measurements currently are being made with an exponential speed control function, as suggested by Miller et al.,[17] under microcomputer control.

The hysteresis shown in Figure 23 at low angular velocities is associated primarily with the fact that, for this experiment, the RRDE was initially stationary. The plot is of current versus program voltage, and the electrode was stationary for some time after the ramp was started, before the DC motor had sufficient torque to overcome the static frictional forces of the system. The disk then started impulsively, and the peak observed in the ring current is associated with the presence of an excess concentration of dissolved zinc that had previously accumulated in the vicinity of the disk. This effect can be overcome satisfactorily by starting with a nonstationary electrode and by measuring the ring and disk currents only while the angular velocity is decreasing.

Table 13 summarizes of the results of a series of experiments in 35 wt% KOH at 25°C, as a function of disk potential, with a programmed sweep from 31.47 to 1.61 Hz. These data conform to an equation of the form

$$I_r = I_r^o + \frac{N}{100} (I_d) \tag{37}$$

where I_r and I_d are the ring and disk currents at the interpolated rotation speeds shown in Table 13, as a function of disk potential; N is the calculated collection efficiency; and I_r^o is the background current due to the evolution of hydrogen on the vitreous carbon ring, which is effectively independent of disk potential.

Table 13

PROGRAMMED ROTATION SPEED RESULTS FOR ZINC IN 35 WT% KOH AT 25°C

(Ring and Disk Currents as a Function of Rotation Speed and Disk Potential).

Disk Potential /mV versus Hg/HgO	ω = 1.61 Hz	ω = 3.76 Hz	ω = 6.27 Hz	ω = 12.57 Hz	ω = 18.87 Hz	ω = 25.17 Hz	ω = 31.47 Hz	Current /mA
-1400	2.58	3.02	3.41	3.86	4.15	4.32	4.46	Disk
	0.83	1.11	1.20	1.20	1.14	1.09	1.00	Ring
-1380	5.40	6.12	6.69	7.30	7.80	8.12	8.40	Disk
	1.53	2.17	2.29	2.33	2.20	2.02	1.98	Ring
-1360	9.60	10.61	11.36	12.22	12.74	13.07	13.40	Disk
	2.78	3.75	4.14	4.13	3.92	3.66	3.33	Ring
-1350	13.80	15.21	16.11	17.22	17.93	18.41	18.78	Disk
	4.05	5.61	6.37	6.63	6.33	5.90	5.23	Ring
-1300	24.9	27.1	28.7	30.8	31.8	32.2	32.6	Disk
	7.2	10.5	11.7	12.1	11.5	10.5	9.6	Ring

Note: Disk acceleration = 0.126 Hz s^{-1}. Ring potential = -1500 mV versus Hg/HgO.

Table 14 shows the results of the regression of the data in Table 13 to equation (37). The tabulated values of the collection efficiency are plotted in Figure 24 versus the angular rotation speed. Also shown in Figure 24 is the theoretical collection efficiency calculated from equation (28) using the computer program in Appendix II.

These results, obtained in KOH solutions, are essentially identical to those obtained previously in NaOH.[2,5] Under all conditions the amount of zinc that is dissolved exceeds the concentration of species that could be reduced at the ring, and the percentage of dissolved material that is collected is a function of the rotation speed. We interpret these data as follows: the decline in collection efficiency at low rotation speeds is an artifact of the RRDE system. That is, when no dissolved product is convected past the ring (as $\omega \rightarrow 0$) the collection efficiency goes to zero. As shown in Figure 24, however, the measured value of N does not attain the theoretical value independent of rotation speed. Instead, N is observed to increase rapidly with ω, achieving a maximum value of 73% of the theoretical value at $\omega \approx 5$ Hz, and then declining approximately linearly with increasing rotation speed. indicating that the dissolution of zinc occurs in at least two sequential steps. The anodic charge transfer process produces a relatively inactive intermediate, which transforms to the electrochemically more active species by chemical reaction in the bulk electrolyte. At long times (low rotation speeds), this second reaction goes to completion, and the concentration of the more reducible product is a maximum. At short times (high transition velocities, high rotation speeds), the initial, less electrochemically active species is at a high concentration, and the collection efficiency

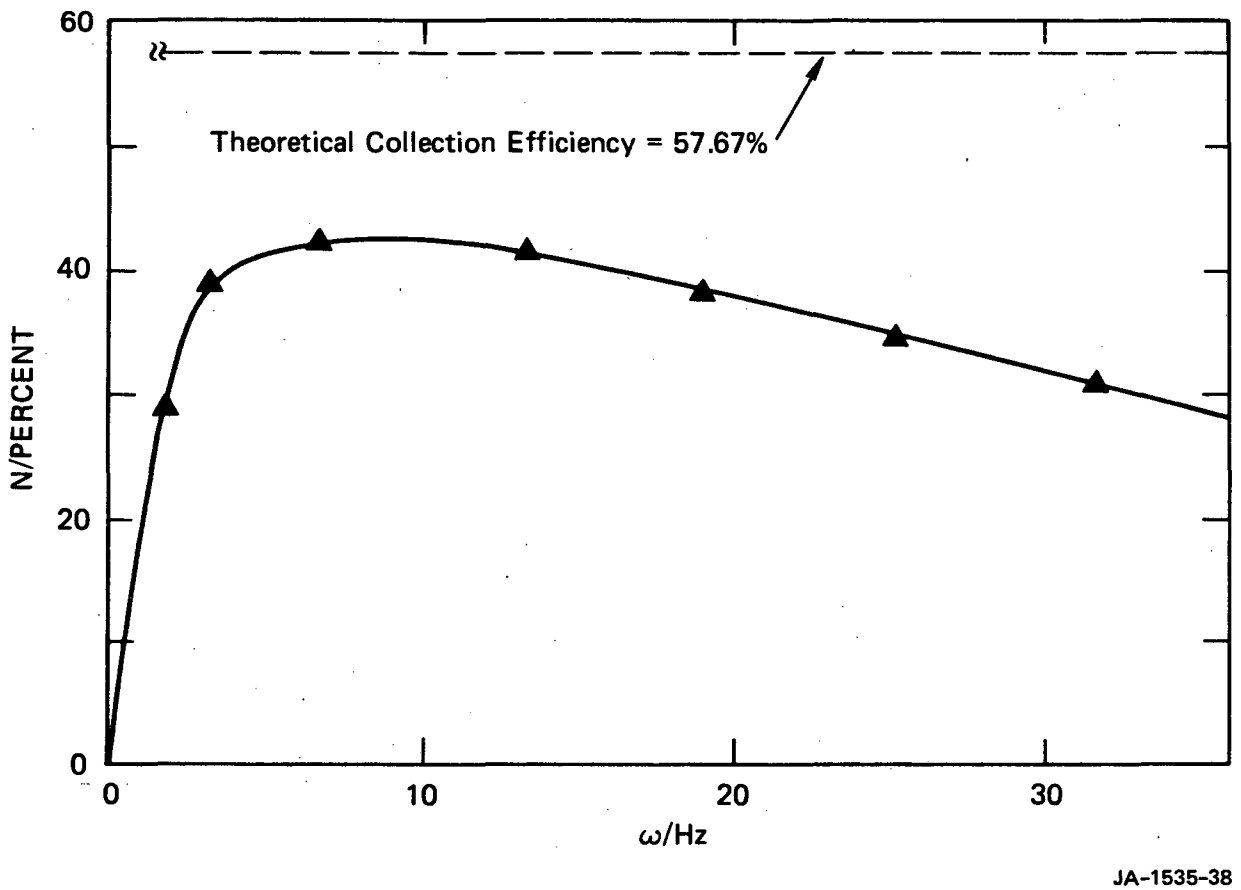

FIGURE 24 COLLECTION EFFICIENCY VERSUS ANGULAR ROTATION SPEED FOR A ZINC/VITREOUS CARBON RRDE IN 35.5 wt% KOH, AT 25°C

Table 14

COLLECTION EFFICIENCY AS A FUNCTION OF ROTATION SPEED: REGRESSION OF RING AND DISK CURRENT DATA IN TABLE 13 TO EQUATION (37)

Rotation Speed/Hz	I_r^o/mA	N/%	Regression Coefficient
1.61	-0.038	28.8	.999
3.76	-0.240	39.2	.998
6.27	-0.437	42.1	.999
12.57	-0.619	41.2	.997
18.87	-0.661	38.1	.998
25.17	-0.617	34.5	.997
31.47	-0.582	31.0	.998

is low. If we postulate that the initially formed inactive intermediate species is $Zn(OH)_2$, then a possible reaction scheme is as follows:

Disk: $$Zn - 2e^- + 2OH^- \rightarrow Zn(OH)_2 \quad (38)$$

Gap: $$Zn(OH)_2 + 2OH^- \rightleftarrows Zn(OH)_4^{2-} \quad (39)$$

Ring: $$Zn(OH)_4^{2-} + 2e^- \rightarrow Zn + 4\ OH^-. \quad (40)$$

On the basis of this postulated reaction sequence, and using the rather simple concept of a mean transit time for the dissolved species between the disk and ring, we can calculate a value for the rate constant in equation (39) from the observed linear dependence of N on rotation velocity.

The radial velocity, dr/dt, of a microscopic volume of electrolyte in the vicinity of a rotating disk electrode at a point (r, y) is

$$\frac{dr}{dt} = 0.5102\ (\bar{\omega}/\lambda)^{1/2}\ r\ \bar{\omega} y \quad , \tag{41}$$

where r is the distance (cm) from the center of rotation, $\bar{\omega}$ is the angular velocity (radians s^{-1}), y is the perpendicular distance from the electrode, and λ is the kinematic viscosity of the solution. Bruckenstein and Feldman[30] assumed that the path of a particle generated at the disk electrode at radius r_i, and ultimately reaching the ring electrode at radius r_o, can be described in terms of an average trajectory. integration of equation (41) yields

$$\ln(r_o/\ r_i) = 0.5102\ (\omega^3/\lambda)^{1/2} \int_o^{t'} y\ dt\ . \tag{42}$$

Assuming that $y = (Dt)^{1/2}$ (i.e., that convection parallel to the electrode takes place, on average, in a plane one mean diffusion length above the electrode surface), and that equal times are required to traverse the path normal to the electrode on leaving the disk and returning to the ring electrode, then from equation (42) the mean transit time, τ, is given by,

$$\tau = \left(\frac{0.718}{\omega}\right)\left(\frac{\lambda}{D}\right)^{1/3} \left(\log \frac{r_o}{r_i}\right)^{2/3} \tag{43}$$

where ω is expressed in revolutions per second (Hz).

The kinematic viscosity and diffusion coefficient for 35.5 wt% KOH at 25°C interpolated from literature tabulations[27,32] are as follows:

$$\lambda = 2.269 \times 10^{-2} \text{ stokes} \quad ; \quad D = 2.3 \times 10^{-5}\ cm^2\ s^{-1} \quad .$$

Further, we can treat the source of the dissolved species as the disk radius (see Figure 8) for which half the area is inside (and half outside),

$$r_i = (r_1^2/2)^{1/2} \quad , \tag{44}$$

and similarly for the ring,

$$r_o = [(r_3^2 + r_2^2)/2]^{1/2} \quad . \tag{45}$$

Thus, equation (43) becomes

$$\tau = \left(\frac{7.15}{\omega}\right) \left(\log\left[\left(\frac{r_3^2 + r_2^2}{r_1^2}\right)^{1/2}\right]\right)^{2/3} \quad . \tag{46}$$

In this initial analysis we will assume that the rate of the homogeneous reaction, equation (39), is determined by the concentration of hydroxyl ions at the disk and the local concentration of the electrochemical dissolution products. Thus,

$$\frac{d[Zn(OH)_4^-]}{dt} = k\,[OH^-]^2[Zn(OH)_2] \quad , \tag{47}$$

where k is the homogeneous rate constant.

The concentration of reducible (zincate) ions at time t can be determined from

$$\frac{dA}{dt} = kc^2Z \quad , \tag{48}$$

where $A = [Zn(OH)_4^-]$

c = bulk OH^- concentration

$Z = [Zn(OH)_2] = Z^o - A$

Z^0 = Concentration of $Zn(OH)_2$ at the disk.

A solution to (48) with the boundary condition that $A = 0$ at $t = 0$ is

$$A = Z^o[1 - \exp(-kc^2t)] \quad . \tag{49}$$

However, the relative collection efficiency is

$$N' = \frac{N_{obs}}{N_{theo}} = \frac{A}{Z^o} \quad . \tag{50}$$

That is, the observed collection efficiency is determined by the mean local concentration of zincate at the ring, while the collection efficiency predicted by equation (28) is based on the complete conversion of zinc hydroxide to zincate. As $t \to \infty$, $A \to Z^o$.

Substituting equation (46) for the transit time into equation (49), we obtain

$$N' = \frac{N_{obs}}{57.67} = 1 - \exp\left[\frac{-7.15\ kc^2}{\omega}\left(\frac{r_1^2 + r_2^2}{r_3^2}\right)^{1/2}\right] \tag{51}$$

A regression of the measured collection efficiency versus rotation speed data presented in Table 13, for frequencies greater than 10 Hz, to an equation of the form

$$\omega = - M/\ln\left(1 - \frac{N}{57.67}\right) \quad , \tag{52}$$

where $M = 7.15kc^2\left(\frac{r_1^2 + r_2^2}{r_3^2}\right)$

yields a value of M = 33.5 with a regression coefficient of 0.998. This is an unexpectedly good fit of the measured relative collection efficiency to the form predicted by our simple model. From the calculated value of M and the known bulk electrolyte concentration and electrode radii, we can calculate an approximate value for the homogeneous rate constant,

$$k \approx 2.4 \times 10^{-2} \quad \text{mol}^{-2}\ \text{s}^{-1} \quad ,$$

for c = 8.474 molal, r_1 = 0.76 cm, r_2 = 0.41 cm, r_3 = 0.32 cm.

Thus, we are able to obtain a value for the rate constant in support of our hypothesis that a homogeneous reaction converts an electrochemically less active initial product to a species that is electro-reducible on the ring. This treatment should not, however, be taken as definitive. In particular, the difficulty in defining an average trajectory for the ions between dissolution at the disk and reduction at the ring will lead to a considerable error in the calculated "mean transit time." The presence of a porous "prepassive" film also may have a considerable influence on the RRDE hydrodynamics and on the homogeneous (and heterogeneous) reaction kinetics.

4.4 The Influence of Zincate Concentration

For a reaction sequence of the type described in equations (38) to (40), one might expect to observe an influence of the bulk dissolved zinc concentration on the discharge process. Such an influence was observed previously[2,4,5] in NaOH solutions. In particular, the effective collection efficiency was found to increase with increasing dissolved zinc concentration.

A series of experiments was performed to determine the influence of dissolved zinc on the dissolution and passivation of zinc in KOH and on the measured AC impedance response. Zinc was dissolved in initially zincate-free, 30 wt% KOH at progressively higher concentrations up to complete saturation. To achieve known zincate concentrations, strips of high-purity zinc metal were polarized anodically using a counter electrode in an external chamber. In no case was the dissolution current allowed to exceed 1 amp, and the total immersed area of zinc strips was chosen to be sufficient to avoid passivation of the dissolving anodes. Electrolytes with filtered using a plastic gauze to remove undissolved zinc grains.

In all except the initially zincate-free solution, the background zincate level was too high to allow accurate ring measurements, and the results of these RRDE experiments will not be described in this section.

Figure 25 shows complete discharge curves for a rotating zinc disk in initially zincate-free 30 wt% KOH. The forward and reverse potentiodynamic sweeps are shown separately for clarity. Following the initial Tafel and linear discharge regions (discussed in Section 4.2), the electrode enters a prepassive region in which the current becomes constant or decreases slightly to a constant value with increasing potential. The

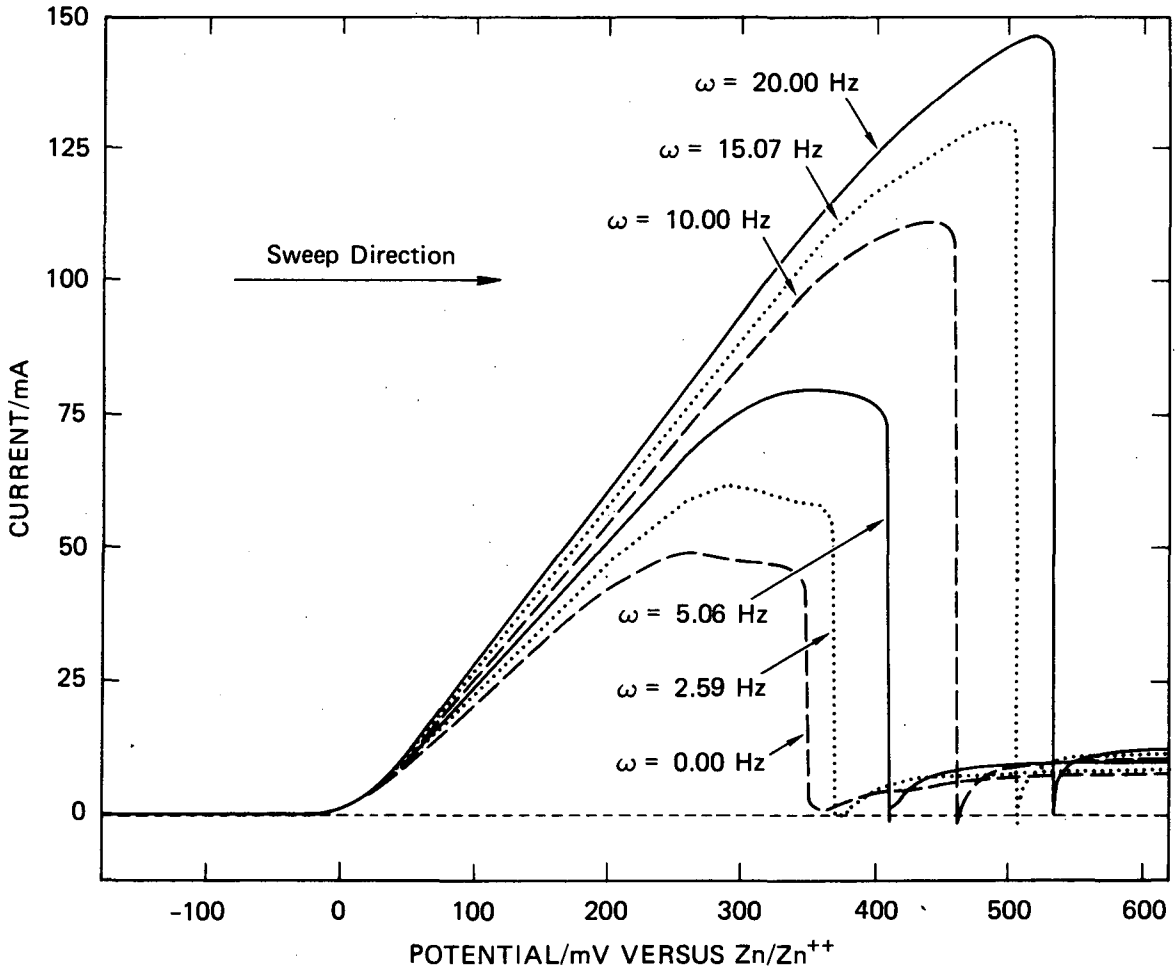

(a) FORWARD (ANODIC) POTENTIODYNAMIC SWEEP

JA-1535-39

FIGURE 25 THE RESULTS OF POTENTIODYNAMIC SWEEP EXPERIMENTS FOR A ZINC ELECTRODE IN INITIALLY ZINCATE-FREE 30 wt% KOH AT 25°C, AS A FUNCTION OF ELECTRODE ROTATION SPEED

Sweep rate = 10 mV s^{-1}.

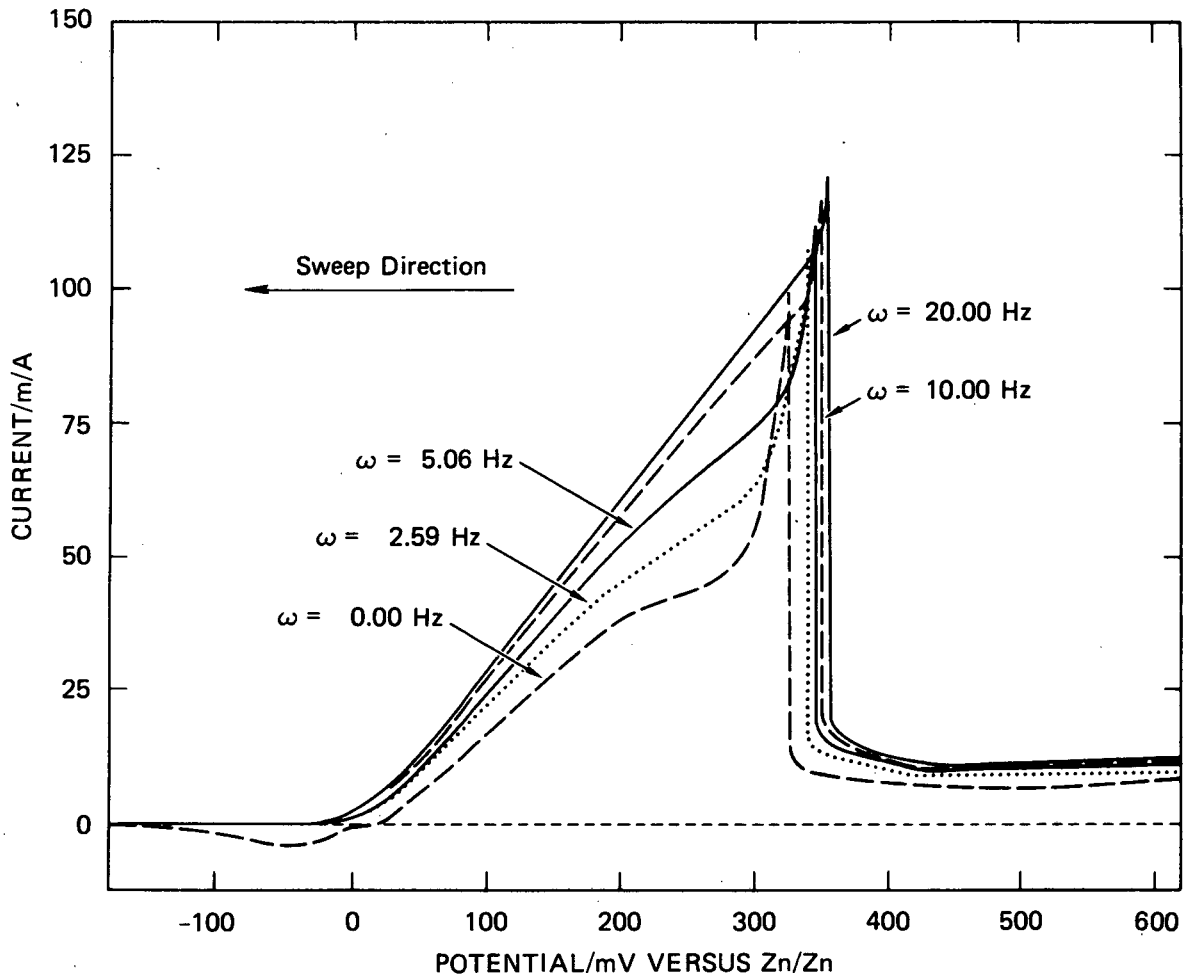

(b) REVERSE (CATHODIC) POTENTIAL SWEEP

JA-1535-40

FIGURE 25 THE RESULTS OF POTENTIODYNAMIC SWEEP EXPERIMENTS FOR A ZINC ELECTRODE IN INITIALLY ZINCATE-FREE 30 wt% KOH AT 25°C, AS A FUNCTION OF ELECTRODE ROTATION SPEED (Concluded)

Sweep rate = 10 mV s^{-1}.

current then decreases abruptly. In the vicinity of this discontinuity we describe the electrode surface as pseudopassive since, under a range of hydrodynamic conditions, the electrode may oscillate between active and passive dissolution levels. At higher potentials the electrode achieves a stable, limiting low current, independent of potential.

On the reverse potential sweep, reactivation occurs abruptly at a potential somewhat less than the prepassive to pseudopassive transition. After an initial current transient, the electrode current follows that of the positive sweep, with very little hysteresis except at the lowest convection rates.

Figure 26 shows the current oscillation observed at a constant potential, following a potential step from the potential of zero current (0 mV versus Zn/Zn^{++}). When stepped to potentials < 385 mV the electrode remains active. At 395 mV the electrode undergoes an active/passive/active transition once, then remains active, while at 400 mV, the electrode oscillates with nearly constant amplitude and period, effectively indefinitely. For potential-step values > 405 mV, the electrode passivates and remains passive.

The characteristics described above for the potentiodynamic discharge of Zn in 30 wt% KOH are all observed in the presence of zincate, up to saturation levels. In particular, the variation of the slope of the linear discharge region, the passivation onset potential, the reactivation potential, and the potential at which the electrode undergoes a stable oscillation are of interest in elucidating possible discharge and passivation mechanisms. Table 15 contains a summary of these parameters measured in 30 wt% KOH at 25°C as a function of electrode rotation speed and zincate concentration.

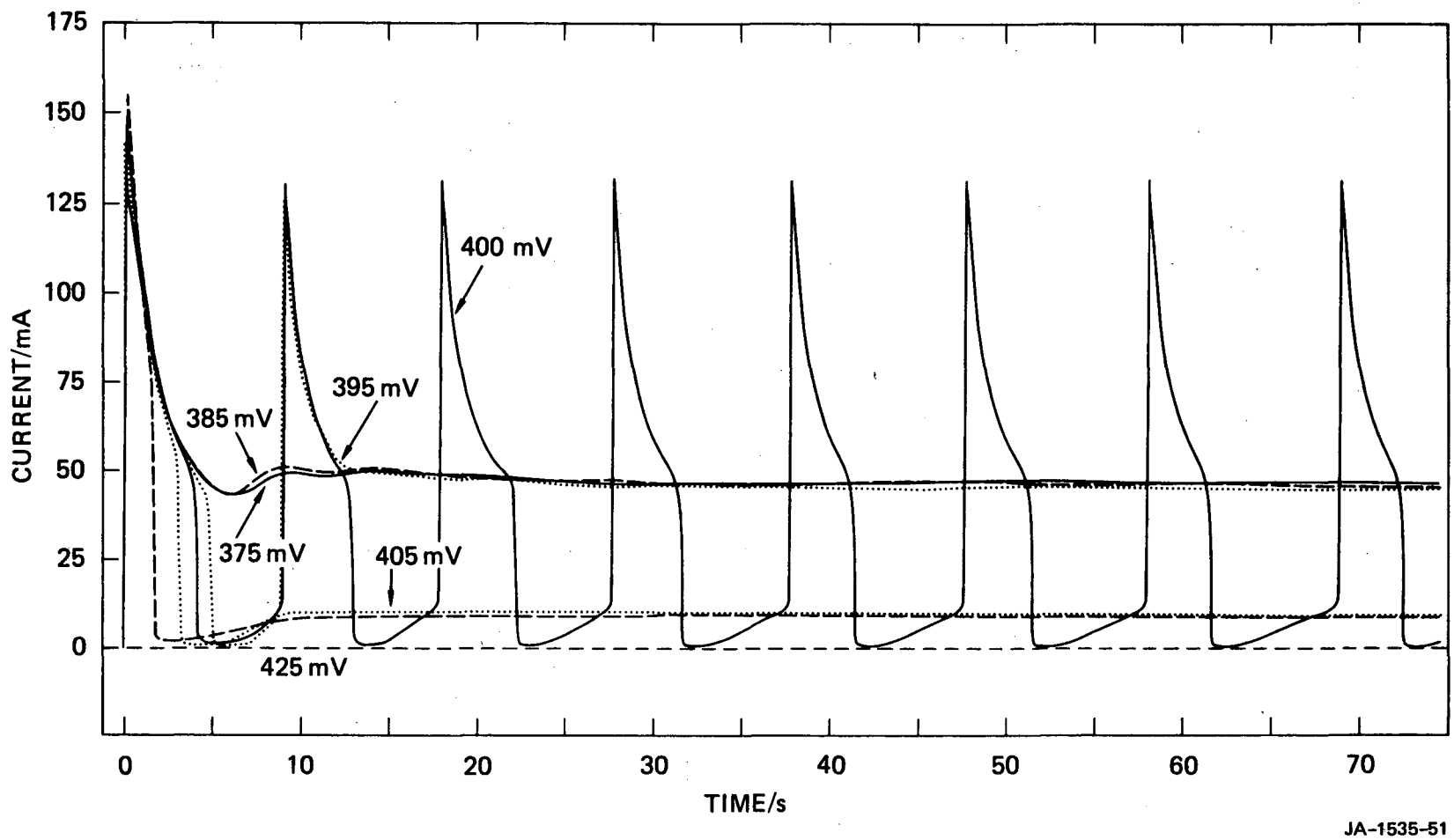

FIGURE 26 THE RESULTS OF POTENTIAL-STEP EXPERIMENTS FOR A ZINC ELECTRODE IN INITIALLY ZINCATE-FREE 30 wt% KOH AT 25°C, AS A FUNCTION OF POTENTIAL-STEP AMPLITUDE

Initial potential = 0 mV versus Zn/Zn^{++}.

Table 15

SUMMARY OF THE INFLUENCE OF ZINCATE ION CONCENTRATION ON THE MEASURED POTENTIODYNAMIC DISCHARGE PARAMETERS IN 30 WT% KOH
All Data at T = 25° ± 1°C, ν = 1 mV s^{-1}.

Dissolved Zinc Concentration /mol cm^{-3}	Rotation Speed /Hz	Slope of Linear Region /Ω cm^{-2}	$\vec{V}_p^*$ /mV	$\overleftarrow{V}_a^*$ /mV	V_{osc}^* /mV
1.60×10^{-7}	20.00	4.83	617	437	400
2.67×10^{-7}	15.07	5.13	589	436	---
0.62×10^{-7}	10.00	5.34	544	431	---
3.02×10^{-7}	5.04	5.74	493	426	---
3.73×10^{-7}	2.59	6.15	452	421	---
4.34×10^{-7}	0.00	6.63	432	407	---
2.04×10^{-5}	20.00	4.45	597	399	361
2.05×10^{-5}	10.03	4.76	521	388	---
2.05×10^{-5}	4.99	5.00	459	382	---
2.06×10^{-5}	1.49	5.41	414	377	---
2.06×10^{-5}	0.00	6.09	398	362	---
1.39×10^{-4}	20.04	4.22	582	367	333
1.39×10^{-4}	10.02	4.22	582	367	333
1.39×10^{-4}	4.99	4.86	443	356	---
1.39×10^{-4}	2.69	5.40	394	351	---
1.39×10^{-4}	0.00	5.69	372	338	---
3.82×10^{-4}	20.08	4.08	483	353	None
3.82×10^{-4}	9.99	4.40	426	351	---
3.82×10^{-4}	4.99	4.61	381	345	---
3.82×10^{-4}	2.49	5.08	362	340	---
3.82×10^{-4}	0.00	5.62	330	329	---
++	20.01		638	353	---
++	10.02	5.31	552	361	---
++	4.99	5.90	476	356	---
++	2.49	6.52	419	350	---
++	0.00	6.98	390	337	---

* Potentials measured with respect to a zinc electrode in the same electrolyte.
++Zincate removed, concentration unknown.
---Not measured.

Figure 27 shows a plot of 1/R versus $\omega^{-1/2}$, as a function of dissolved zinc concentration. These data correspond roughly to a family of straight lines. With the exception of the last data set in Table 15, however, these lines exhibit a striking characteristic of increasing dissolution rate (decreasing R) with increasing dissolved-zinc concentration. At constant rotation speed, R decreases with the logarithm of the dissolved-zinc concentration:

$$R = K - 0.401 \log ([Zn^{++}]) \tag{53}$$

where $[Zn^{++}]$ is expressed in mol cm^{-3}, and R in Ω cm^{-2}. For $\omega^{1/2} = 1$, K = 3.821 and the regression coefficient $r^2 = 0.998$.

This variation of the dissolution resistance, which characterizes the linear current/voltage discharge region of zinc, cannot be attributed to a variation in the uncompensated electrolyte resistance associated with changing specific conductivity in the electrolyte. Since the total amount of zinc dissolved accounts for only 0.38 moles/kg in an approximately 7 molal solution, we would expect this effect to be much less. Since we can postulate an overall cell reaction of the type

$$Zn + 2OH^- + 2H_2O \rightleftarrows Zn(OH)_4^= + H_2\uparrow \quad , \tag{54}$$

the in-situ electrooxidation of zinc will result in no net change in the availability of charge carriers. Indeed, the decrease in OH^- concentration in favor of the less mobile zincate ion is likely to result in a small <u>decrease</u> in electrolyte conductivity.

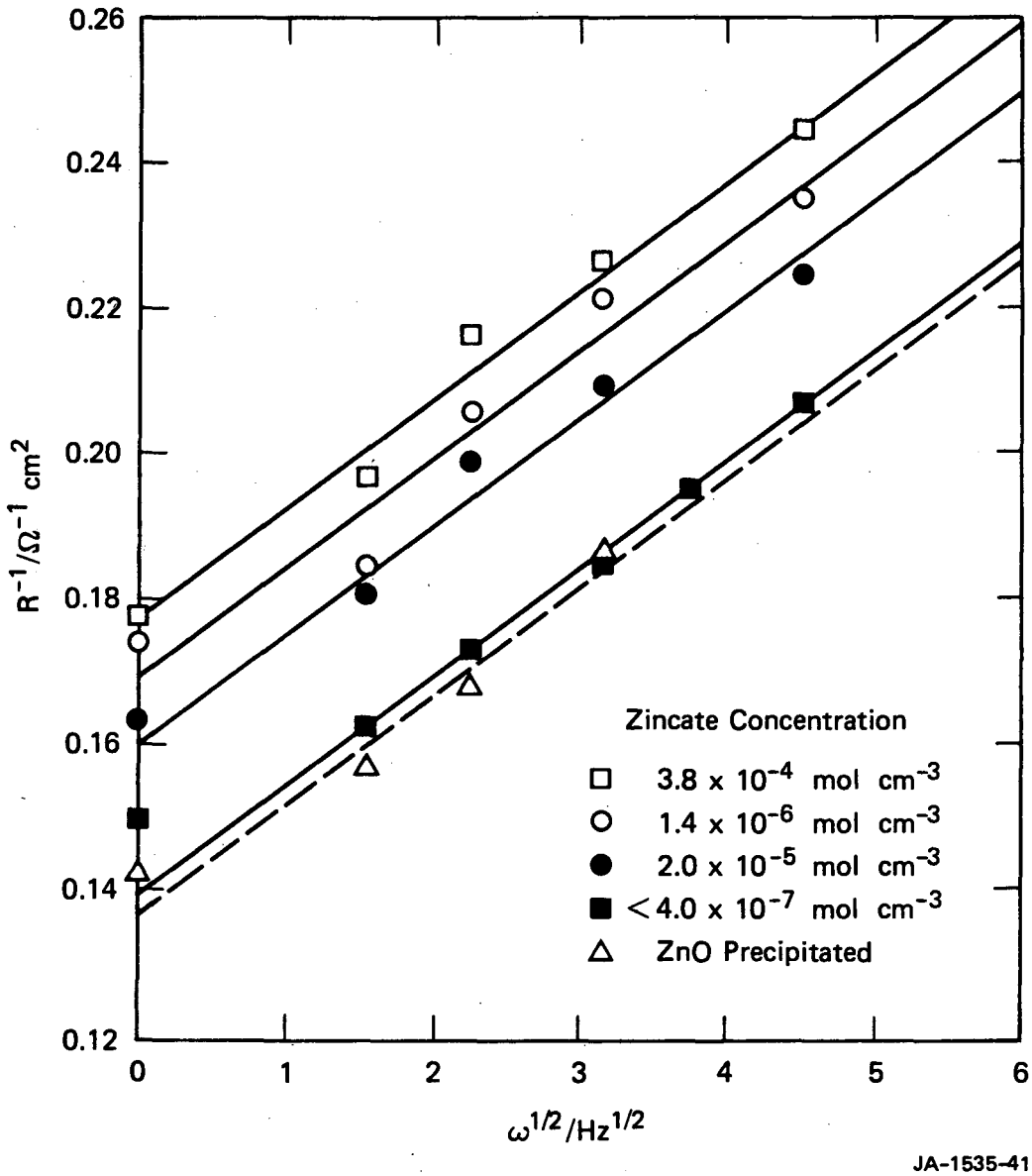

FIGURE 27 THE INFLUENCE OF DISSOLVED-ZINC CONCENTRATION ON THE POTENTIODYNAMIC DISSOLUTION RATE OF ZINC IN 30 wt% KOH AT 25°C

The results indicated by the dashed line in Figure 27 were obtained following an experiment to reduce the dissolved-zinc concentration. A total charge of 250,400 coulombs was impressed between spiral platinum wire electrodes in zincate-concentrated electrolyte. At the termination of current, a considerable mass of zinc metal was present at the cathode, and a crystalline ZnO deposit was apparent at the anode. The dashed line indicates that the dissolution resistance increased in the absence of dissolved zinc. The dissolution resistance at the termination of the experiment was marginally greater than that in the initially zincate-free solution, probably as a consequence of a decrease in electrolyte concentration (decrease in conductivity) associated with the precipitation of ZnO.

It is clear that increasing the zincate ion concentration results in a significant increase in the rate of discharge of a zinc electrode at overpotentials up to 100 or 200 mV. However, as the concentration of dissolved zinc increases in the bulk electrolyte phase, the useful potential "window" decreases before the onset of pseudopassivation and passivation behavior. This effect is shown in Figure 28, in which the potential at which passivation occurs on the anodic potentiodynamic sweep is plotted versus electrode rotation speed, as a function of zincate concentration. The passivation onset potential decreases monotonically with decreasing convection rate and increasing zincate concentration. Both these trends are to be expected if passivation is due to precipitation from a critically supersaturated solution.

Because these experiments were performed under potentiodynamic sweep conditions, several effects combine to produce the trends shown in

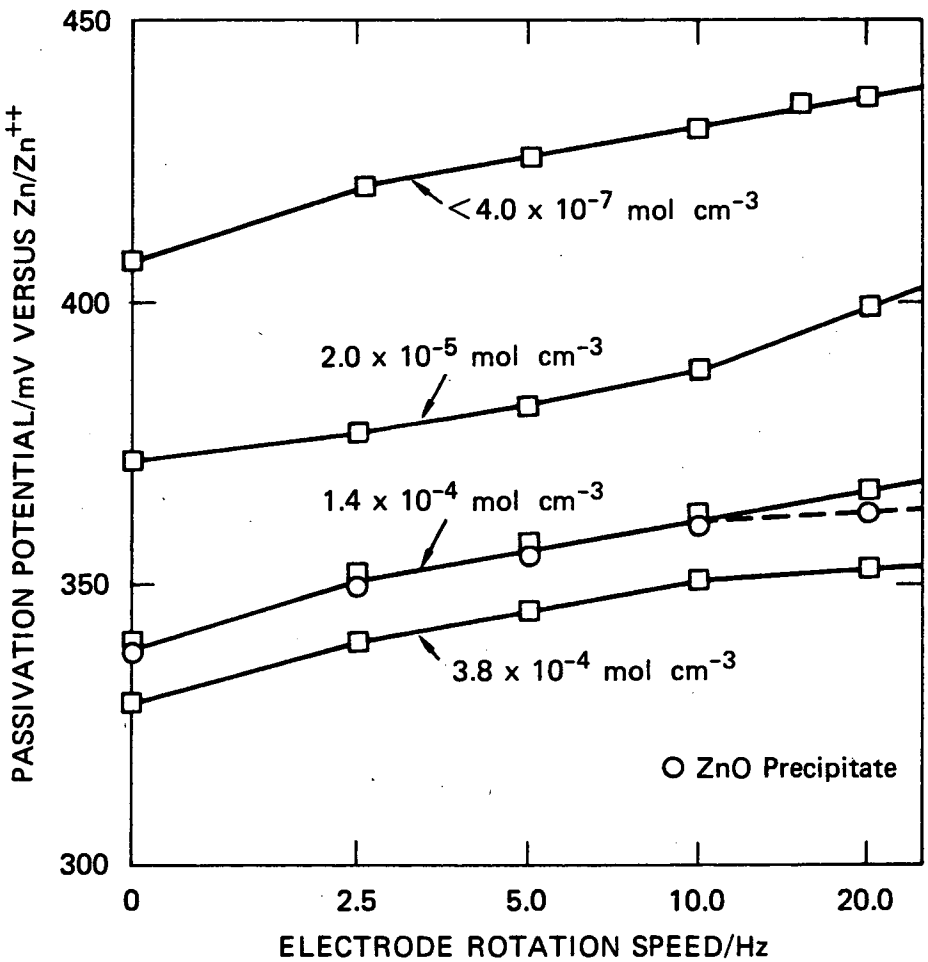

JA-350583-50R

FIGURE 28 THE PASSIVATION POTENTIAL OF ZINC VERSUS ELECTRODE ROTATION SPEED IN 30 wt% KOH AT 20°C, AS A FUNCTION OF ZINCATE CONCENTRATION

Potential sweep rate = 10 mV s^{-1}.

Figure 28. The critical level of supersaturation necessary for passivation presumably is the concentration of the zincate ion zincate concentration, achieved as the result of a dynamic equilibrium between the dissolution (discharge) and the diffusion rates. At low zincate concentrations and/or large rotation speeds, the diffusion rate is high, resulting in a large value of the passivation onset potential. At high zincate concentrations, the diffusion rate is low but the dissolution rate is high, resulting in passivation at lower potentials.

A plausible interpretation of these data is that the dissolution reaction is autocatalytic, possibly following a scheme of the type proposed by Armstrong and Bell[31] and Epelboin et al.,[32] involving a Zn^+ intermediate.

$$Zn(OH)_4^{2-} + Zn + \rightarrow 2Zn^+_{ads} + 4OH^- \tag{55}$$

$$Zn^+_{ads} - e^- \rightarrow Zn^{++} \tag{56}$$

Since anodic dissolution is observed in the complete absence of dissolved zincate, reaction (55) must be considered as occurring in parallel with a direct two-electron oxidation process (or a two-step process that does not involve zincate ions):

$$Zn - e^- \rightarrow Zn^+_{ads} \tag{57}$$

$$Zn^+_{ads} - e^- \rightarrow Zn^{++} \quad . \tag{58}$$

4.5 AC Impedance Results

In the previous sections we have developed an empirical model for the discharge of zinc in KOH, in terms of a convection-independent term and a term proportional to the thickness of the diffusion layer [equation (35)]. From the results of potentiodynamic sweep experiments as a function of dissolved-zinc concentration, we observed that discharge can be partly characterized in terms of parallel processes involving a convection independent conductance proportional to log (bulk zincate ion concentration), and a convection-dependent term [K in equation (53)]. We proposed that these observations could be explained in terms of an autocatalytic process involving an adsorbed Zn^+ species [equations (55) and (56)].

A series of AC impedance measurements was performed as a function of DC voltage, electrode rotation speed, zincate concentration, and temperature, using the methods described in Section 2.4 and elsewhere.[2,8] By conducting measurements over a very wide frequency range (10^{-3} to 10^{-4} Hz), the contributions to the convection independent terms (uncompensated electrolyte resistance, charge transfer impedance, and double-layer capacitance) and the diffusional processes (Warburg impedance) could easily be resolved. More importantly, the autocatalytic process represented by equation (56) should result in characteristic inductive behavior at low frequencies.[31-35]

Figure 29 shows results obtained at an anodic overpotential of approximately 100 mV for a zinc disk rotated at 10 Hz in a 35.5 wt% KOH solution, containing a small amount of zincate. The presence of an inductive loop is clearly evident in the impedance locus plot, with the impedance doubling back on itself in the three decades of frequency

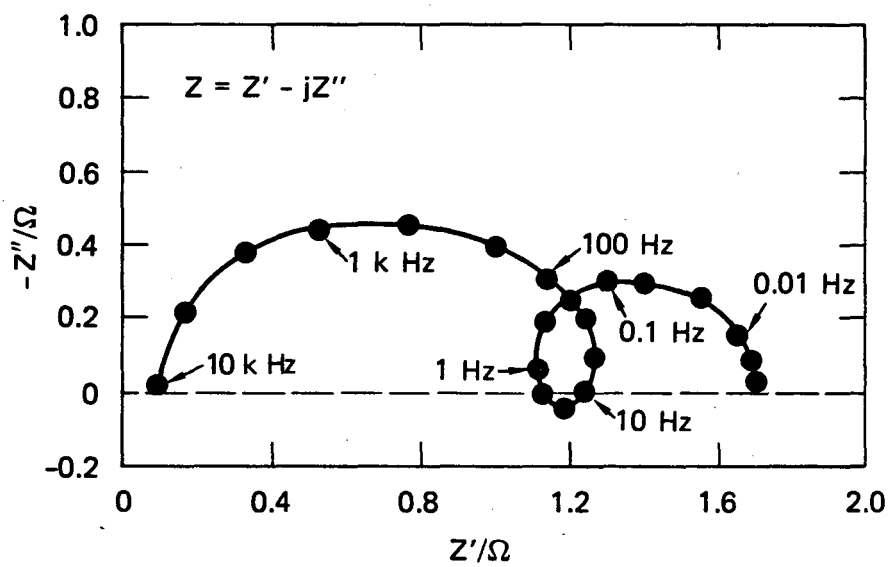

JA-350583-49

FIGURE 29 IMPEDANCE LOCUS SHOWING INDUCTIVE LOOP FOR Zn IN 35.5% KOH

Electrode rotation = 10 Hz, DC potential = -1350 mV versus Hg/HgO, Temperature = 25°C.

between 0.1 and 100 Hz. At frequencies lower than 0.1 Hz, the impedance response is associated principally with diffusional processes. At frequencies above 100 Hz, the impedance response is that of the charge transfer resistance (R_{ct} = 1.0 Ω) shunted by the double-layer capacitance. At limiting high frequencies, the impedance locus intersects with the real axis at the value of the uncompensated electrolyte resistance ($R_u \simeq 0.1$ Ω). The measured impedance response conforms to an equivalent circuit of the type shown in Figure 30.

The results shown in Figure 31 were obtained as a function of the rotation speed of a zinc disk electrode, held potentiostatically within the linear current/voltage discharge region, in initially zincate-free KOH. As expected, the high-frequency behavior (which is determined by R_u and the parallel combination of R_{ct} and C_{dl}) is relatively uninfluenced by electrode rotation speed. At low frequencies the impedance reponse is that expected for diffusion within a Nernst diffusion layer at finite thickness; that is, the impedance decreases with increasing rotation speed. At large rotation speeds and very low frequencies, the inductive effect due to the autocatalytic process can be seen as the impedance locus curves back toward the imaginary axis.

The data for nonzero rotation speeds in Figure 31 can be extrapolated to remove this inductive impedance, and used to estimate the low-frequency intercept associated with the diffusional process, R_{lf}. We find that for this data set,

$$R_{lf} = 2.91 + 7.88\ \omega^{-1/2} \quad ,$$

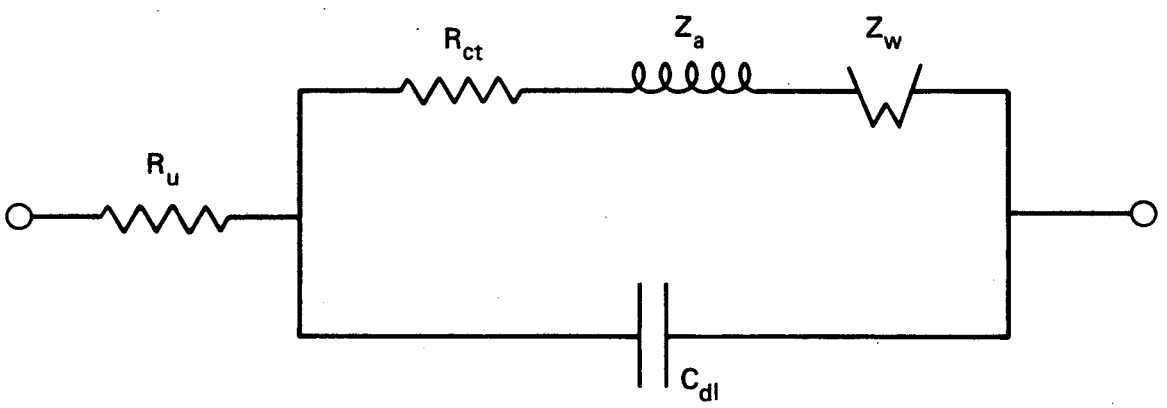

R_u = Uncompensated Electrolyte Resistance

R_{ct} = Charge Transfer Resistance

Z_a = Inductance Due to Adsorbed Species and/or Autocatalytic Effects

Z_w = Warburg Diffusional Impedance

C_{dl} = Double-Layer Capacitance

JA-1535-42

FIGURE 30 EQUIVALENT CIRCUIT FOR THE IMPEDANCE OF A ZINC ELECTRODE UNDERGOING DISCHARGE AT MODERATE ANODIC OVERPOTENTIALS

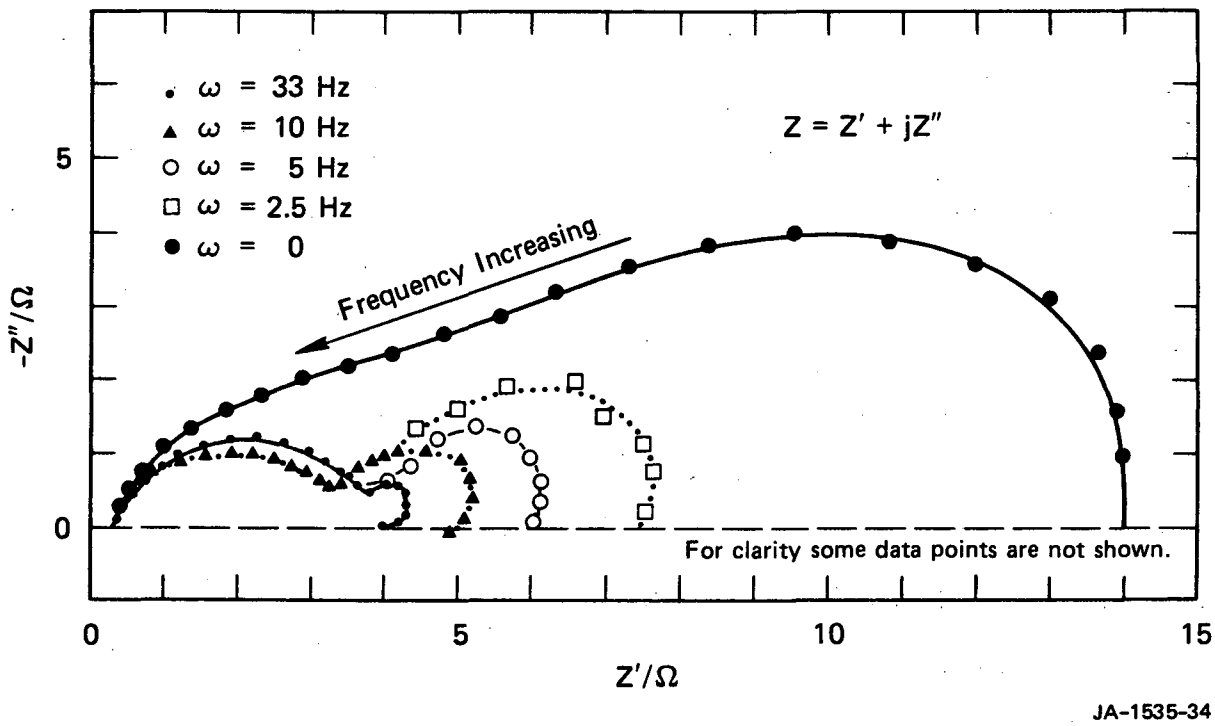

FIGURE 31 THE INFLUENCE OF ROTATION SPEED ON THE DISSOLUTION KINETICS FOR A ZINC DISK HELD AT +75 mV VERSUS Zn/Zn^{++}, IN 36 wt% KOH AT 25°C

with a regression coefficient of 0.992. Thus, the low-frequency (DC) resistance comprises a rotation-independent term (2.91 Ω = $R_u + R_{ct}$) and a rotation-dependent term (= 7.88 $\omega^{-1/2}$).

Both the diffusional impedance and the inductive impedance associated with an autocatalytic process may be influenced by the concentration of dissolved zincate ion. If the sequence of diffusional processes has a rate determined by the diffusion of zincate reactant to the interface (on charge) or the diffusion of zincate product from the interface (on discharge), then the overall rate will be influenced by the concentration of zincate ions in the bulk electrolyte. The bulk electrolyte zincate concentration and this diffusional flux will influence the autocatalytic process if this process involves a zincate ion intermediate [e.g. equation (55)]. Figures 32(a), 32(b) and 32(c) show the influence of zincate ion concentration on the measured impedance locus at 0 mV (equilibrium), -50 mV (charge) and +50 mV (discharge) anodic overvoltage, respectively. Under equilibrium conditions we observe, in Figure 32a, a family of curves with a trend towards decreasing impedance with increasing dissolved zincate concentration. Over a very wide range of frequencies down to the DC limit, these impedance data are dominated by a finite Warburg diffusional impedance. The data in Figure 32(a) are re-plotted in Figure 33(a), as a function of $\omega^{-1/2}$. At low frequencies (large $\omega^{-1/2}$) these plots are straight lines, with a slope equal to the Warburg diffusion coefficient, σ, which can be expressed as[8,23]

$$\sigma = \sigma_O + \sigma_R \tag{59}$$

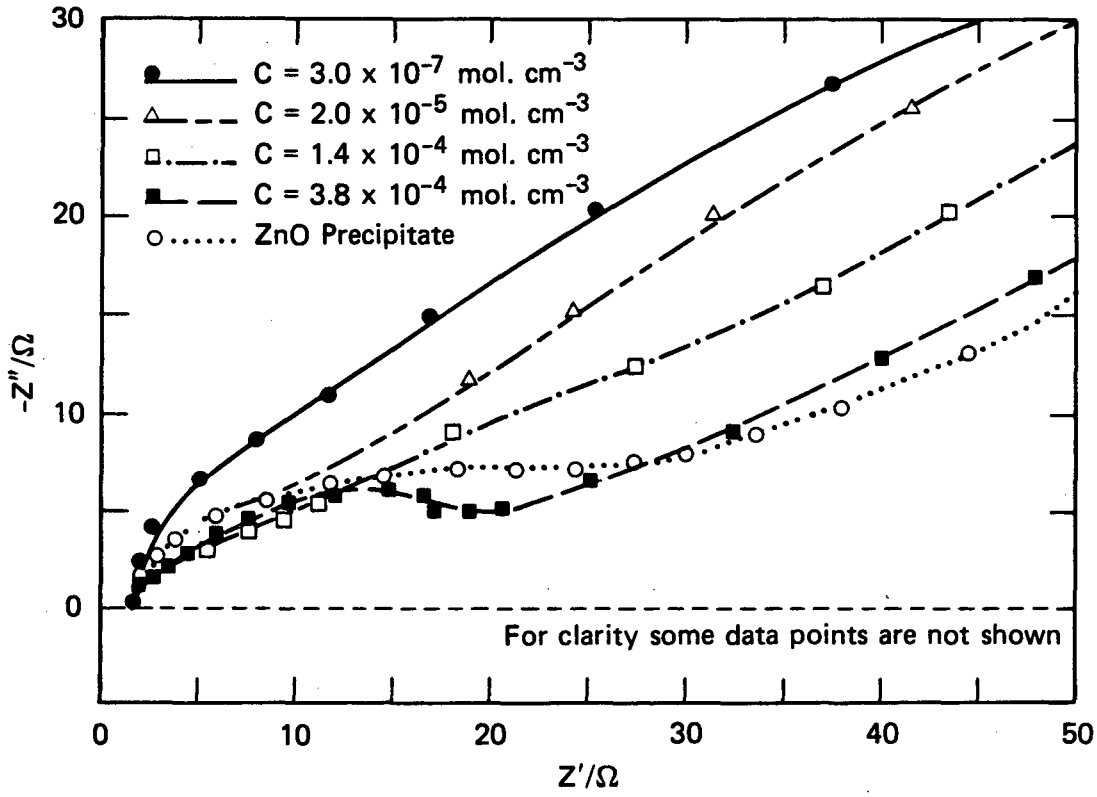

(a) MEASURED AT 0 mV VERSUS Zn/Zn^{++}

JA-1535-43

FIGURE 32 THE INFLUENCE OF ZINCATE ION CONCENTRATION ON THE IMPEDANCE LOCUS IN 30 wt% KOH, AT 25°C

Rotation speed = 10.0 Hz

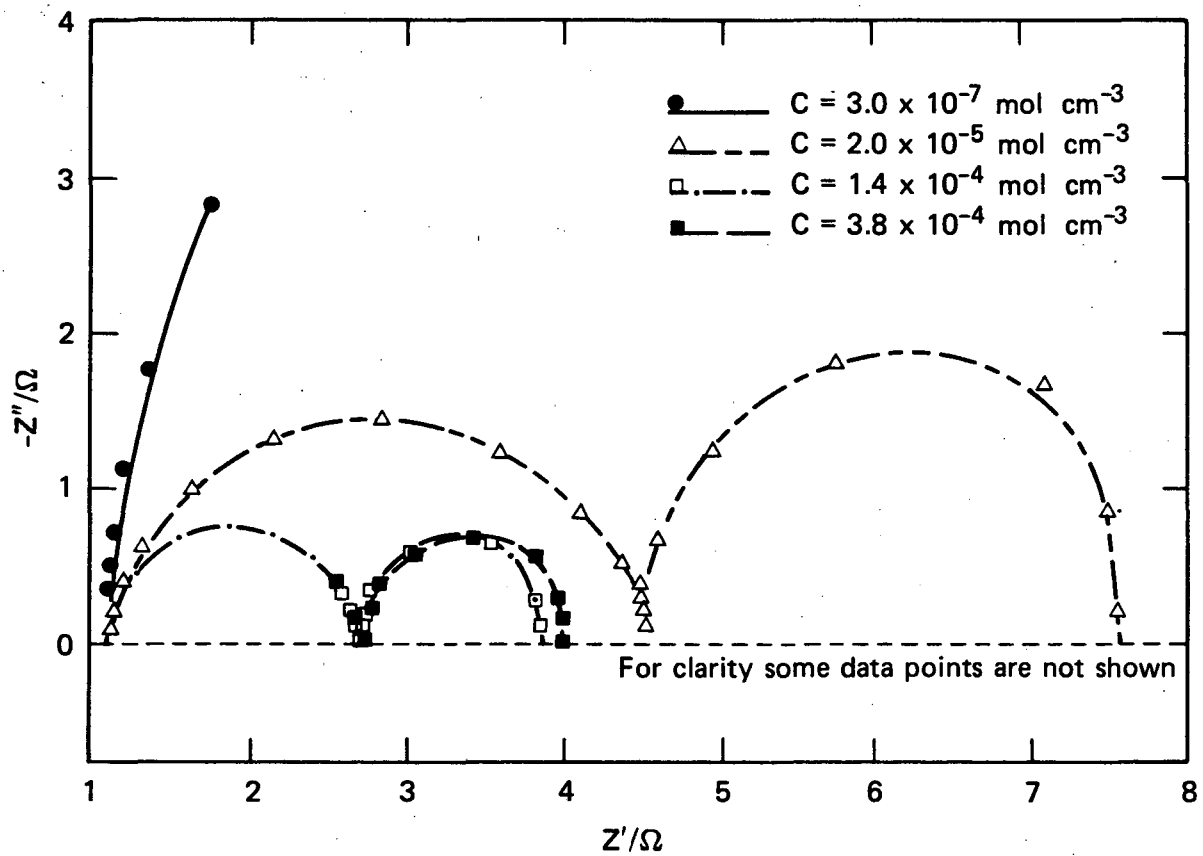

(b) MEASURED AT -50 mV VERSUS Zn/Zn^{++}

JA-1535-44

FIGURE 32 THE INFLUENCE OF ZINCATE ION CONCENTRATION ON THE IMPEDANCE LOCUS IN 30 wt% KOH, AT 25°C (Continued)

Rotation speed = 10.0 Hz.

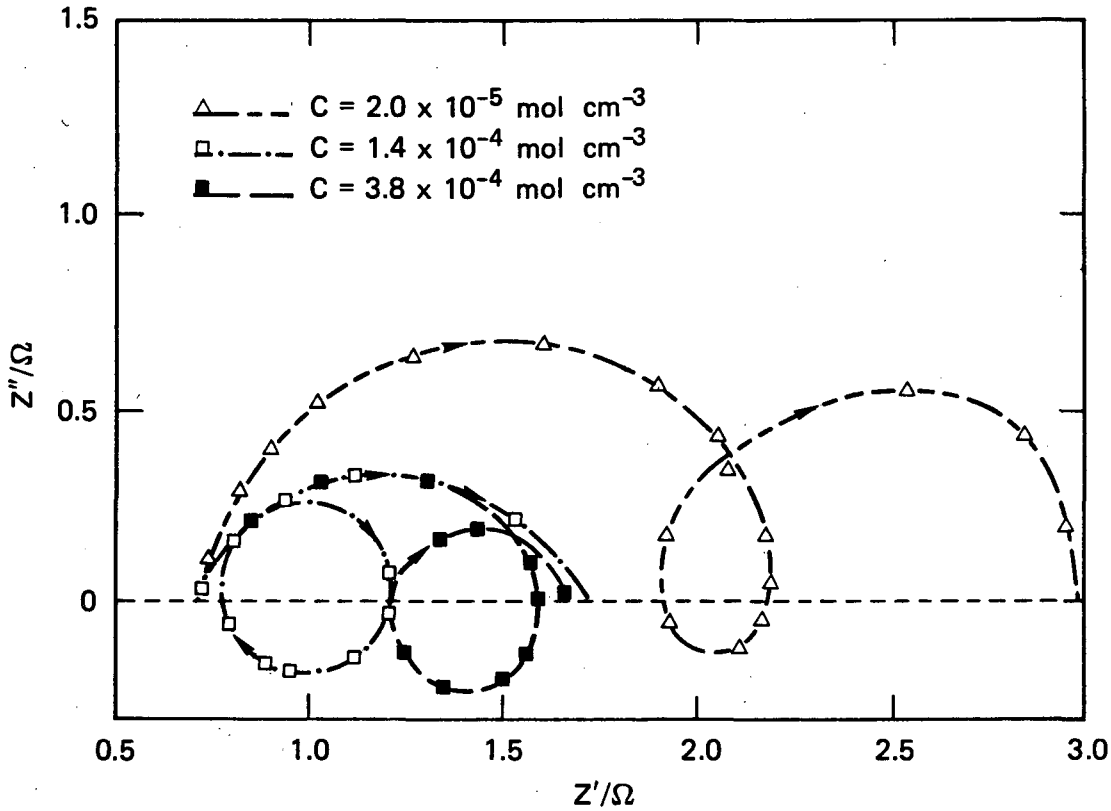

(c) MEASURED AT +50 mV VERSUS Zn/Zn^{++}

JA-1535-45

FIGURE 32 THE INFLUENCE OF ZINCATE ION CONCENTRATION ON THE IMPEDANCE LOCUS IN 30 wt% KOH, AT 25°C (Concluded)

Rotation speed = 10.0 Hz.

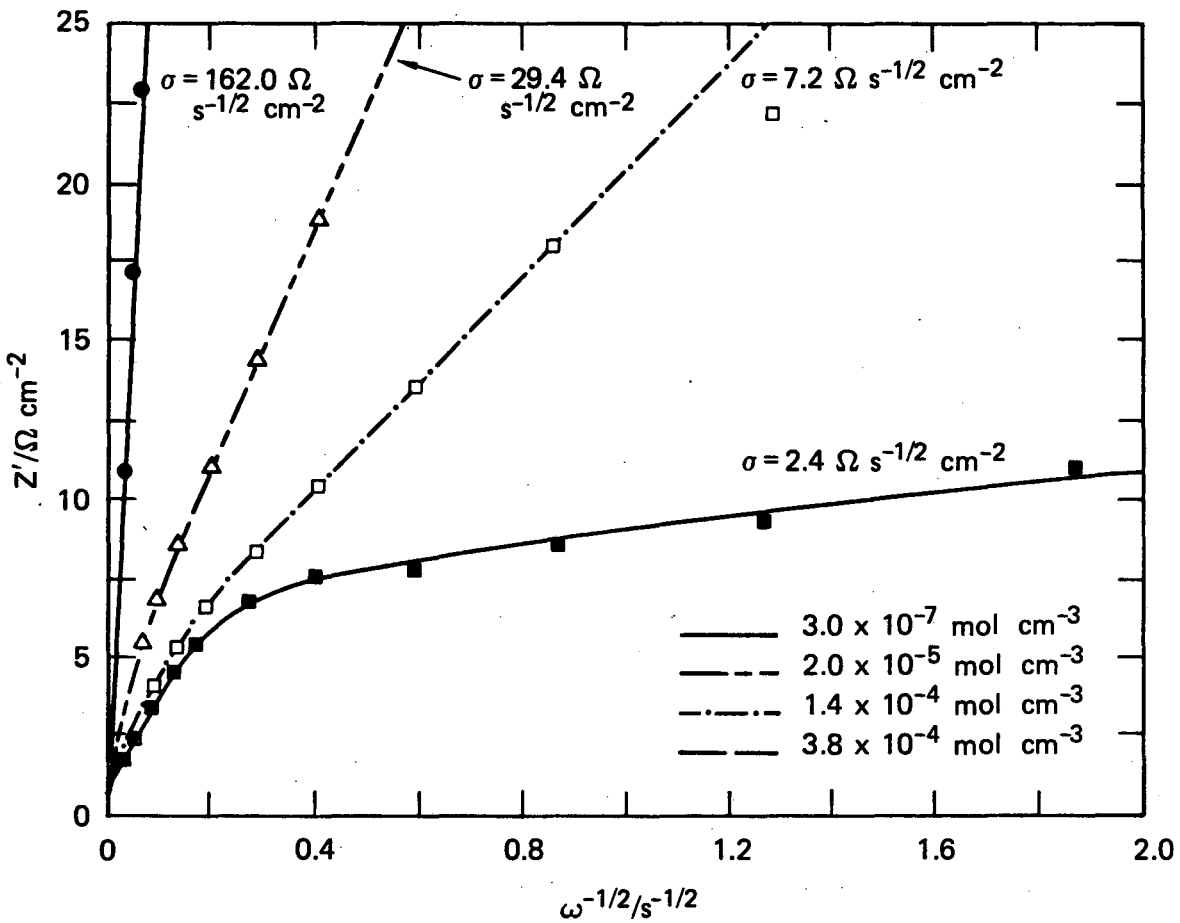

(a) PLOTTED FOR THE DATA IN FIGURE 32a

JA-1535-46

FIGURE 33 THE REAL COMPONENT OF IMPEDANCE VERSUS $\omega^{-1/2}$, AS A FUNCTION OF ZINCATE CONCENTRATION

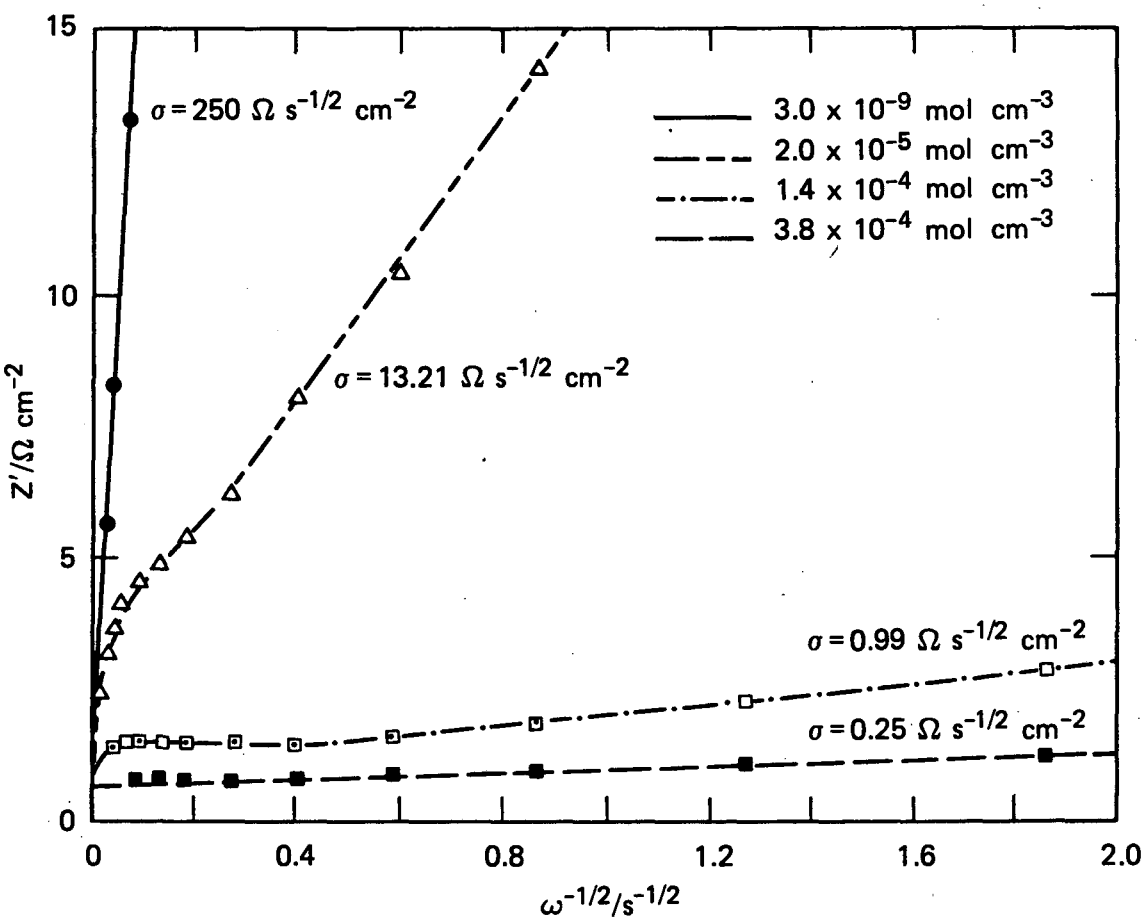

(b) PLOTTED FOR THE DATA IN FIGURE 32b

JA-1535-47

FIGURE 33 THE REAL COMPONENT OF IMPEDANCE VERSUS $\omega^{-1/2}$, AS A FUNCTION OF ZINCATE CONCENTRATION, FOR THE DATA IN FIGURE 32b (Concluded)

$$\sigma_O = \left[\frac{RT}{n^2F^2(2)^{1/2}}\right] \left[\frac{D_R^{-1/2} \exp(-\beta\eta)}{\alpha c_R \exp(\alpha\eta) + \beta c_O \exp(-\beta\eta)}\right] \tag{60}$$

$$\sigma_R = \left[\frac{RT}{n^2F^2(2)^{1/2}}\right] \left[\frac{D_R^{-1/2} \exp(-\alpha\eta)}{\alpha c_R \exp(\alpha\eta) + \beta c_O \exp(-\beta\eta)}\right] , \tag{61}$$

where α and β are the anodic and cathodic transfer coefficients, η is the applied DC overvoltage, and subscripts "O" and "R" refer to oxidation and reduction reactions, respectively.

Close to the equilibrium potential ($\eta \approx 0$), σ is a function of both the anodic and cathodic transfer coefficients, diffusion coefficient, and bulk concentrations. However, at potentials removed from the equilibrium potential, one process is dominant, and at large cathodic overvoltages equations (59) to (61) simplify to

$$\sigma = \frac{RT}{\beta n^2F^2c_R\ (2D_R)^{1/2}} \quad . \tag{62}$$

Figure 33(b) shows a plot of the real component of the impedance, measured at -50 mV, versus $\omega^{-1/2}$, as a function of zincate concentration. The values of σ that characterize the straight-line portions of these plots can be fitted to equation (62). If we assume that the concentration of reducible species (c_R) is identical to the known dissolved-zinc concentration, then we obtain the following regression equation.

$$\frac{1}{\sigma} = -9.116 + 10948\ [Zn^{++}]: \quad r^2 = 0.993.$$

The regression coefficient of 0.993 indicates that these data are a reasonably good fit to a straight line. We can calculate the diffusion coefficient, D_R, from the slope of regression line

$$\frac{d(1/\sigma)}{dc_R^b} = 10948 = \frac{A\ n^2F^2(2D_R)^{1/2}}{RT} \quad ,$$

where superscript "b" refers to bulk concentration. Assuming $\beta = 1/2$, we obtain $D_R = 1.08 \times 10^{-6}\ cm^2\ s^{-1}$, which is a plausible value for the zincate ion diffusing in concentrated KOH.

The preceding calculation suggests that the charging process proceeds in a relatively straight foward fashion, with the diffusional impedance dominated by the diffusion of reactant (i.e., zincate) to the electrode surface. However, the impedance locus plots in Figure 32(c) indicate that the discharge process is considerably more complex. In this case mass transport limitation may be imposed by the diffusion of OH^- ions to the interface, as well as the diffusion of product ("zincate") away. Unfortunately, at a rotation speed of 10 Hz the overall interfacial impedance contains terms associated with charge transfer and autocatalytic (inductive) processes, and we were not able to calculate σ from the data in Figure 32(c).

Figures 34(a) and 34(b) show impedance data taken at elevated temperatures in 35.5 wt% KOH, at 0 and +50 mV versus Zn/Zn^{++}, respectively. At the very low zincate ion concentrations present for these experiments, the inductive impedance is not dominant even at 50 mV anodic overpotential, and we were able to calculate σ as a function of electrolyte temperature. These data are presented in Table 16.

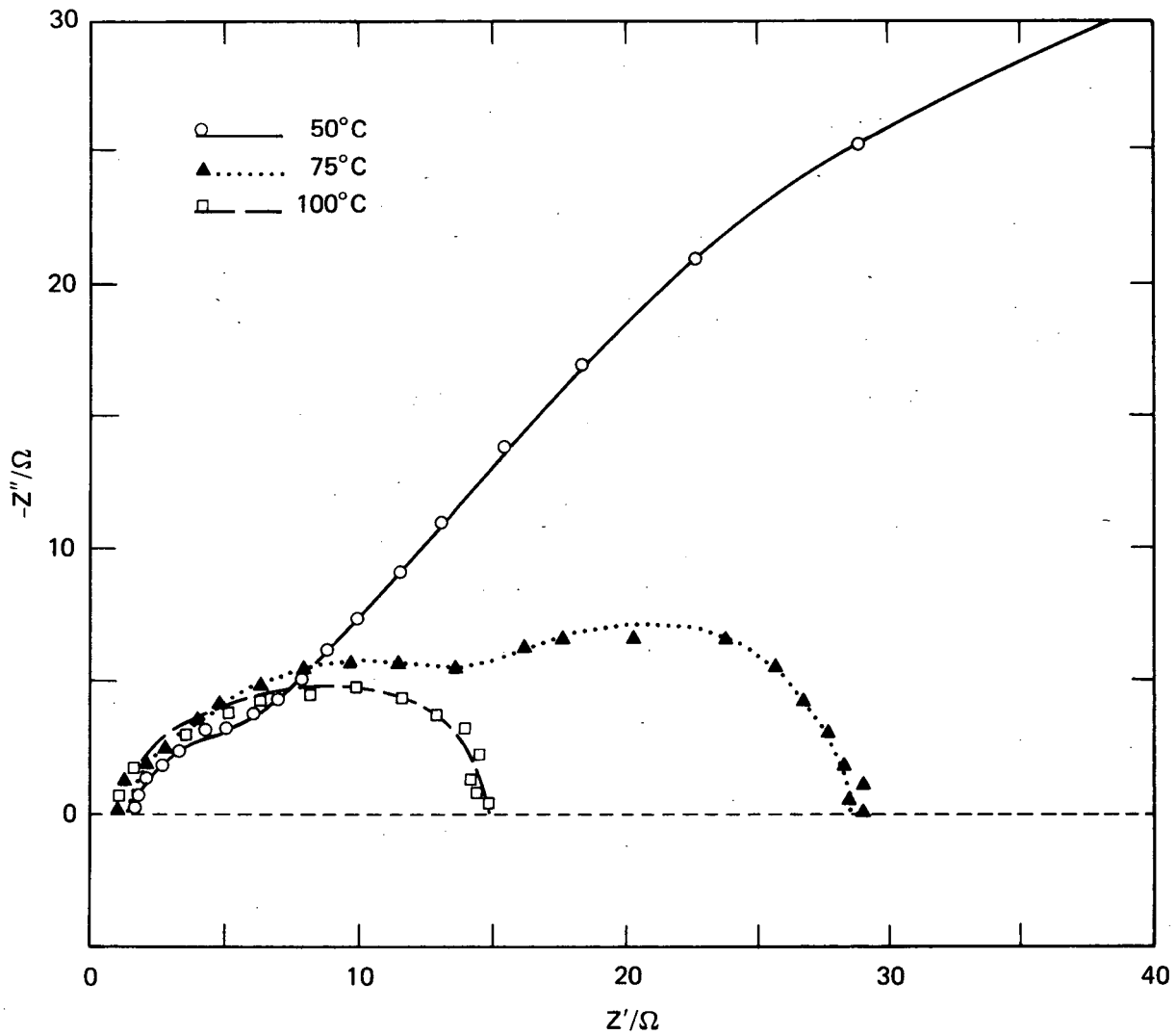

(a) MEASURED AT 0 mV VERSUS Zn/Zn^{++}

JA-1535-48

FIGURE 34 THE INFLUENCE OF TEMPERATURE ON THE IMPEDANCE LOCUS IN ZINCATE-FREE 35.5 wt% KOH

Rotation speed = 10.0 Hz.

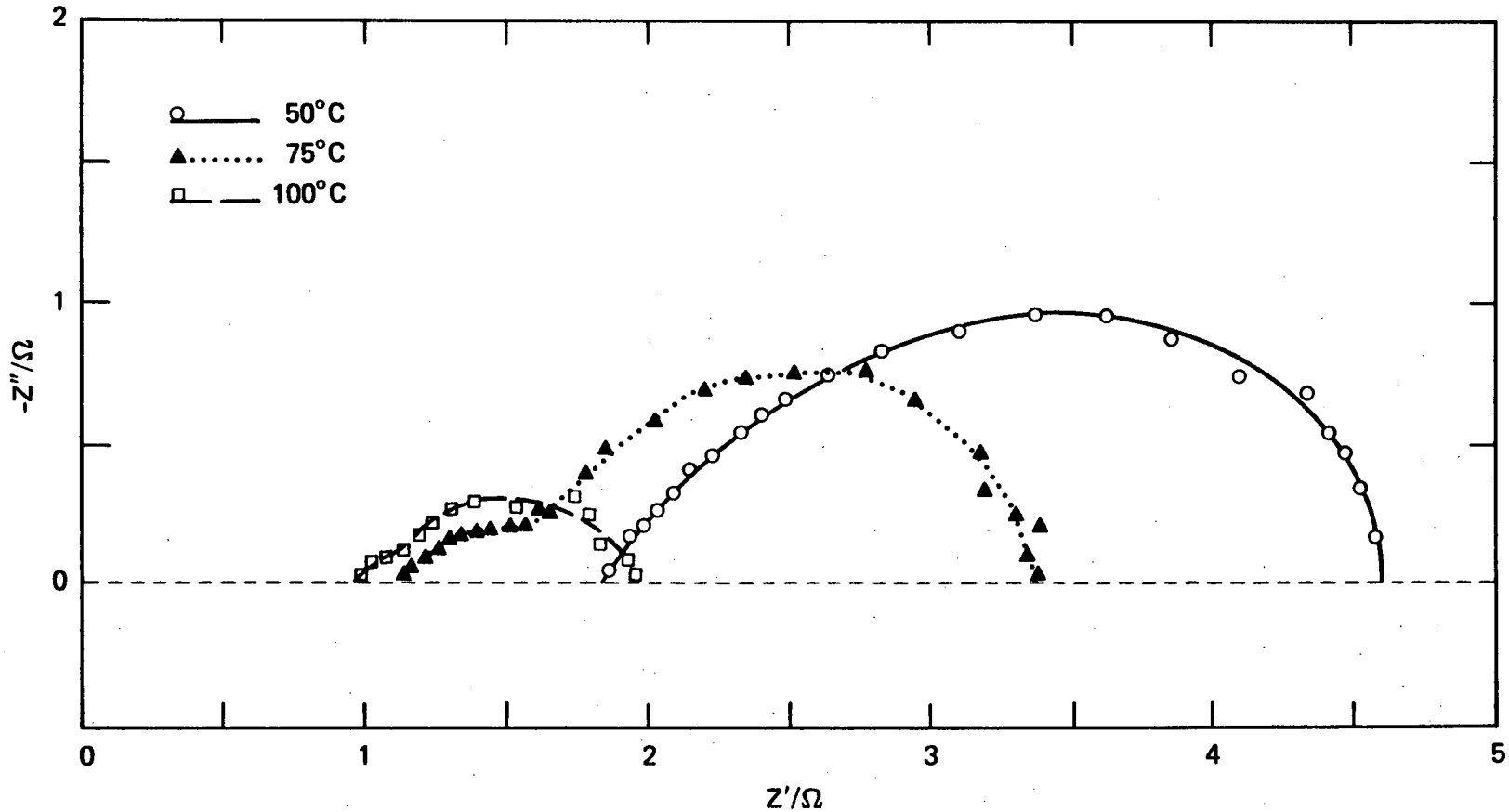

(b) MEASURED AT 50 mV VERSUS Zn/Zn^{++}

JA-1535-49

FIGURE 34 THE INFLUENCE OF TEMPERATURE ON THE IMPEDANCE LOCUS IN ZINCATE-FREE 35.5 wt% KOH (Concluded)
Rotation speed = 10.0 Hz.

Table 16

THE WARBURG DIFFUSION COEFFICIENT CALCULATED FROM THE IMPEDANCE MEASURED IN 35.5 WT% KOH

T/K	Φ/mV	$\sigma/\omega s^{-1/2} cm^{-2}$	$\frac{\sigma}{T}$ /Ω s^{-1} K^{-1} cm^{-2}
273	0	53.33	1.95×10^{-1}
298	0	22.14	7.43×10^{-2}
323	0	6.30	1.95×10^{-2}
348	0	1.92	5.52×10^{-3}
373	0	0.82	2.20×10^{-3}
273	50	35.71	1.31×10^{-1}
298	50	20.86	7.00×10^{-2}
323	50	9.04	2.80×10^{-2}
348	50	1.72	4.94×10^{-2}
373	50	0.40	1.07×10^{-3}

The last column in Table 16 displays σ normalized by the absolute temperature. With reference to equation (62), these data should display a residual temperature dependence only associated with the inverse square root of the diffusion coefficient. It is surprising, therefore, that σ/T displays a parabolic temperature dependence, as shown in Figure 35. This fit is almost exact, and the solid line in Figure 35 is the regression fit of the data obtained at η = 50 mV to an equation of the form

$$\frac{\sigma}{T} = a_0 + a_1 T + a_2 T^2 \quad . \tag{63}$$

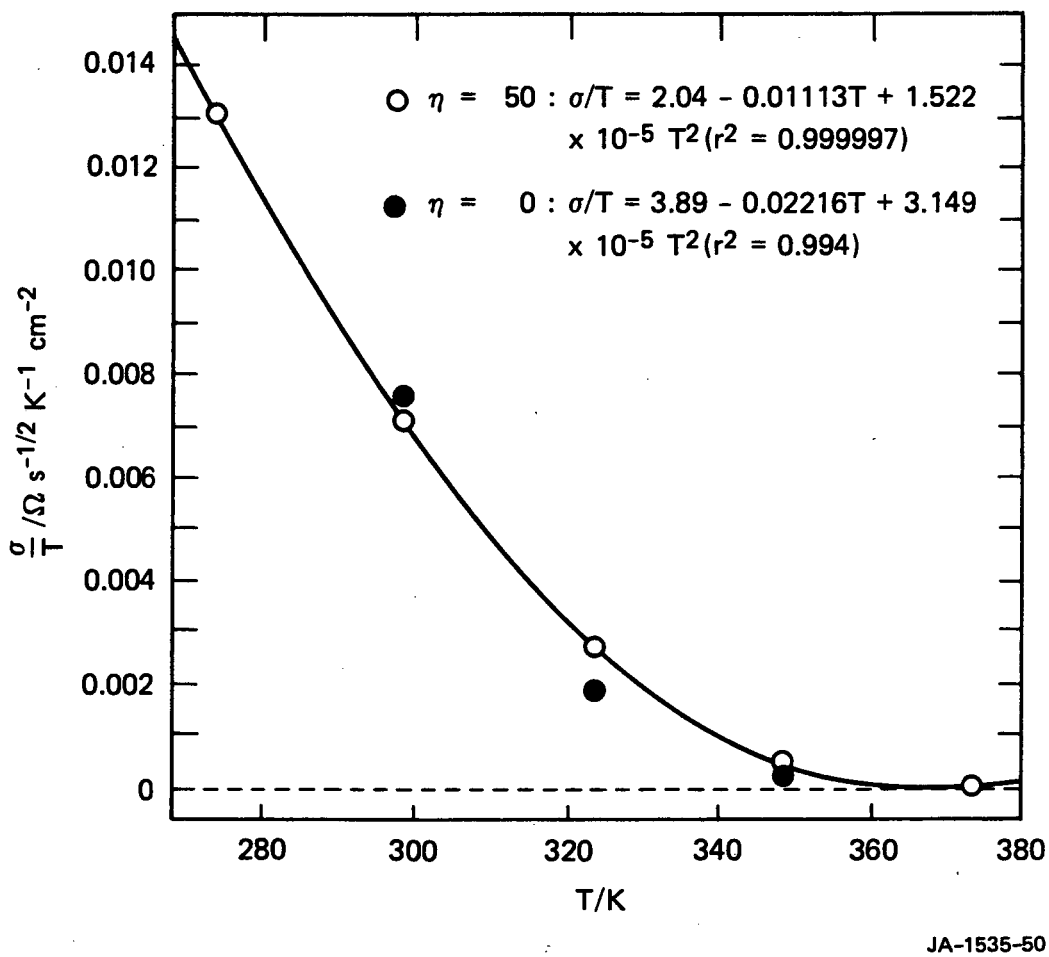

FIGURE 35 σ/T VERSUS T MEASURED IN ZINCATE-FREE 35.5 wt% KOH, AT 0 AND +50 mV ANODIC OVERPOTENTIAL

At present we have no explanation for the observed temperature dependence of σ. Experiments are under way to measure more carefully the influence of temperature and zincate concentration on the reaction resistance and the autocatalytic inductive impedance, as well as on σ, in order to develop a quantitative model for the discharge of zinc in concentrated alkali.

5 SUMMARY AND CONCLUSIONS

5.1 Introduction

A series of experiments has been performed in an attempt to elucidate the mechanisms of charge and discharge of iron and zinc electrodes in 30 and 35 wt% KOH. Particular emphasis has been directed toward determining possible operating limitations and modes of failure of batteries employing these electrodes, when operated at extremes of temperature.

The principal experimental methods used in this investigation were potential-sweep voltammetry and coulometry, rotating ring disk electrode and AC impedance measurements. Measurements on iron electrodes were confined to the influence of temperature at a single KOH concentration. Measurements on zinc electrodes also included the influence of KOH and dissolved zinc concentrations.

5.2 Observations of Iron Electrodes

Cyclic voltammetry as a function of potentiodynamic sweep rate was used to identify the mechanisms of dissolution and passivation of iron and to measure the kinetics of charge and discharge. It is apparent that under the experimental conditions of potentiodynamic cycling (which corresponds to rapid charging and discharging), the discharge rate is limited by the resistance of electrolyte in pores within the growing oxide. On subsequent charging after the formation of a homogeneous oxide film, the maximum charge rate is determined by the oxide resistance. This

resistance increases monotonically with decreasing temperature, and under extremely low ambient temperature conditions (< 0°C) this large film resistance could result in a substantially reduced charge acceptance rate for the iron electrode.

The results of AC impedance experiments support those derived from potentiodynamic cycling. During charging, charge acceptance is limited by diffusion and migration of ions within the oxide film. From results at high frequencies, we have calculated the exchange-current density for the interfacial charge transfer reaction. This increases from 3.76 mA cm^{-2} at 0°C to 9.98 mA cm^{-2} at 100°C.

The results of rotating ring disk electrode experiments show that dissolution of iron metal and oxide occurs within defined regions of potential during both the charge and discharge cycles. With experiments involving variation of the ring potential from reducing to oxidizing, we have identified the dissolved species that occur in each of six regions of potential. By integrating under disk and associated ring oxidation and reduction peaks, we have been able to quantify the extent of dissolution associated with each charge and discharge process, and to determine the effects of temperature on the dissolution phenomenon. Within the potential region of interest for an iron battery electrode, the extent of dissolution increases with increasing temperature. Thus, dissolution accounts for 0.08% of the total electrode charge at 0°C, increasing to more than 7.5% at 75°C. It is clear that electrode dissolution may severely limit coulombic efficiency at elevated temperatures and may cause problems associated with shape change if iron electrodes are repeatedly cycled at high temperatures.

From the results of the experiments previously described, and by using tabulated results[3] of our previous thermodynamic calculations, we have been able to postulate a comprehensive charge and discharge reaction scheme for the iron electrode in concentrated hydroxide. In particular, the results of potentiodynamic sweep RRDE experiments has been extremely useful in determining which reactions involve dissolved intermediates. The detailed reaction sequences in Figure 20 for high- and low-temperature conditions are shown separately. This proposed mechanism should be regarded not as definitive but as a working hypothesis to further experi mentation. Simplified versions of the oxidation and reduction reaction sequences at high and low temperatures are presented in Figure 21.

5.3 Observations of Zinc Electrodes

In contrast to the iron electrode, in which charge/discharge kinetics are controlled by the electrode/electrolyte interfacial impedance and oxide film resistance, the discharge of zinc prior to passivation is dominated by mass transport processes. Accordingly, potentiodynamic studies of Zn were performed with rotational speed as the principal independent variable.

The discharge of zinc initially follows a Butler-Volmer rate law, but this rapidly gives way to a linear current/voltage region before the onset of pre-passive, pseudopassive, and true passive behavior. The linear region covers most of the potential "window" of interest in the discharge of zinc battery electrodes, and this region has received most of our attention. We have made a number of experimental observations of the discharge behavior of rotating zinc disk and ring- disk electrodes, which

are described fully in Section 4 of this report and in previous publications.[2-8] We have observed a number of empirical laws of behavior that have yet to be molded into a cohesive model for the mechanisms of discharge of zinc in concentrated hydroxide electrolytes.

The critical observations can be summarized as follows:

(1) The slope that characterizes the linear discharge region defines a resistance ($R = dV/dI$), which can be separated into a convection independent term (R°) and a term that depends on the electrode rotation speed.

(2) With increasing temperature the rotation-dependent and rotation-independent terms change monotonically in such a way as to increase the dissolution rate at constant voltage.

(3) With increasing dissolved-zinc concentration, the convection-dependent term changes in such a way as to increase the dissolution rate at constant voltage to an extent roughly proportional to the logarithm of the total dissolved-zinc concentration.

(4) The potential at which the electrode passivates increases with increasing electrode rotation speed or decreasing-dissolved zinc concentration.

(5) The collection efficiency measured for a zinc RRDE decreases with increasing electrode rotation speed. From a simple analysis based on the concept of a mean transit time between disk and ring, we were able to show that this variation is consistent with the production of an electroreducible species by a first-order homogeneous chemical reaction in the electrolyte phase.

(6) At low dissolved-zinc concentrations in the bulk electrolyte and low anodic overpotentials, the impedance of the zinc electrode is dominated by diffusion within a finite diffusion layer. This diffusional impedance has the same dependence on rotation speed dependence as that noted in (1).

(7) At large dissolved-zinc concentrations and large (> 20 mV) anodic overpotentials, the impedance of the zinc electrode displays an inductive loop characteristic of autocatalytic behavior.

(8) The Warburg diffusion coefficient, σ, measured in the range 0 to +50 mV, is proportional to the inverse of the dissolved zinc concentration. That is, diffusional limitation of zinc electrode dissolution (discharge) is imposed by the transport of the final product material to the electrode.

(9) With increasing temperature the Warburg diffusion coefficient normalized by temperature, σ/T, decreases with a well-obeyed parabolic temperature dependence.

On first inspection many of these results are unexpected, and some apparently are in conflict. For example, σ/T is expected to have a residual temperature dependence associated only with the inverse square root of the diffusion coefficient and not that described in observation (9). Likewise, the autocatalytic behavior suggested by observations (3), (7), and (8) is unusual; and a diffusional process that gives rise to a resistance independent of discharge current, as indicated by observations (1) and (6), is not typically associated with electrode dissolution.

5.4 A Model for the Dissolution and Passivation of Zinc

We believe that our observations of the discharge behavior of zinc electrodes can be explained by a single cohesive model for the dissolution and passivation of zinc in concentrated alkali. The basic tenets of this model are as follows.

To remain as general as possible, we have previously described the ultimate product of the dissolution of zinc as "dissolved zinc." This product is frequently described in the literature as "zincate," and we will assume this species to be $Zn(OH)_4^{=}$.

We propose that the dissolution of zinc in 30 or 35 wt% KOH that is initially devoid of zincate proceeds initially via two one-electron transfer reactions of the form

$$\text{Slow:} \quad Zn - e^- \rightarrow Zn^+_{ads} \tag{64}$$

$$\text{Fast:} \quad Zn^+_{ads} - e^- + 2OH^- \rightarrow Zn(OH)_2 \quad . \tag{65}$$

Reaction (64) is slow and rate determining. At very low anodic overpotential ($0 < \eta < 10$ mV), in the absence of dissolved zinc, a Tafel law behavior is observed corresponding to

$$I = i_o \exp\,[\eta RT/\alpha\eta F] \quad . \tag{66}$$

We postulate that $Zn(OH)_2$ is an intermediate product that reacts chemically to produce the ultimate product, zincate, as follows:

$$Zn(OH)_2 + 2OH^- \rightarrow Zn(OH)_4^= \quad . \tag{67}$$

Zinc hydroxide forms on the electrode at all potentials more positive than the reversible potential for equation (65). This material is porous and only loosely adherent (as observed by Breiter[28]). We propose that the electrochemically formed $Zn(OH)_2$ is in chemical equilibrium with the zincate product:

$$Zn(OH)_2 + 2OH^- \rightleftarrows Zn(OH)_4^= \quad . \tag{68}$$

Under RRDE conditions, only $Zn(OH)_4^=$ is detectable on the ring [$Zn(OH)_2$ is uncharged and solid], and the collection efficiency is less than that predicted theoretically, by the amount of $Zn(OH)_2$ that is convected beyond

the radius of the ring. When the equilibrium rate constant for reaction (68) is low or the rotation speed high, the observed collection efficiency will be decreased, as indicated by observation (5) above.

When the local zincate concentration is increased, an alternative to reaction (64) becomes feasible;

$$Zn + Zn(OH)_4^{=} \rightarrow 2Zn^{+}_{ads} + 4OH^{-} \quad . \tag{69}$$

It is this disproportionation reaction that provides the autocatalytic effect noted by observations (3), (7), and (8). It should be noted that the electrochemical reaction (64) and the disproportionation reaction are parallel pathways that occur simultaneously at different rates.

We are now able to explain the seemingly anomalous influence of mass transport on the dissolution rate. The evidence of potentiodynamic sweep and AC impedance measurements indicates clearly that the discharge of Zn electrodes at an overvoltage of more than 10 or 20 mV is rate limited by mass transport within a finite diffusion layer. Yet rate limitation due to the diffusion of OH^- <u>to</u> the electrode would result in a current plateau (i.e., a resistance tending to infinity as the current is increased) rather than the observed constant "diffusional resistance." Also, the rate of diffusion of product <u>from</u> the electrode should become less as the bulk concentration of product is increased, but the opposite is observed.

We suggest that mass transport limitation is imposed by the diffusion of zincate <u>to</u> the electrode surface. This diffusional flux can be expressed simply as

$$J = D \frac{c^o - c^i}{\delta} \quad , \tag{70}$$

where δ is the diffusion layer thickness (and is proportional to the inverse square root of the rotation speed), and c is the zincate concentration (superscripts "o" and "i" refer to the "outside" and "interface" sides of the diffusion layer, respectively). The predicted dependence of J on the bulk concentration of zincate and on the rotation speed clearly is well obeyed. What is not quite so clear is the dependence of J on the overall current density. We can assume that under mass-transport limited conditions, the concentration of zincate at the interface is zero (c^i = 0). To predict the observed linear dependence of current (αJ) on overvoltage, therefore, c^o must increase linearly with current [equation (67)]. Since zincate is in equilibrium with the initial product, $Zn(OH)_2$, we simply require a linear increase with current of the $Zn(OH)_2$ concentration at the outside of the diffusion layer.

Figure 36 presents a general, qualitative picture of our proposed reaction scheme for the case where the autocatalytic step [reaction (2) in Figure 36] is completely under mass transport control. With increasing bulk zincate concentration, the diffusional flux of zincate to the interface is increased [Figure 36(a)], and the reaction current at constant voltage is proportionally increased. Figure 36(b) shows the effect of increasing the applied voltage. As the voltage is increased, reactions

(1) $Zn - e^- \rightarrow Zn^+$

(2) $Zn + Zn(OH)_4^= \rightarrow 2Zn^+ + 4OH^-$

(3) $Zn^+ - e^- + 2OH^- \rightarrow Zn(OH)_2$

(4) $Zn(OH)_2 + 2OH^- \rightarrow Zn(OH)_4^=$

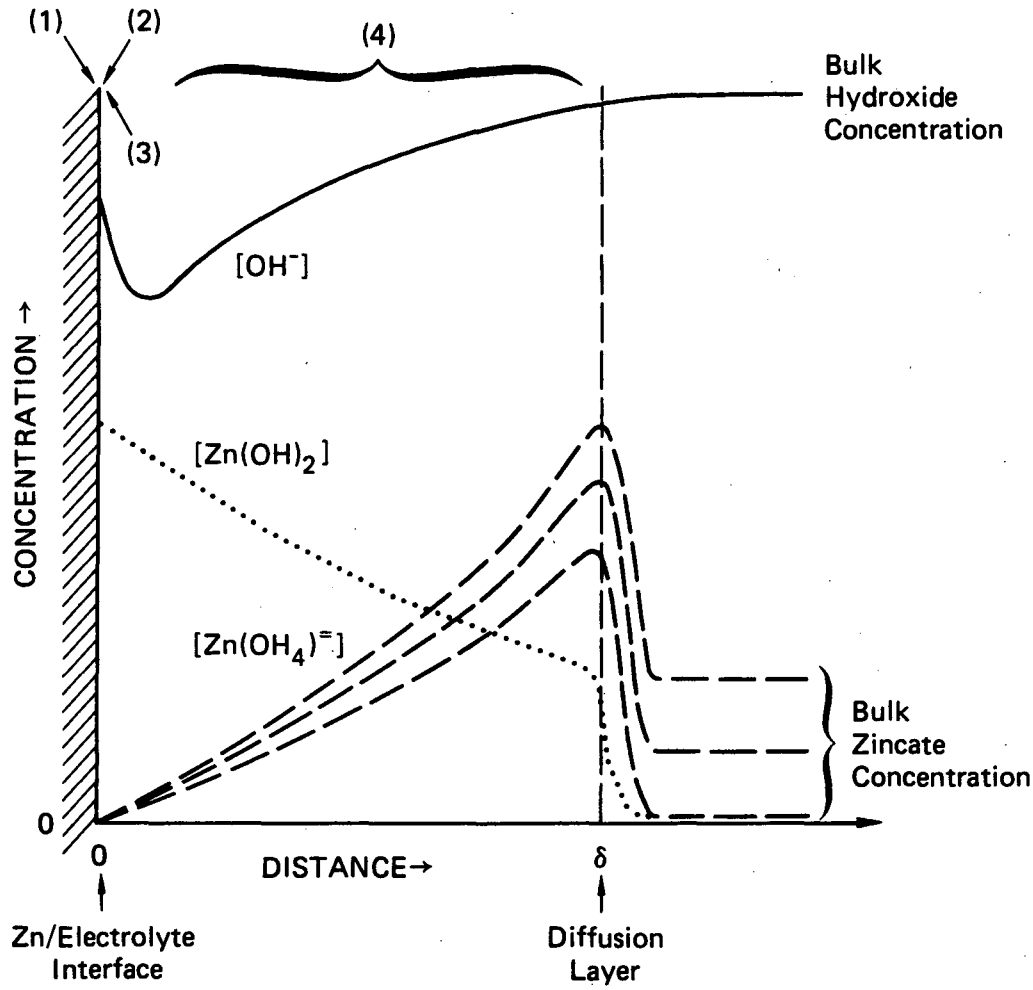

(a) THE INFLUENCE OF BULK ZINCATE ION CONCENTRATION

JA-1535-52

FIGURE 36 REACTIONS AND DIFFUSION PROFILES FOR THE PROPOSED MECHANISM OF THE ELECTROCATALYTIC DISSOLUTION OF ZINC UNDER MASS TRANSPORT CONTROL

(1) $Zn - e^- \rightarrow Zn^+$

(2) $Zn + Zn(OH)_4^= \rightarrow 2Zn^+ + 4OH^-$

(3) $Zn^+ - e^- + 2OH^- \rightarrow Zn(OH)_2$

(4) $Zn(OH)_2 + 2OH^- \rightarrow Zn(OH)_4^=$

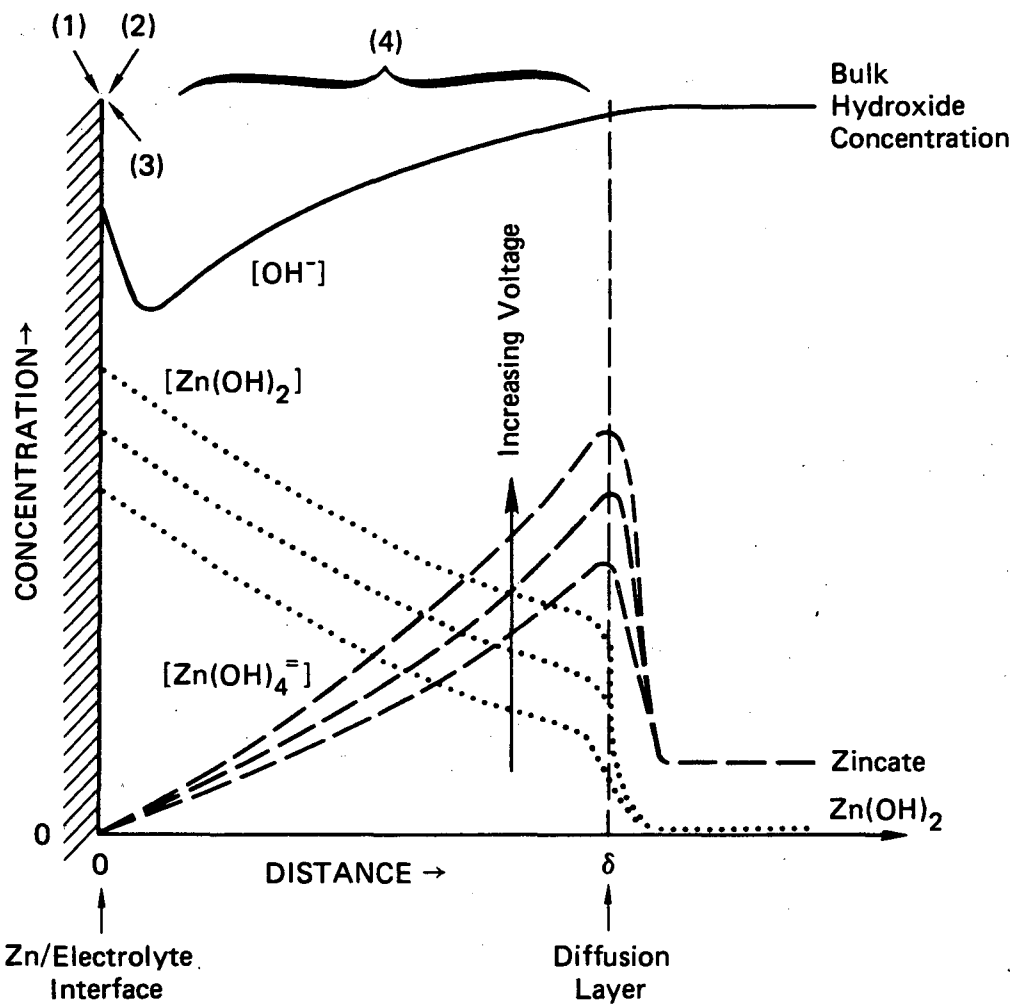

(b) THE INFLUENCE OF APPLIED POTENTIAL

JA-1535-53

FIGURE 36 REACTIONS AND DIFFUSION PROFILES FOR THE PROPOSED MECHANISM OF THE ELECTROCATALYTIC DISSOLUTION OF ZINC UNDER MASS TRANSPORT CONTROL (Concluded)

(1) and (3) proceed at higher rates,* and the concentration of $Zn(OH)_2$ at the interface increases. Since $Zn(OH)_2$ and $Zn(OH)_4^{=}$ are in equilibrium via reaction (4), the increase in voltage and the increase in bulk zincate concentration both result in a higher zincate flux to the electrode and thus in a higher current. Decreasing the thickness of the diffusion layer (e.g., by increasing the rotation speed) has a similar effect on the zincate diffusion flux and the current. It should be noted that reaction (4) procedes very slowly, and it is probable that equilibrium conditions are not attained within the diffusion layer, particularly at low temperatures. This does not affect the qualitative significance of the model since we require only that reaction (4) procedes to the right at a finite rate within the boundary layer.

Electrode passivation occurs in a two-step process that involves the formation of prepassive and true passive films. When the reaction rate is increased (by increasing the anodic overvoltage), a porous film begins to accumulate on the electrode. At some point the transport of material across this prepassive film becomes rate limiting, and the slope of the current/voltage curve begins to decrease ($R = dV/dI \rightarrow \infty$). Under some conditions a potential region in which the current is independent of voltage can be seen prior to passivation. This effect is associated with mass transport limitation in the prepassive film, <u>not</u> in the free electrolyte phase. Under these conditions the electrolyte composition in

*We have described the case in which reaction (2) is completely controlled by the diffusion of zincate, but in reality the rate of this reaction also would increase as the anodic overvoltage is increased.

the pores may become very different from that of the bulk electrolyte, and we propose that passivation occurs when the pH at the base of the pores becomes sufficiently low to favor the formation of ZnO over $Zn(OH)_2$ as the initial product:

$$Zn^{+} - e^{-} + 2\bar{O}H \rightarrow ZnO + H_2O \quad . \tag{71}$$

ZnO is nonporous and relatively insoluble in the electrolyte. Following formation of the true passive ZnO film, the current drops to a low value and the residual prepassive film material dissolves, leaving an exposed ZnO surface. In this condition one of two things can happen. If the transport of OH^- through the ZnO is sufficient to maintain the film thickness in a steady state with the dissolution reaction, then the film remains passive. If the high-field migration rate is too low, the film will dissolve and the electrode will again establish the prepassive conditions. Hydroxide ions will be depleted within the pores of the prepassive film, ZnO will form, the electrode will passivate, etc. This cycle may repeat indefinitely.

It is important to notice that, since we consider reaction (4) to occur with a variable rate throughout the diffusion layer, the diffusion profiles are not linear. For example, three factors influence the $[OH^-]$ profile. Hydroxide ions are consumed in the overall reaction, reaction (4) occurs with a variable rate throughout the diffusion layer and reaction (2) releases hydroxide in the vicinity of the interface. This nonlinearity and the complexity of the proposed reaction scheme contribute greatly to the difficulty of translating the qualitative model described above, and shown schematically in Figure 35, into a quantitative model for the dissolution of zinc.

5.5 Conclusions

The models we have developed for the dissolution and passivation of iron and zinc in concentrated alkali have a number of important consequences for the use of iron/nickel oxide and zinc/nickel oxide batteries. It is apparent that oxidation and subsequent reduction of Fe electrodes is largely impeded by migration and diffusion processes within the oxide film. Thus, discharge and charge acceptance rates might well be improved by modifying the film structure, possibly by the addition of suitable dopant ions. It is clear also that the various dissolution processes observed for iron reflect integral steps in the mechanisms of charge and discharge. Suppressing the solubility of these species without providing an alternative reaction path will result only in decreased reaction rate. Nevertheless, intelligent use of the reaction scheme that we have proposed might well lead to a class of additives that will alleviate the problem of coulombic inefficiencies due to dissolution at high temperature, without kinetic losses at low temperatures.

Our model for zinc involves autocatalysis and mass transport limitation by the zincate ion, and two-stage passivation involving $Zn(OH)_2$ and ZnO. A conclusion is that this model provides a mechanism for "shape change" of zinc electrodes. If the reaction initially proceeds at a greater rate in one part of the electrode than another (e.g., edge > center due to the primary current distribution), then, because the product catalyzes the reaction, the two rates will diverge. In a more normal reaction scheme, the presence of product tends to impede the forward reaction, and rates tend to become uniform over an electrode surface. For an autocatalytic reaction of the type proposed, initial nonuniformities

are amplified during discharge. This is an extension of the model proposed by McBreen[36] in which asymetric dissolution is attributed to the nonuniform primary current distribution. We invoke the concept of autocatalysis to explain the persistance (in fact acceleration of) current nonuniformity following the accumulation of product in the vicinity of the electrode. The data presented by McBreen[36] for early cycles of a zinc negative electrode, show flat current profiles for the inner regions of a zinc plate, while the currents at the peripheral sections accelerates with discharge time, consistent with our model.

5.6 Suggestions for Further Work

The models proposed for the dissolution and passivation of zinc and iron require further testing, and a number of specific experiments are suggested.

(1) A series of potential-step experiments should be performed in zincate-free KOH, to examine the evolution of the diffusion layer and the autocatalytic process. In the complete absence of dissolved zinc, only the direct one-electron transfer ($Zn - e^- \rightarrow Zn^+$) can occur. By following the current transients following a potential step from zero to an anodic overvoltage, it should be possible to destinguish the direct from the autocatalytic process in the overall reaction.

(2) The formation of prepassive and passive films should be followed directly, using optical, semiconductor, and AC impedance techniques. In particular, since $Zn(OH)_2$ and ZnO are likely to be semiconductors, following the photocurrent as a function of electrode potential should yield valuable information regarding the existence, nature, and thickness of any films present.

(3) The results of these and further experiments should be applied in a quantitative way to refine the present model or improve the modeling work of others.[37]

(4) Semiconductor electrochemistry techniques also may be of great value in determining the nature and conductivity of the oxide films formed during the discharge of iron. Light effects should be used to evaluate the role and utility of dopants intended to increase oxide conductivity, thus reducing kinetic losses in low-temperature operation.

(5) Further RRDE studies should be performed at elevated temperatures to determine which electrolyte additives increase and which decrease the dissolution of iron.

5.7 Comment

It is apparent that the learning curve for the development of iron/nickel oxide and zinc/nickel oxide alkaline battery electrodes is approaching a plateau, and that further engineering modifications and phenomenological computer modeling will produce little improvement. Both techniques require input regarding the underlying nature of the processes being investigated.

It is our belief that the missing information, that is a prerequisite for a breakthrough in battery technology, is a detailed knowledge of the reaction sequences and mechanics that constitute the overall reaction mechanism. We believe that this report represents a step in this direction.

REFERENCES

1. "Power Systems for Electric Vehicles," U.S. Department of Health, Public Service Publication No. 999-AP-37 (1967).

2. M.C.H. McKubre and D. D. Macdonald, "The Temperature Limitations of Alkaline Battery Electrodes," Volume I, Final Report to DOE, Contract EM-78-C-01-5159, 1979.

3. D. D. Macdonald and M.C.H. McKubre, "The Temperature Limitations of Alkaline Battery Electrodes," Volume II, Final Report to DOE, Contract EM-78-C-01-5159, 1979.

4. M.C.H. McKubre and D. D. Macdonald, J. Electrochem. Soc. 127, 632 (1980).

5. M.C.H. McKubre and D. D. Macdonald, J. Electrochem. Soc. 128, p. 524 (1981).

6. M.C.H. McKubre and D. D. Macdonald, IECEC 15, 1207 (1980).

7. D. D. Macdonald and M.C.H. McKubre, "Electrochemical Impedance Techniques in Corrosion Sciences," Symposium on Progress in Electrochemical Testing, ASTM, May 1979.

8. D. D. Macdonald and M.C.H. McKubre, " Impedance Measurements in Electrochemical Systems," in Modern Aspects of Electrochemistry, Vol. 15 (1980), J. O'M Bockris and B. E. Conway, Eds.

9. M.C.H. McKubre and D. D. Macdonald, "Electronic Instrumentation for Electrochemical Studies," in Comprehensive Treatise of Electrochemistry, J. O'M Bockris, B. C. Conway, E. Yeager, and R. E. White, Eds., submitted for publicaton.

10. W. J. Blaedel and V. W. Meloche, Elementary Quantitative Analysis, Harper and Row, New York (1963).

11. Analog Devices Data-Acquisition Databook, Analog Devices, Inc., Norwood, Mass., 1982.

12. AD521 Data Sheet, Analog Devices, Inc., Norwood, Mass., 1981.

13. U. Bertocci, Corrosion 35, 211 (1979).

14. U. Bertocci and J. L. Mullen, in ASTM Proc. Electrochemical Corrosion Testing," F. Mansfeld and U. Bertocci, Eds, (San Francisco, 1981).
15. M.C.H. McKubre, "the Use of Harmonic Analysis to Determine Corrosion Rates," paper No. 135 in 160th Meeting of the Electrochemical Society, Denver, 1981.

16. M.C.H. McKubre, "The Electrochemical Measurements of Corrosion Rates in Cathodically Protected Systems," Final Report: Phase I, under EPRI Contract RP 1689-7-1, 1981.

17. B. Miller, M. I. Bellavance and S. Bruckenstein, Analytical Chem. 44, 1983 (1966).

18. S. Bruckenstein, M. I. Bellavance and S. Bruckenstein, J. Electrochem. Soc. 120, 1351 (1973).

19. K. Tokuda and S. Bruckenstein, J. Electrochem. Soc. 122, 1316 (1975).

20. G. Blanc, I. Epelboin, C. Gabrielli, and M. Keddam, J. Electronal. Chem. 62, 59 (1975).

21. C. Deslouis, I. Epelboin, C. Gabrielli, and B. Tribollet, J. Electroanal. Chem. [82], 251 (1977).

22. Y. Beers, Theory of Error, Addison-Wesley, Cambridge, Mass. (1975).

23. D. D. Macdonald, Transient Techniques in Electrochemistry, Plenum, New York (1977).

24. W. J. Muller, Trans. Faraday Soc. 27, 737 (1931.

25. W. J. Albery and S. Bruckenstein, Trans. Faraday Soc. 62, 1920 (1966).

26. Y. U. Pleskov and V. Y. Filinovskii, The Rotating Disk Electrode, Consultants Bureau, New york (1971).

28. R. W. Powers and M. W. Breiter, J. Electrochem. Soc. 116, 719 (1969).

29. H. Kato, T. Yoshaimura and M. Yamashita, Nippon Kagaku Kaishu, 122, 309 (1964).

30. S. Bruckenstein and G. A. Feldman, J. Electroanal. Chem. 9, 395 (1965).

31. R. D. Armstrong and M. F. Bell, J. Electroanal. Chem. 55, 201 (1974).

32. I. Epelboin, M. Ksouri, and R. Wiart J. Electrochem. Soc.)122), 1206 (1975).

33. I. Epelboin, M. Ksouri, and R. Wiart, J. Electroanal. Chem. 75, 113, (1977).

34. I. Epelboin, E. Lejag, and R. Wiart, Compt. Rend. Acad. Sci. Paris, [274C], 178 (1972).

35. R. D. Armstrong and A. A. Metcalfe, J.Electroanal. Chem. 71, 5 (1976).

36. J. McBreen, J. Electrochem. Soc., 119, 1620 (1972).

37. W. G. Sunu and D. N. Bennion, J. Electrochem. Soc., 127, 2007 (1980).

APPENDIX I

DMS4 (DATA MANAGEMENT SYSTEM)

```
1  REM DMS4 15/APR/1982
2  REM KEITHLEY MODEL 192 DMM
3  REM MOUNTAIN HARDWARE CLOCK
10  REM MODIFICATION OF SOLARTRON DMS TO INCORPORATE VARIABLE INTEGRATION & SOFTWARE DIFFERENCING
30  REM BY M.C.H.MCKUBRE  AUG/28/1981
100  HIMEM: 36300: LOMEM: 24577
120  TEXT : HOME : SPEED= 230: VTAB 5: PRINT "SOLARTRON 1172/1174/1250"
140  VTAB 10: PRINT  TAB( 5)"IMPEDANCE"
160  PRINT : PRINT  TAB( 15)"MEASUREMENT"
180  PRINT : PRINT  TAB( 27)"SYSTEM"
200  PRINT : PRINT : PRINT : FOR II = 1 TO 40: PRINT "$+";: NEXT II: SPEED= 255
220  VTAB 22: PRINT "WHAT IS THE DATA ARRAY LENGTH ? ": VTAB 24: CALL  - 868:ZN = 120: PRINT ZN;: INPUT
"  ";ZQ$: IF ZQ$ = "" THEN 260
240 ZN =  INT ( VAL (ZQ$)): IF ZN < 3 OR ZN > 300 THEN  PRINT  CHR$ (7): GOTO 220
260  PRINT : PRINT : PRINT "SAVE PARAMETER ARRAY ? ";: GET ZD$(0): PRINT " ND"
280 ZN% = 32: IF ZD$(0) <  > "Y" THEN ZN% = 0: VTAB 23: HTAB 25: CALL  - 868: PRINT "ND"
300  DIM ZN(5,ZN),ZM(32),ZZ(9),ZT(25),ZR(25),EZ(4),AA(3),ZE%(1)
320  PRINT  CHR$ (4);"BLOAD B.FRA"
340 ZZ% = 18: REM  IEEE-488 ADDRESS
360 ZT(0) =  LOG (10):ZT(1) = 1 / ZT(0):ZT(2) = 6E - 10:ZR(2) = 1:ZR(3) = 0
380  REM : DEFAULT DATA
400 ZM(0) = 1: REM INITIAL HARMONIC
420 ZM(1) = 0: REM LOCAL
440 ZM(2) = 4: REM DC BIAS/INPUT REJECT ON
460 ZM(3) = 1: REM CARRIER OFF
480 ZM(4) = 2: REM SINEWAVE
500 ZM(6) = 3: REM DISPLAY OPERATING FREQ.
520 ZM(7) = 2: REM LOG. SWEEP
540 ZM(8) = 1: REM SWEEP OFF
560 ZM(9) = 6: REM INPUT AUTORANGING
580 ZM(11) = 1: REM MEASUREMENT MODE
600 ZM(12) = 1: REM Y INPUT CHANNEL
620 ZM(13) = 2: REM DISPLAY REAL,IMAG.
640 ZM(14) = 1: REM MINIMUM DELAY
660 ZM(15) = 1: REM MINIMUM INTEGRATION
680 ZM(16) = 9999: REM MAXIMUM FREQUENCY
700 ZM(17) = 1: REM MINIMUM FREQUENCY
720 ZM(18) = 1: REM DISPLAY FREQUENCY
740 ZM(19) = 1: REM OPERATING FREQUENCY
760 ZM(20) = 0.1: REM AC OUTPUT VOLTAGE
780 ZM(21) = 0.1: REM AC VOLTAGE DISPLAYED
```

```
800 ZM(22) = 10: REM LINEAR DELTA FREQ.
820 ZM(23) = 10: REM LOG POINTS PER DECADE
840 ZM(24) = 0: REM DC BIAS VOLTAGE
860 ZM(25) = 1: REM SERIES MEASURING RESISTANCE
880 ZM(26) = 0: REM // STANDARD CAPACITANCE
900 ZM(27) = 1: REM IMPEDANCE SCALE FACTOR
920 ZM(28) = 0: REM INITIAL DC VOLTAGE
940 ZM(29) = 0: REM FINAL DC VOLTAGE
960 ZM(30) = ZN: REM FREQUENCY POINTS PER VOLTAGE
980 ZM(31) = 0: REM
1000 ZM(32) = 0: REM
1020 CQ% = 3: REM  (Y/X) MODE
1040 LI = 9999: IF ZR(4) = 1174 THEN LI = LI * 140: REM UPPER F LIMIT
1060 BP(0) = 0: REM DELAY IN SECONDS
1080 BP(1) = LI: REM BREAK TO INTEGRATION * 10
1100 BP(2) = LI: REM BREAK TO INTEGRATION * 100
1120 BP(3) = LI: REM BREAK TO INTEGRATION * 1000
1140 S% = 6: REM BOOT FROM SLOT #6
1160 D% = 1: REM DRIVE #1
1180 VB% =  PEEK (1150): REM BOOTVOLUME
1200 V% = VB%: REM CORVUS VOLUME VARIABLE
1220 PL% = ZN%: REM LENGTH OF PARAMETER FILE LOAD
1240  HOME : VTAB 9:ZD$(0) = "MEASUREMENT":ZD$(1) = "DATA ANALYSIS": PRINT : PRINT ZD$(0);" (M)": PRINT
: PRINT "OR": PRINT : PRINT ZD$(1);" (D)": PRINT
1260  VTAB 16: HTAB 2: PRINT "WELL ? ";: GET ZQ$: PRINT ZD$(0): IF ZQ$ = "D" THEN  HTAB 2: VTAB 16: CALL
 - 868: PRINT ZD$(1): GOTO 1460
1280  HOME : VTAB 9: PRINT "LOADING DMS4.MAIN"
1300  HOME : VTAB 5: PRINT "WHICH INSTRUMENT ARE YOU USING ?": PRINT : PRINT : PRINT "1....1172": PRINT
: PRINT "2....1174": PRINT : PRINT "3....1250": PRINT : PRINT "WELL ? ";:
1320  GET ZQ$: IF ZQ$ =  CHR$ (13) THEN ZR(4) = 1172: GOTO 1380
1340 ZZ(3) =  INT ( VAL (ZQ$)): IF ZZ(3) < 1 OR ZZ(3) > 3 THEN  PRINT  CHR$ (7): GOTO 1300
1360 ZR(4) = 1172: IF ZZ(3) < 1 THEN ZR(4) = 1174: IF ZZ(3) > 2 THEN ZR(4) = 1250
1380  PRINT ZR(4): VTAB 20: PRINT "IS CLOCK AVAILABLE (Y/N) ? ";: GET ZD$(0):CL% = 1: PRINT "NO": IF ZD$
(0) <  > "Y" THEN CL% = 0: VTAB 20: HTAB 28: CALL  - 868: PRINT "NO"
1400 NP% = 0: REM LAST PROGRAM MARKER
1420  PRINT  CHR$ (4);"BLOAD CHAIN,A520"
1440  CALL 520"DMS4.MAIN,D1"
1460  VTAB 22: PRINT "LOADING DMS4.ANALYSIS"
1480  PRINT  CHR$ (4);"BLOAD CHAIN,A520"
1500  CALL 520"DMS4.ANALYSIS"
1520  END
1540  REM  NP%=0 => DMS#
1560  REM  NP%=1 => DMS#.MAIN
1580  REM  NP%=2 => DMS#.BODE
1600  REM  NP%=3 => DMS#.NYQUIST
1620  REM  NP%=4 => DMS#.ANALYSIS
1640  REM  NP%=5 => DMS#.RCR FIT
1660  REM  NP%=6 => DMS#.LINEAR FIT
1680  REM  NP%=7 => DMS#.DATA MANIPULATE
30000  REM AUTO-LIST UTILITY BY ROBERT WEAVER
30020  TEXT : HOME : SPEED= 255
30030  VTAB 5: CALL  - 868: INPUT "ENTER FILE NAME: ";DN$:L = LEN (DN$)
```

```
30040  IF L > 48 THEN  VTAB 20: PRINT "LIMIT TO 48 CHARACTERS": PRINT  CHR$ (7): FOR I = 0 TO 200: NEXT
I: GOTO 30030
30060  PRINT  CHR$ (4);"PR#1": PRINT  CHR$ (15)
30065  PRINT  CHR$ (9);"52P": PRINT  CHR$ (9);"F"
30070 L =  INT (24 - L / 2)
30080  PRINT  CHR$ (9);"K"
30090  PRINT  CHR$ (14);
30100  PRINT  TAB( L)DN$:L = L - 1
30120  FOR I = 1 TO  LEN (DN$) + 2:DU$ = DU$ +  CHR$ (95): NEXT I
30150  PRINT  CHR$ (14);
30160  PRINT  TAB( L)DU$
30170  PRINT  CHR$ (9);"122N": PRINT  CHR$ (9);"112R": PRINT  CHR$ (9);"11L"
30180  PRINT  CHR$ (15)
30190  PRINT  CHR$ (9);"A"
30200  LIST : PRINT
30210  PRINT  CHR$ (12)
30220  PRINT  CHR$ (18): PRINT  CHR$ (4);"PR#0": END
```

DMS4.MAIN

```
1  REM   DMS4.MAIN 17/JUN/1982
2  REM KEITHLEY DVM ON IEEE-488 BUS
10  HIMEM: 36300: GOSUB 20000: IF NP% = 0 THEN  GOSUB 1500
1000  HOME : PRINT
1100  PRINT : PRINT "PROGRAM OPTIONS ARE:"
1120  PRINT : PRINT "  1...SET UP SOLARTRON"
1140  PRINT : PRINT "  2...RESET (INITIALIZE)"
1160  PRINT : PRINT "  3...TAKE MEASUREMENTS"
1180  PRINT : PRINT "  4...CHAIN BODE PLOT"
1200  PRINT : PRINT "  5...CHAIN NYQUIST PLOT"
1220  PRINT : PRINT "  6...SAVE DATA ON DISK"
1230  PRINT : PRINT "  7...RETRIEVE DATA FROM DISK"
1240  PRINT : PRINT "  8...CHANGE CONFIGURATION"
1245  PRINT : PRINT "  9...CHAIN ANALYSIS PROGRAM"
1250  PRINT : PRINT "  0...EXIT PROGRAM"
1260 ZZ(3) = 0: VTAB (23):ZZ(4) = 0:ZZ(5) = 9: GOSUB 10100
1280  IF ZE%(0) = 1 THEN 1000
1300  ON ZZ(3) GOTO 2000,1400,3000,4000,5000,6000,7000,8000,9700
1320  HOME : VTAB 9: PRINT "EXIT PROGRAM": PRINT : PRINT "TYPE GOTO 1000 TO RESUME": END
1400  GOSUB 1500: GOTO 1000
1500  HOME : PRINT "INITIALISE"
1520 ZZ% = 18: GOSUB 20010: GOSUB 26000
1540  FOR II = 0 TO 24: IF II = 1 OR II = 5 OR II = 10 THEN  NEXT II
1560 ZA% =  INT (II + 0.5): GOSUB 21000: NEXT II:S% = 6:D% = 1:V% = VB%
1580  GOSUB 29000: REM KEITHLEY
1600  RETURN
2000  REM  SET PARAMETER ROUTINE
2020  HOME : VTAB 5: PRINT "SET UP SOLARTRON UNDER:": PRINT : PRINT "  LOCAL (=L) , OR PROGRAM (=P) CONT
ROL ?": PRINT
2040  GET ZD$(0): IF ZD$(0) = "L" THEN  PRINT " LOCAL": GOTO 2100
2060  IF ZD$(0) = "P" THEN  PRINT " PROGRAM": GOTO 2200
2080  PRINT " FAILED": FOR II = 0 TO 1000: NEXT II: GOTO 2000
2100  GOSUB 25000: REM  LOCAL
2120  VTAB 12: PRINT "SET CONTROLS": PRINT "DON'T INITIATE MEASUREMENTS"
2140  PRINT "HIT 'R' TO RESUME  ": GET ZD$(0)
2160  IF ZD$(0) <  > "R" THEN 2120
2180  GOTO 1000
2200  REM PROGRAM CONTROL
2220 ZM(0) = 1: REM FUNDAMENTAL
2240  VTAB 15:ZZ(3) = BP(0):ZZ(4) = 0:ZZ(5) = 1000:ZZ(6) = 0: PRINT "DELAY IN SECONDS = ";: GOSUB 10100:
 IF ZE%(0) = 1 THEN 2240
2260 BP(0) = ZZ(3)
```

```
2280  FOR II = 1 TO 3
2300  VTAB 15 + 2 * II:ZZ(3) = BP(II):ZZ(4) = 0.0001:ZZ(5) = LI: PRINT "BREAK POINT FREQ. #";II;" = ";: GOSUB
10100: IF ZE%(0) = 1 THEN 2300
2320 BP(II) = ZZ(3): NEXT II
2340  HOME : IF ZR(4) = 1174 THEN 2440
2360  VTAB 3:ZZ(3) = ZM(28):ZZ(4) =  - 9.99:ZZ(5) = 9.99:ZZ(6) = 0: PRINT "INITIAL DC VOLTAGE = ";: GOSUB
10100: IF ZE%(0) = 1 THEN 2360
2380 ZM(28) = ZZ(3):ZM(24) = ZM(28):ZA% = 24: GOSUB 21000
2400  VTAB 5:ZZ(3) = ZM(29):ZZ(4) =  - 9.99:ZZ(5) = 9.99:ZZ(6) = 0: PRINT "FINAL  DC  VOLTAGE = ";: GOSUB
10100: IF ZE%(0) = 1 THEN 2400
2420 ZM(29) = ZZ(3)
2440  VTAB 8:ZZ(3) = ZM(17):ZZ(4) = 0.0001:ZZ(5) = LI: PRINT "MINIMUM FREQUENCY = ";: GOSUB 10100: IF ZE
%(0) = 1 THEN 2440
2460 ZM(17) = ZZ(3):ZA% = 17: GOSUB 21000
2480  VTAB 10:ZZ(3) = ZM(16):ZZ(4) = ZM(17):ZZ(5) = LI: PRINT "MAXIMUM FREQUENCY = ";: GOSUB 10100: IF Z
E%(0) = 1 THEN 2480
2500 ZM(16) = ZZ(3):ZA% = 16: GOSUB 21000
2520  VTAB 12:ZZ(3) = ZM(20):ZZ(4) = 0.01:ZZ(5) = 9.99:ZZ(6) = 0: PRINT "AC OUTPUT VOLTAGE = ";: GOSUB 1
0100: IF ZE%(0) = 1 THEN 2520
2540 ZM(20) = ZZ(3):ZA% = 20: GOSUB 21000:ZM(21) = ZZ(3):ZA% = 21: GOSUB 21000
2560  IF ZR(4) = 1174 THEN 2700
2580  IF ZM(28) = ZM(29) OR ZM(16) = ZM(17) THEN ZM(30) = ZN: GOTO 2640
2600  VTAB 15:ZZ(3) = ZM(30):ZZ(4) = 2:ZZ(5) = ZN / 2:ZZ(6) = 1: PRINT "# OF FREQUENCY STEPS = ";: GOSUB
10100: IF ZE%(0) = 1 THEN 2600
2620 ZM(30) = ZZ(3)
2640  VTAB 17:ZZ(3) = ZM(4):ZZ(4) = 1:ZZ(5) = 3:ZZ(6) = 1: PRINT "WAVEFORM:"
2660  PRINT "   1=TRIANGULAR": PRINT "   2=SINE": PRINT "   3=SQUARE": GOSUB 10100: IF ZE%(0) = 1 THEN 2
640
2680 ZM(4) = ZZ(3):ZA% = 4: GOSUB 21000
2700  IF CL% = 0 THEN 1000
2720  HOME : GOSUB 12000: VTAB 5: PRINT "THE DATE IS:  ";ZZ(4): VTAB 7: PRINT "THE TIME IS:  ";ZZ(5)
2740  VTAB 12: PRINT "AT WHAT TIME WOULD YOU LIKE": VTAB 14: PRINT "MEASUREMENTS TO BEGIN ?"
2760  VTAB 16: INPUT "HH.MM ";ZQ$: GOTO 1000
3000  HOME : PRINT "TAKING MEASUREMENTS IN MODE # ";CQ%
3010  VTAB 3: PRINT "IMPEDANCE SCALE FACTOR = ";ZM(27)
3020  POKE 34,3: REM SET TEXT WINDOW
3030 ZA% = 19:ZM(19) = ZM(17): GOSUB 21000:ZA% = 18:ZM(18) = ZM(17): GOSUB 21000
3040 FMPX = (ZM(16) / ZM(17)) ^ (1 / (ZM(30) - 1))
3050 VADD = 0: IF ZM(30) < ZN THEN VADD = (ZM(29) - ZM(28)) / ( INT (ZN / ZM(30) - 0.5))
3060 ZN(0,0) = 1
3070 ZN(0,1) = ZN(0,0) + ZM(30) - 1
3080  FOR II = 1 TO BP(0) * 441 * 60: NEXT II
3090  FOR JZN = ZN(0,0) TO ZN(0,1)
3100  FOR II = 1 TO BP(0) * 441: NEXT II: REM DELAY IN SECONDS
3110 ZM(15) = 1: IF ZM(19) > BP(1) THEN ZM(15) = 2: IF ZM(19) > BP(2) THEN ZM(15) = 3: IF ZM(19) > BP(3)
 THEN ZM(15) = 4
3120 ZA% = 15: GOSUB 21000: REM  SET INTEGRATION
3130  IF CQ% = 4 OR CQ% < 0 THEN 3170
3140 ZA% = 12:ZM(12) = 1: GOSUB 21000: REM  SET 'X'
3150 ZN% = JZN - 1: GOSUB 22000: REM MEASURE
3160 X1 = ZN(1,JZN):X2 = ZN(2,JZN): REM   INITIAL 'X'
3170 ZA% = 12:ZM(12) = 2: GOSUB 21000: REM  SET 'Y' MODE
```

```
3180 ZN% = JZN - 1: GOSUB 22000: REM  MEASUREMENT
3190  VTAB 5: CALL  - 868: PRINT "FREQUENCY = ";ZN(0,JZN);: HTAB 24: PRINT "TOTAL # ";ZN
3200  VTAB 7: CALL  - 868: PRINT "REAL 'Y'  = ";ZN(1,JZN);:ZN(3,JZN) = ZN(1,JZN): GOSUB 9000
3210  VTAB 8: CALL  - 868: PRINT "IMAG. 'Y' = ";ZN(2,JZN);:ZN(4,JZN) = ZN(2,JZN): GOSUB 9000
3220  IF CQ% = 4 THEN 3280
3230 ZA% = 12:ZM(12) = 1: GOSUB 21000: REM SET 'X'
3240 ZN% = JZN - 1: GOSUB 22000: IF CQ% < 0 THEN 3260
3250 ZN(1,JZN) = (ZN(1,JZN) + X1) / 2:ZN(2,JZN) = (ZN(2,JZN) + X2) / 2: REM  'X' MEAN
3260  VTAB 10: CALL  - 868: PRINT "REAL 'X'  = ";ZN(1,JZN);: GOSUB 9000
3270  VTAB 11: CALL  - 868: PRINT "IMAG. 'X' = ";ZN(2,JZN);: GOSUB 9000
3280 ZM(19) = ZM(19) * FMPX: IF ZM(19) > 59 AND ZM(19) < 61 THEN 3280
3290  IF ZM(19) > LI THEN ZM(19) = LI
3300 ZA% = 19: GOSUB 21000: REM SET NEW FREQUENCY
3310 ZA% = 18:ZM(18) = ZM(19): GOSUB 21000: REM SET DISPLAY F
3320  REM CALCULATE IMPEDANCE
3330  IF  ABS (CQ%) = 1 THEN ZZ(1) = ZN(1,JZN):ZZ(2) = ZN(2,JZN):ZZ(3) = ZN(3,JZN) - ZN(1,JZN):ZZ(4) = Z
N(4,JZN) - ZN(2,JZN)
3340  IF  ABS (CQ%) = 2 THEN ZZ(1) = ZN(3,JZN) - ZN(1,JZN):ZZ(2) = ZN(4,JZN) - ZN(2,JZN):ZZ(3) = ZN(1,JZ
N):ZZ(4) = ZN(2,JZN)
3350  IF  ABS (CQ%) = 3 THEN ZZ(1) = ZN(1,JZN):ZZ(2) = ZN(2,JZN):ZZ(3) = ZN(3,JZN):ZZ(4) = ZN(4,JZN)
3360  IF  ABS (CQ%) = 4 THEN ZZ(1) = ZN(1,JZN):ZZ(2) = ZN(2,JZN):ZZ(3) = 1.000:ZZ(4) = 0.000
3370  GOSUB 9500:ZZ(1) = 1.00 / ZM(25):ZZ(2) = 6.2831853 * ZN(0,JZN) * ZM(26): GOSUB 9500
3380 ZN(1,JZN) = ZZ(3) / ZM(27)
3390 ZN(2,JZN) = ZZ(4) / ZM(27)
3400  GOSUB 9980
3410  VTAB 14: CALL  - 868: PRINT "REAL 'Z'  = ";ZN(1,JZN);: GOSUB 9000
3420  VTAB 15: CALL  - 868: PRINT "IMAG. 'Z' = ";ZN(2,JZN);: GOSUB 9000
3430  VTAB 17: CALL  - 868: PRINT "MAGNITUDE = ";ZN(3,JZN);: GOSUB 9000
3440  VTAB 18: CALL  - 868: PRINT "PHASE/DEG.= ";ZN(4,JZN);: GOSUB 9000
3450  VTAB 23:ZD$(0) = "": GOSUB 29240:ZD$(0) =  MID$ (ZD$(0),5):ZN(3,JZN) =  VAL (ZD$(0)): VTAB 20: CALL
 - 868: PRINT "VOLTAGE   = ";ZN(3,JZN)
3460 ZA% = 1:ZM(1) = 1: GOSUB 21000
3470  IF  PEEK ( - 16384) - 128 = 65 THEN  GOTO 3520: REM ABORT RUN
3480  IF JZN >  = ZN THEN 3520
3490  NEXT JZN
3500 ZM(24) = ZM(24) + VADD:ZA% = 24: GOSUB 21000:ZN(0,0) = JZN
3510 ZM(19) = ZM(17):ZA% = 19: GOSUB 21000: GOTO 3070
3520  POKE 34,0:ZN% = ZN: GOTO 1000
4000  HOME : VTAB 9: PRINT "LOADING BODE PLOT PROGRAM":NP% = 1
4010  PRINT  CHR$ (4);"BLOAD CHAIN,A520,S6,D1,V"VB%
4020  CALL 520"DMS4.BODE,D1"
5000  HOME : VTAB 9: PRINT "LOADING NYQUIST PROGRAM":NP% = 1
5010  PRINT  CHR$ (4);"BLOAD CHAIN,A520,S6,D1,V"VB%
5020  CALL 520"DMS4.NYQUIST,D1"
6000  REM SAVE DATA TO DISK
6020 ZD$(0) = "":ZZ(3) = CQ%: GOSUB 6500:ZZ(3) = 2: GOSUB 6500:ZZ(3) = CL%: GOSUB 6500:ZZ(3) = ZM(2): GOSUB
6500:ZZ(3) = ZM(4): GOSUB 6500:ZZ(3) = ZM(9): GOSUB 6500
6040 ZN(0,0) =  VAL (ZD$(0)):ZN(1,0) = ZN:ZN(2,0) = PL%:ZN(3,0) = ZM(27)
6050  IF CL% <  > 0 THEN  GOSUB 12000: REM CLOCK->ZN(4,0)&ZN(5,0)
6060 ZZ(8) = 78: GOSUB 11400: GOTO 1000
6500 ZD$(0) = ZD$(0) +  STR$ ( INT (ZZ(3) + 0.5)): RETURN
7000  REM  RETRIEVE DATA FROM DISK
```

```
7020 ZZ(8) = 78: GOSUB 11300:ZN% = ZN(1,0): GOTO 1000
8000  REM  MEASUREMENT CONFIGURATION
8020  HOME : VTAB 5: PRINT "WHICH INPUT CONFIGURATION ?"
8040  VTAB 8: PRINT "1......(Y-X)/(X)"
8060  VTAB 10: PRINT "2......(X)/(Y-X)"
8100  VTAB 12: PRINT "3......(Y/X)"
8120  VTAB 14: PRINT "4......Y"
8130  VTAB 16: PRINT "WELL ? ";:ZZ(3) = CQ%:ZZ(4) = 1:ZZ(5) = 4:ZZ(6) = 1
8140  GOSUB 10100: IF ZE%(0) = 1 THEN 8000
8160 CQ% = ZZ(3)
8170  IF CQ% < 4 THEN  VTAB 18: PRINT "2 OR 3 MEASUREMENTS ?  3  ": GET ZD$(0): IF ZD$(0) = "2" THEN CQ%
 = - CQ%: VTAB 18: HTAB 24: PRINT "2"
8180  VTAB 20:ZZ(3) = ZM(25):ZZ(4) = 0.01:ZZ(5) = 1E12:ZZ(6) = 0: PRINT "STANDARD RESISTANCE = ";: GOSUB
10100: IF ZE%(0) = 1 THEN 8180
8200 ZM(25) = ZZ(3)
8220  VTAB 22:ZZ(3) = ZM(26):ZZ(4) = 0:ZZ(5) = 1E - 5:ZZ(6) = 0: PRINT "PARALLEL CAPACITANCE = ";: GOSUB
10100: IF ZE%(0) = 1 THEN 8220
8240 ZM(26) = ZZ(3)
8260  VTAB 24:ZZ(3) = ZM(27):ZZ(4) = 1:ZZ(5) = 1E12:ZZ(6) = 0: PRINT "IMPEDANCE SCALE FACTOR = ";: GOSUB
10100: IF ZE%(0) = 1 THEN 8260
8280 ZM(27) = ZZ(3)
8300  GOTO 1000
9000  REM DISPLAY COUNTER ROUTINE
9010  HTAB 30: PRINT "# ";JZN;"   ": RETURN
9240  PR# 3: PRINT "∂(:": PRINT "'";ZD$(0);"X'": PRINT "∂?;∂H:": PR# 0: INPUT ZD$(0): IN# 0: RETURN
9500  REM COMPLEXDIVISION
9520 ZZ(5) = ZZ(1) * ZZ(1) + ZZ(2) * ZZ(2)
9540 ZZ(6) = (ZZ(3) * ZZ(1) + ZZ(4) * ZZ(2)) / ZZ(5)
9560 ZZ(4) = (ZZ(4) * ZZ(1) - ZZ(3) * ZZ(2)) / ZZ(5)
9580 ZZ(3) = ZZ(6): RETURN
9700  HOME : VTAB 9: PRINT "LOADING ANALYSIS PROGRAM":NP% = 1
9710  PRINT  CHR$ (4);"BLOAD CHAIN,A$20,S6,D1,V"VB%
9720  CALL 520"DMS4.ANALYSIS,D1"
9730  RETURN
9970  REM MAG. & PHASE
9980 ZN(3,JZN) =  SQR (ZN(1,JZN) * ZN(1,JZN) + ZN(2,JZN) * ZN(2,JZN))
9982  IF ZN(1,JZN) = 0 THEN ZN(1,JZN) = 1E - 10
9985 ZN(4,JZN) =  ATN (ZN(2,JZN) / ZN(1,JZN)) * (180 / 3.141592654)
9990 ZN(5,JZN) =  LOG (ZN(3,JZN)) / ZT(0): RETURN
10000  REM  Y/N SUBR
10010 ZE%(0) = 0: INPUT " ";ZD$(0): IF  LEFT$ (ZD$(0),1) = "Y" THEN ZZ(3) = 2: RETURN
10020  IF  LEFT$ (ZD$(0),1) = "N" OR ZD$(0) = "" THEN ZZ(3) = 1: RETURN
10030 ZE%(0) = 1: GOSUB 10050: RETURN
10050  REM  ERROR SUBR
10060  PRINT  CHR$ (7):ZE%(0) = 1: RETURN
10100  REM  I/P SUBR
10110  CALL  - 868
10120 ZE%(0) = 0: PRINT ZZ(3): INPUT "  ";ZD$(0): IF ZD$(0) = "" THEN ZZ(7) = ZZ(3): GOTO 10170
10130  FOR I = 1 TO  LEN (ZD$(0)):ZQ$ =  MID$ (ZD$(0),I,1)
10140  IF ZQ$ = "+" OR ZQ$ = "-" OR ZQ$ = " " OR ZQ$ = "." OR ZQ$ = "E" THEN 10160
10150  IF ZQ$ < "0" OR ZQ$ > "9" THEN 10050
10160  NEXT I:ZZ(7) =  VAL (ZD$(0))
```

```
10170  IF ZZ(7) < ZZ(4) OR ZZ(7) > ZZ(5) THEN 10050
10180 ZZ(3) = ZZ(7): IF ZZ(6) = 1 THEN ZZ(3) =  INT (ZZ(7))
10190  FOR I = 0 TO 200: NEXT I: RETURN
10200  REM  FIXED REAL SUBR
10210  POKE 36336,13: POKE 36337,ZZ(4): POKE 36338,0: POKE 36340,64: GOTO 10240
10220  POKE 36336,14: POKE 36337,ZZ(5): POKE 36338,1: POKE 36340,64: GOTO 10240
10230  POKE 36336,13: POKE 36337,ZZ(6): POKE 36338,1: POKE 36340,64
10240  CALL 36379: PRINT ZN(ZZ(7),I): RETURN
11300  REM  : LOAD ARRAY
11310  GOSUB 11500
11320  POKE 98,90: POKE 99,ZZ(8): CALL 38152
11330  PRINT  CHR$ (4);"BLOAD"ZD$(0);",A" PEEK (38394) +  PEEK (38395) * 256"
11340  RETURN
11400  REM : SAVE ARRAY
11410  GOSUB 11500
11420  POKE 98,90: POKE 99,ZZ(8): CALL 38104
11430  PRINT  CHR$ (4);"BSAVE"ZD$(0)",A" PEEK (38394) +  PEEK (38395) * 256",L" PEEK (38396) +  PEEK (38
397) * 256 + PL% * 5 + 12 *  SGN (PL%)"
11435  PRINT  CHR$ (4);"LOCK"ZD$(0)
11440  RETURN
11500  REM ASK SLOT,DRIVE AND VOLUME
11505 ZZ(3) = 2: HOME : VTAB 9: PRINT "ENTER DISK DRIVE NUMBER..";ZZ(3);"..";
11510  HOME : VTAB 5: PRINT "TO ACCESS FLOPPY DISK USE :": PRINT "    S(4),D(1 OR 2),V(0)": VTAB 8: PRINT
"TO ACCESS CORVUS DISK USE :": PRINT "    S(6),D(1 OR 2),V(1 TO 67)
11515  VTAB 12: PRINT "POINTERS CURRENTLY SET AT :": PRINT : PRINT "    SLOT #";S%: PRINT "   DRIVE #";D
%: PRINT "  VOLUME #";V%
11520  VTAB 19: PRINT "CHANGE POINTERS (Y/N) ? ";: GET ZD$(0): IF ZD$(0) = "N" THEN 11550
11530  HOME : VTAB 5:ZZ(3) = S%:ZZ(4) = 4:ZZ(5) = 6:ZZ(6) = 0: PRINT "    SLOT ";: GOSUB 10120: IF ZE%(0
) = 1 THEN 11530
11532 S% =  INT (ZZ(3) + 0.5)
11535  VTAB 10:ZZ(3) = D%:ZZ(4) = 1:ZZ(5) = 2:ZZ(6) = 0: PRINT "   DRIVE ";: GOSUB 10120: IF ZE%(0) = 1 THEN
11535
11537 D% =  INT (ZZ(3) + 0.5): IF S% <  > 6 THEN V% = 0: GOTO 11550: REM FLOPPY
11540  VTAB 15:ZZ(3) = V%:ZZ(4) = 1:ZZ(5) = 67:ZZ(6) = 0: PRINT "  VOLUME ";: GOSUB 10120: IF ZE%(0) = 1
 THEN 11540
11542 V% =  INT (ZZ(3) + 0.5)
11550  PRINT : PRINT "PRESS ANY KEY TO CATALOG ": GET ZD$(0): PRINT : PRINT  CHR$ (4);"CATALOG,S"S%",D"D
%",V"V%
11560  PRINT : PRINT "ANOTHER CATALOG  Y/N ?  ";: GOSUB 10000: IF ZE%(0) = 1 THEN 11560
11570  IF ZZ(3) = 2 THEN 11500
11580  PRINT : PRINT "FILE NAME WILL BE PRECEDED BY DMS4-": PRINT : INPUT "ENTER FILE NAME = DMS4-";ZD$(
0):ZD$(0) = "DMS4-" + ZD$(0)
11590  RETURN
12000  RETURN : REM  CLOCK
20000  REM  INITIALISATION
20010 ZD$(4) = "@" +  CHR$ (95) +  CHR$ (ZZ% + 64):ZD$(5) = "@" +  CHR$ (95) + "?" +  CHR$ (ZZ% + 32)
20020 ZD$(6) =  CHR$ (4) + "IN#0":ZD$(7) =  CHR$ (4) + "PR#0"
20030 ZD$(8) =  CHR$ (4) + "PR#3":AA$ = "@" +  CHR$ (95) + "(:'":BB$ = "X'@?;@H:"
20040  RETURN
21000  REM  SEND DATA TO FRA
21010  IF ZA% < 0 OR ZA% > 24 THEN ZE%(0) = 1: RETURN
21020  IF ZA% = 5 OR ZA% = 10 THEN ZE%(0) = 1: RETURN
```

```
21030  PRINT ZD$(8): PRINT ZD$(5)
21040  IF ZA% > 15 THEN 21140
21050  IF ZA% = 12 OR ZA% = 0 THEN Z1% = ZM(ZA%): GOTO 21130
21060  IF ZA% = 7 THEN 21090
21070  IF ZA% = 9 THEN 21110
21080 Z1% = ZM(ZA%) - 1: GOTO 21130
21090  IF ZM(ZA%) = 1 THEN Z1% = 0: GOTO 21130
21100 Z1% = 4: GOTO 21130
21110  IF ZM(ZA%) < 6 THEN Z1% = ZM(ZA%) + 1: GOTO 21130
21120 Z1% = ZM(ZA%) + 2
21130  PRINT ":'T2"; CHR$ (ZA% + 48); STR$ (Z1%);"'": GOTO 21450
21140  IF ZA% < 20 THEN  GOTO 21160
21150  ON ZA% - 19 GOTO 21230,21250,21300,21320,21370
21160  ON ZA% - 16 GOTO 21180,21190,21200
21170 ZD$(1) = "F": GOTO 21210
21180 ZD$(1) = "N": GOTO 21210
21190 ZD$(1) = "6": GOTO 21210
21200 ZD$(1) = "7"
21210 Z2% = 6: IF ZM(ZA%) = 0 THEN 21460
21220  GOTO 21410
21230 Z2% = 5:ZD$(1) = "G": IF ZM(ZA%) = 0 THEN 21460
21240 ZD$(1) = "60": GOTO 21410
21250 ZD$(1) = "3": IF ZM(ZA%) = 0 THEN 21460
21260 Z3% =  INT ( LOG (ZM(ZA%)) /  LOG (10) + 1E - 6)
21270 ZP =  INT (ZM(ZA%) * 10 ^ 3) * 10 ^ 4: IF ZP = 0 THEN ZP =  INT (ZP * 10 + 1E - 6)
21280 ZD$(3) = "": IF Z3% <  > 0 THEN  FOR ZI = 1 TO  ABS (Z3%):ZD$(3) = ZD$(3) + "0": NEXT ZI
21290 ZD$(3) = ZD$(3) +  STR$ (ZP): GOTO 21440
21300 Z2% = 6:ZD$(1) = ">": IF ZM(ZA%) = 0 THEN 21460
21310  GOTO 21410
21320 ZD$(1) = "?": IF ZM(ZA%) = 0 THEN 21460
21330 ZD$(3) =  STR$ (ZM(ZA%) * 10 ^ 6)
21340  IF  LEN (ZD$(3)) = 6 THEN ZD$(3) = "00" + ZD$(3): GOTO 21440
21350  IF  LEN (ZD$(3)) = 7 THEN ZD$(3) = "0" + ZD$(3): GOTO 21440
21360  GOTO 21440
21370 ZD$(1) = "C": IF ZM(ZA%) = 0 THEN 21460
21375 ZD$(1) = "C0":ZD$(2) = "0000": IF ZM(ZA%) < 0 THEN ZD$(2) = "0010"
21380 ZZ(3) =  ABS (ZM(ZA%)): IF ZZ(3) < 1 THEN ZD$(1) = "C00"
21385  IF ZZ(3) < 0.1 THEN ZD$(1) = "C000"
21390 ZD$(3) =  STR$ ( INT (ZZ(3) * 10 ^ 2 + 6E - 5)) + ZD$(2): GOTO 21440
21400  IF ZM(ZA%) = 0 THEN Z3% = 0: GOTO 21430
21410 Z3% =  INT ( LOG (ZM(ZA%)) /  LOG (10) + 1E - 6)
21420 Z4% = 4: IF ZA% = 20 THEN Z4% = 3
21430 ZD$(3) =  STR$ ( INT (ZM(ZA%) * 10 ^ (Z2% - Z3%) + ZT(2))) +  STR$ (Z3% + Z4%)
21440  PRINT ":'T1";ZD$(1);ZD$(3);"'"
21450  PRINT ZD$(6): PRINT ZD$(7): RETURN
21460 ZD$(3) = "00000000": GOTO 21440
21470  IF ZA% = 5 OR ZA% > 6 THEN 21490
21480 ZD$(3) =  LEFT$ (ZD$(3),7) + "4"
21490  GOTO 21440
22000  REM  MEASUREMENT ROUTINE
22010 ZE%(0) = 0: IF ZN% >  = ZN THEN ZE%(0) = 2: RETURN
22020 ZN% = ZN% + 1: PRINT ZD$(8)
```

```
22030  PRINT ZD$(5);":'S111T2;0T2;2'"
22040  IF  PEEK (49331) < 64 THEN 22040
22050  PRINT ZD$(5);":'T37'": GOSUB 28000
22060 ZZ(1) = ZR:ZZ(2) = ZS
22070  PRINT ZD$(5);":'T4<'": GOSUB 28500:ZR(0) = ZR
22080  IF ZR(0) = 1 THEN  PRINT ZD$(5);":'T3I'": GOSUB 28000:ZZ(3) = ZR:ZZ(4) = ZS: PRINT ZD$(5);":'T3M'
": GOSUB 28000:ZZ(5) = ZR:ZZ(6) = ZS
22090  IF ZR(0) = 2 THEN  PRINT ZD$(5);":'T31'": GOSUB 28000:ZZ(3) = ZR:ZZ(4) = ZS: PRINT ZD$(5);":'T35'
": GOSUB 28000:ZZ(5) = ZR:ZZ(6) = ZS
22100  IF ZR(0) = 3 THEN  PRINT ZD$(5);":'T39'": GOSUB 28000:ZZ(3) = ZR:ZZ(4) = ZS: PRINT ZD$(5);":'T3='
": GOSUB 28000:ZZ(5) = ZR:ZZ(6) = ZS
22110  PRINT ZD$(5);":'T48'": GOSUB 28500
22120  IF ZR <  > 0 AND ZN% >  = ZN THEN ZR = 0:ZE%(0) = 1
22130  IF ZR <  > 0 THEN  PRINT ZD$(5);":'S111T2;0T2;2'"
22140 ZN(0,ZN%) = (ZZ(1) / 1000) * 10 ^ (ZZ(2) - ( INT (ZZ(2) / 10) * 10) - 4)
22150 ZT =  - 5 + (ZZ(4) - ( INT (ZZ(4) / 10) * 10) - 4)
22160 ZZ(3) = ((ZZ(3) * 100) +  INT (ZZ(4) / 100)) * 10 ^ ZT
22170 ZT =  INT (ZZ(4) / 10):ZT = ZT - ( INT (ZT / 10) * 10)
22180  IF ZT > 3 THEN ZZ(3) = 10E20
22190  IF ZT = 1 OR ZT = 5 THEN ZZ(3) = ZZ(3) *  - 1
22200 ZN(1,ZN%) = ZZ(3)
22210 ZT =  - 5 + (ZZ(6) - ( INT (ZZ(6) / 10) * 10) - 4)
22220 ZZ(5) = ((ZZ(5) * 100) +  INT (ZZ(6) / 100)) * 10 ^ ZT
22230 ZT =  INT (ZZ(6) / 10):ZT = ZT - ( INT (ZT / 10) * 10)
22240  IF ZT > 3 THEN ZZ(5) = 10E20
22250  IF ZT = 1 OR ZT = 5 THEN ZZ(5) = ZZ(5) *  - 1
22260 ZN(2,ZN%) = ZZ(5)
22270  IF ZR <  > 0 THEN ZN% = ZN% + 1: GOTO 22040
22280  PRINT ZD$(5);":'T2;0'"
22290  PRINT ZD$(7): PRINT ZD$(6)
22300  RETURN
24000  IF ZA% < 0 THEN ZE%(0) = 1: RETURN
24010  IF ZA% <  = 24 OR ZA% = 31 THEN 24030
24020 ZE%(0) = 1: RETURN
24030  PRINT ZD$(8): PRINT ZD$(5)
24040  IF ZA% < 16 THEN 24310
24050  ON ZA% - 15 GOTO 24080,24090,24100,24110,24120
24060  ON ZA% - 20 GOTO 24150,24180,24220,24250
24070  PRINT ":'T3;'": GOSUB 28000: GOSUB 27210:ZP = ZR: GOTO 24470
24080  PRINT ":'T3F'": GOTO 24440
24090  PRINT ":'T3N'": GOTO 24440
24100  PRINT ":'T36'": GOTO 24440
24110  PRINT ":'T37'": GOTO 24440
24120  PRINT ":'T3G'": GOSUB 28000:ZP = ZR * 10 ^ ( - 5 + (ZS - ( INT (ZS / 10) * 10))): IF ZP < 0.01 THEN
ZP = 0.01
24130  IF ZP > 9.99 THEN ZP = 9.99
24140  GOTO 24470
24150  PRINT ":'T33'": GOSUB 28000:ZP = ZR / 1000: IF ZP < 0.01 THEN ZP = 0.01
24160  IF ZP > 9.99 THEN ZP = 9.99
24170  GOTO 24470
24180  PRINT ":'T3>'": GOSUB 28000:ZP = ZR * 10 ^ ((ZS - ( INT (ZS / 10) * 10)) - 7): IF ZP < 1E - 7 THEN
ZP = 1E - 7
```

```
24190 ZZ(5) = 9999: IF ZR(4) = 1174 THEN ZZ(5) = 999900
24200  IF ZP > ZZ(5) THEN ZP = ZZ(5)
24210  GOTO 24470
24220  PRINT ":'T3?'": GOSUB 28000:ZP = ZR / 100: IF ZP < 0.2 THEN ZP = 0.2
24230  IF ZP > 99.99 THEN ZP = 99.99
24240  GOTO 24470
24250  PRINT ":'T3C'": GOSUB 28000:Z8% =  INT ((ZS -  INT (ZS / 100) * 100) / 10)
24260  IF Z8% = 1 THEN ZR = ZR *  - 1
24270 ZP = ZR / 100: IF  ABS (ZP) < 0.01 THEN ZP = 0.01: GOTO 24290
24280  IF  ABS (ZP) > 9.99 THEN ZP = 9.99
24290  IF Z8% = 1 THEN ZP = ZP *  - 1
24300  GOTO 24470
24310  PRINT ":'T4"; CHR$ (ZA% + 48);"'": GOSUB 28500: PRINT ZD$(7): PRINT ZD$(6)
24320  IF ZA% = 10 THEN ZP = ZR - 1: RETURN
24330  IF ZA% = 12 OR ZA% = 0 THEN ZP = ZR: RETURN
24340  IF ZA% = 1 THEN 24380
24350  IF ZA% = 9 THEN 24480
24360  IF ZA% = 7 THEN 24410
24370 ZP = ZR + 1: RETURN
24380  IF ZR = 0 THEN ZP = 1: RETURN
24390  IF ZR = 8 THEN ZP = 2: RETURN
24400 ZE%(0) = 1: RETURN
24410  IF ZR = 0 THEN ZP = 1: RETURN
24420  IF ZR = 4 THEN ZP = 2: RETURN
24430 ZE%(0) = 1: RETURN
24440  GOSUB 28000: GOSUB 27200:ZP = ZR:ZZ(5) = 9999: IF ZR(4) = 1174 THEN ZZ(5) = 999900
24450  IF ZP < 1E - 4 THEN ZP = 1E - 4
24460  IF ZP > ZZ(5) THEN ZP = ZZ(5)
24470  PRINT ZD$(7): PRINT ZD$(6): RETURN
24480  IF ZR = 8 THEN ZP = 6: RETURN
24490  PRINT ZD$(8): PRINT ZD$(5): PRINT "'T4:'": GOSUB 28500: PRINT ZD$(6): PRINT ZD$(7):ZP = ZR - 1: RETURN

25000  PRINT ZD$(8): PRINT ZD$(5) + ":'S001'" + ZD$(5) +  CHR$ (1) + ":": PRINT ZD$(6): PRINT ZD$(7): RETURN

26000  PRINT ZD$(8): PRINT ZD$(5); CHR$ (4);":": PRINT ZD$(6): PRINT ZD$(7): RETURN
27200 Z7% = 1
27210 ZE%(0) = 0:Z6 = ((ZR * 100) +  INT (ZS / 100)) / 100000
27220  IF Z7% = 1 THEN  GOTO 27260
27230 Z8% =  INT ((ZS -  INT (ZS / 100) * 100) / 10)
27240  IF Z8% = 1 OR Z8% = 5 THEN Z6 = Z6 *  - 1
27250  IF Z8% > 3 THEN ZE%(0) = 1
27260 ZR = Z6 * 10 ^ ((ZS - ( INT (ZS / 10) * 10)) - 4):Z7% = 0: RETURN
28000  PRINT ZD$(4);":": PRINT ZD$(7)
28010  VTAB 23: INPUT ZR,ZD$(0):ZS =  VAL (ZD$(0))
28020  PRINT ZD$(8): RETURN
28500  PRINT ZD$(4);":": PRINT ZD$(7): VTAB 23: INPUT ZR
28510  PRINT ZD$(8): RETURN
29000  REM KEITHLEY MODEL 192 SET-UP
29010 ZD$(0) = "Y(LF)": GOSUB 29240
29020 ZD$(0) = "T1F0R0K0Q0S3M0Z0W1": GOSUB 29240: RETURN
29240  REM TALK TO KEITHLEY
29260  PRINT ZD$(8): PRINT AA$;ZD$(0);BB$: PRINT ZD$(7): INPUT ZD$(0): PRINT ZD$(6): RETURN
```

DMS4.ANALYSIS

```
1  REM DMS4.ANALYSIS 10/MAY/1982
10  HIMEM: 36300: PRINT  CHR$ (4)"BRUN B.VMOVE"
20  ONERR  GOTO 9400
30 ZN% = ZN: CALL 37312
100  FOR I9 = 0 TO 3:HOLD(I9) = BP(I9): NEXT I9
575  IF X% > 20 AND X% < 270 AND Y% > 10 AND Y% < 170 THEN  DRAW 11 AT X%,Y%
1000  TEXT : HOME : PRINT
1100  PRINT : PRINT "PROGRAM OPTIONS ARE:"
1120  PRINT : PRINT "  1...ANALYSIS OPTIONS"
1140  PRINT : PRINT "  2...DISPLAY OPTIONS"
1160  PRINT : PRINT "  3...CHAIN DMS4.MAIN"
1180  PRINT : PRINT "  4...CHAIN BODE PLOT"
1200  PRINT : PRINT "  5...CHAIN NYQUIST PLOT"
1220  PRINT : PRINT "  6...SAVE DATA ON DISK"
1230  PRINT : PRINT "  7...RETRIEVE DATA FROM DISK"
1240  PRINT : PRINT "  8...CHANGE CONFIGURATION"
1245  PRINT : PRINT "  9...INPUT DATA-FILES"
1250  PRINT : PRINT "  0...EXIT PROGRAM"
1260 ZZ(3) = 0: VTAB (23):ZZ(4) = 0:ZZ(5) = 9: GOSUB 10100
1280  IF ZE%(0) = 1 THEN 1000
1300  ON ZZ(3) GOTO 1500,2000,3000,4000,5000,6000,7000,8000,9000
1320  HOME : VTAB 9: PRINT "EXIT PROGRAM": PRINT : PRINT "TYPE GOTO 1000 TO RESUME": END
1500  HOME : VTAB 5: PRINT "ANALYSIS OPTIONS ARE: ": PRINT
1520  PRINT : PRINT "  1...SUBTRACT A CONSTANT "
1540  PRINT : PRINT "  2...CHAIN DATA MANIPULATE"
1560  PRINT : PRINT "  3...CHAIN LINEAR REGRESSION"
1580  PRINT : PRINT "  4...CHAIN RCR REGRESSION"
1700  PRINT : PRINT "  0...RETURN TO MAIN MENU"
1760 ZZ(3) = 0: VTAB (23):ZZ(4) = 0:ZZ(5) = 4: GOSUB 10100
1780  IF ZE%(0) = 1 THEN 1500
1800  ON ZZ(3) GOTO 1840,1920,1940,1970
1820  GOTO 1000
1840  HOME : VTAB 5: PRINT "SUBTRACT A CONSTANT": PRINT : PRINT "FROM WHICH COLUMN ? ": PRINT
1860 ZZ(3) = 0: VTAB (12):ZZ(4) = 1:ZZ(5) = 4: GOSUB 10100
1880  IF ZE%(0) = 1 THEN 1860
1890 II = ZZ(3): VTAB 16: INPUT "VALUE TO BE SUBTRACTED = ";ZZ(3): GOSUB 9999
1900  FOR JZN = 1 TO ZN:ZN(II,JZN) = ZN(II,JZN) - ZZ(3)
1910  NEXT JZN: GOTO 1000
1920  HOME : VTAB 9:NP% = 4: PRINT "LOADING DMS4.DATA MANIPULATE"
1924 VB% = 6
1925  PRINT  CHR$ (4);"BLOAD CHAIN,A520,S6,D1,V"VB%:VB% = 6
1930  CALL 520"DMS4.DATA MANIPULATE"
```

```
1940  HOME : VTAB 9:NP% = 4: PRINT "LOADING DMS4.LINEAR REGRESSION"
1950  PRINT  CHR$ (4);"BLOAD CHAIN,A520,S6,D1,V"VB%
1960  CALL 520"DMS4.LINEAR REGRESSION"
1970  HOME : VTAB 9:NP% = 4: PRINT "LOADING DMS4.RCR REGRESSION"
1980  PRINT  CHR$ (4);"BLOAD CHAIN,A520,S6,D1,V"VB%
1990  CALL 520"DMS4.RCR REGRESSION"
2000  HOME : VTAB 5: PRINT "DISPLAY OPTIONS ": PRINT
2020  PRINT : PRINT "FOR EACH AXIS YOU MUST CHOOSE": PRINT : PRINT "A COLUMN (0 = II) ": PRINT : PRINT "
AND AN OPERATOR"
2040  PRINT : PRINT : PRINT "REMEMBER !!!!!!!!!!": PRINT : PRINT "THIS PROGRAM WILL ATTEMPT ": PRINT : PRINT
"TO OFFSET YOUR STUPIDITY"
2060  PRINT : PRINT : PRINT "LOG(0)=-4": PRINT : PRINT "LOG(-X)=LOG(X)": PRINT : PRINT "1/0=1E10"
2070  PRINT : GET ZQ$
2080  TEXT : HOME : VTAB 9: PRINT "X AXIS ": PRINT : GOSUB 2800: GOSUB 2900
2090 BP(0) = II:BP(1) = ZZ(3):AA(0) = X1:AA(1) = X2
2100  HOME : VTAB 9: PRINT "Y AXIS ": PRINT : GOSUB 2800: GOSUB 2900
2110 BP(2) = II:BP(3) = ZZ(3):AA(2) = X1:AA(3) = X2
2200  REM
2300 ZZ(0) = 1E30:ZZ(1) =  - ZZ(0):ZZ(2) =  - ZZ(1):ZZ(3) =  - ZZ(2)
2310  GOSUB 9999
2320  FOR I = 1 TO ZN%: REM MIN/MAX
2340 II = BP(0):ZE%(0) = 1:AA% = 0: GOSUB 2600: REM  X
2350  IF ZZ(0) > ZZ(5) THEN ZZ(0) = ZZ(5)
2360  IF ZZ(1) < ZZ(5) THEN ZZ(1) = ZZ(5)
2380 II = BP(2):ZE%(0) = 3:AA% = 2: GOSUB 2600: REM  Y
2385  IF ZZ(2) > ZZ(5) THEN ZZ(2) = ZZ(5)
2390  IF ZZ(3) < ZZ(5) THEN ZZ(3) = ZZ(5)
2395  NEXT I:I = 0: GOSUB 15000:I = 2: GOSUB 15000: REM SCALE AXES
2399  GOTO 12000
2400  HGR2 : SCALE= 1: ROT= 0: HCOLOR= 3
2420  HPLOT 20,170 TO 20,10 TO 270,10 TO 270,170 TO 19,170 TO 19,9 TO 271,9 TO 271,171 TO 19,171
2440  FOR II = 20 TO 270 STEP 25: HPLOT II,8 TO II,11: HPLOT II,169 TO II,172: NEXT II
2460  FOR II = 10 TO 170 STEP 16: HPLOT 18,II TO 21,II: HPLOT 269,II TO 271,II: NEXT II
2480  GOSUB 12500: REM LABEL AXES
2500  REM  PLOT DATA
2550  FOR I = 1 TO ZN%
2555 II = BP(0):ZE%(0) = 1:AA% = 0: GOSUB 2600: REM   X
2560 X% =  INT (270.5 + (250 / (ZZ(1) - ZZ(0))) * (ZZ(5) - ZZ(1)))
2565 II = BP(2):ZE%(0) = 3:AA% = 2: GOSUB 2600: REM   Y
2570 Y% =  INT (10.5 + (160 / (ZZ(2) - ZZ(3))) * (ZZ(5) - ZZ(3)))
2575  IF X% > 20 AND X% < 270 AND Y% > 10 AND Y% < 170 THEN  HPLOT X%,Y%
2580  NEXT I: GOSUB 16000: REM SCALE FACTORS
2585  GET ZQ$: IF ZQ$ = "F" THEN  GOTO 1000
2590  GOTO 12000
2600 ZZ(6) = I: IF II < 6 THEN ZZ(6) = ZN(II,I): REM POINT CALCULATE
2610 ZZ(6) = AA(AA%) + AA(AA% + 1) * ZZ(6)
2620  ON BP(ZE%(0)) GOTO 2660,2680,2700,2720,2730,2750
2640 ZZ(5) = ZZ(6): RETURN
2660  IF ZZ(6) = 0 THEN ZZ(5) =  - 4: RETURN
2665  IF ZZ(6) < 0 THEN ZZ(5) =  LOG ( - ZZ(6)) /  LOG (10): RETURN
2670 ZZ(5) =  LOG (ZZ(6)) /  LOG (10): RETURN
2680  IF ZZ(6) = 0 THEN ZZ(5) =  - 1E10: RETURN
```

```
2685 ZZ(5) = 1 / ZZ(6): RETURN
2700 ZZ(5) = ZZ(6) * ZZ(6): RETURN
2720 ZZ(5) =  SQR ( ABS (ZZ(6))): RETURN
2730 ZZ(6) =  ABS (ZZ(6)): IF ZZ(6) > 1E20 THEN ZZ(5) = 1E10: RETURN
2740 ZZ(5) = 1 / ( SQR (ZZ(6))): RETURN
2750 ZZ(5) =  EXP (ZZ(6)): RETURN
2799  END
2800  VTAB 10: CALL  - 958: PRINT "PLOT WHICH COLUMN ? "
2820 ZZ(3) = 0: VTAB (12):ZZ(4) = 0:ZZ(5) = 6: GOSUB 10100
2840  IF ZEZ(0) = 1 THEN 2000 LIST 1900
2860 II = ZZ(3): RETURN
2900  HOME : VTAB 5: PRINT "WHAT OPERATOR ?": PRINT
2920  PRINT : PRINT "  1...LOG"
2930  PRINT : PRINT "  2...RECIPROCAL"
2940  PRINT : PRINT "  3...SQUARE"
2950  PRINT : PRINT "  4...SQUARE ROOT"
2955  PRINT : PRINT "  5...INVERSE SQUARE ROOT"
2957  PRINT : PRINT "  6...EXP"
2960  PRINT : PRINT "  0...NONE"
2970 ZZ(3) = 0: VTAB (23):ZZ(4) = 0:ZZ(5) = 6: GOSUB 10100
2975  IF ZEZ(0) = 1 THEN 2900
2980 X1 = 0:X2 = 1: PRINT : PRINT "MORE ARITHMETIC (Y/N) ? ": GET ZD$(0): IF ZD$(0) = "N" THEN  RETURN
2985  HOME : VTAB 12: PRINT "Z = A + B*Z": VTAB 15: INPUT "A = ";X1: PRINT : INPUT "B = ";X2
2990  RETURN
3000  HOME : VTAB 9: PRINT "LOADING DMS4.MAIN":NPZ = 4
3005  FOR I9 = 0 TO 3:BP(I9) = HOLD(I9): NEXT I9
3010  PRINT  CHR$ (4);"BLOAD CHAIN,A520,S6,D1,V"VBZ
3020  CALL 520"DMS4.MAIN,D1"
4000  HOME : VTAB 9: PRINT "LOADING BODE PLOT PROGRAM":NPZ = 4
4010  PRINT  CHR$ (4);"BLOAD CHAIN,A520,S6,D1,V"VBZ
4020  CALL 520"DMS4.BODE,D1"
5000  HOME : VTAB 9: PRINT "LOADING NYQUIST PROGRAM":NPZ = 4
5010  PRINT  CHR$ (4);"BLOAD CHAIN,A520,S6,D1,V"VBZ
5020  CALL 520"DMS4.NYQUIST,D1"
6000  REM SAVE DATA TO DISK
6020 ZD$(0) = "":ZZ(3) = CQZ: GOSUB 6500:ZZ(3) = 4: GOSUB 6500:ZZ(3) = ZN(2): GOSUB 6500:ZZ(3) = ZN(7): GOSUB
6500:ZZ(3) = ZN(4): GOSUB 6500:ZZ(3) = ZN(9): GOSUB 6500
6040 ZN(0,0) =  VAL (ZD$(0)):ZN(1,0) = ZN:ZN(2,0) = ZN(20):ZN(3,0) = ZN(25):ZN(4,0) = ZN(26):ZN(5,0) = Z
N(27)
6060 ZZ(8) = 78: GOSUB 11400: GOTO 1000
6500 ZD$(0) = ZD$(0) +  STR$ ( INT (ZZ(3) + 0.5)): RETURN
7000  REM  RETRIEVE DATA FROM DISK
7020 ZZ(8) = 78: GOSUB 11300:ZNZ = ZN(1,0):ZN$ = ZD$(0): GOTO 1000
8000  REM   MEASUREMENT CONFIGURATION      :RETURN
9000  TEXT : HOME : VTAB 5: PRINT "RANDOM ACCESS DATA-INPUT":I = 0
9020  INPUT "WHICH DATA FILE ?  DATA-";N$:N$ = "DATA-" + N$
9040  PRINT : PRINT "ROOM FOR ";ZN - I;" MORE POINTS"
9060  PRINT : INPUT "FIRST DATA POINT = ";ZZ(1)
9080  PRINT : INPUT " LAST DATA POINT = ";ZZ(2)
9100  IF ZZ(2) < ZZ(1) OR I + ZZ(2) - ZZ(1) > ZN THEN  PRINT  CHR$ (7): GOTO 9040
9120  GOSUB 17000: PRINT : PRINT "MORE DATA (Y/N)? ";: GET ZD$(0): PRINT ZD$(0): IF ZD$(0) <  > "N" THEN
9020
```

```
9140  FOR II = I + 1 TO ZN:ZN(0,II) = 1E4:ZN(1,II) = 0:ZN(2,II) = 0:ZN(3,II) = 0:ZN(4,II) = 0:ZN(5,II) =
1: NEXT II: GOTO 1000
9400  REM ERR HANDLING ROUTINE
9410  TEXT
9420  PRINT : PRINT : PRINT "ERROR # "; PEEK (222): PRINT : PRINT "IN LINE #"; PEEK (218) +  PEEK (219) *
256
9460  PRINT : PRINT "HIT A KEY TO CONTINUE ";: GET ZQ$
9480  PRINT : GOTO 1000
9500  REM COMPLEX DIVISION
9520 ZZ(5) = ZZ(1) * ZZ(1) + ZZ(2) * ZZ(2)
9540 ZZ(6) = (ZZ(3) * ZZ(1) + ZZ(4) * ZZ(2)) / ZZ(5)
9560 ZZ(4) = (ZZ(4) * ZZ(1) - ZZ(3) * ZZ(2)) / ZZ(5)
9580 ZZ(3) = ZZ(6): RETURN
9999  PRINT : PRINT : INVERSE : PRINT "....CALCULATING....": NORMAL : RETURN
10000  REM  Y/N SUBR
10010 ZE%(0) = 0: INPUT " ";ZD$(0): IF  LEFT$ (ZD$(0),1) = "Y" THEN ZZ(3) = 2: RETURN
10020  IF  LEFT$ (ZD$(0),1) = "N" OR ZD$(0) = "" THEN ZZ(3) = 1: RETURN
10030 ZE%(0) = 1: GOSUB 10050: RETURN
10050  REM  ERROR SUBR
10060  PRINT  CHR$ (7):ZE%(0) = 1: RETURN
10100  REM  I/P SUBR
10110  CALL  - 868
10120 ZE%(0) = 0: PRINT ZZ(3): INPUT "  ";ZD$(0): IF ZD$(0) = "" THEN ZZ(7) = ZZ(3): GOTO 10170
10130  FOR I = 1 TO  LEN (ZD$(0)):ZQ$ =  MID$ (ZD$(0),I,1)
10140  IF ZQ$ = "+" OR ZQ$ = "-" OR ZQ$ = " " OR ZQ$ = "." OR ZQ$ = "E" THEN 10160
10150  IF ZQ$ < "0" OR ZQ$ > "9" THEN 10050
10160  NEXT I:ZZ(7) =  VAL (ZD$(0))
10170  IF ZZ(7) < ZZ(4) OR ZZ(7) > ZZ(5) THEN 10050
10180 ZZ(3) = ZZ(7): IF ZZ(6) = 1 THEN ZZ(3) =  INT (ZZ(7))
10190  FOR I = 0 TO 200: NEXT I: RETURN
10200  REM  FIXED REAL SUBR
10210  POKE 36336,13: POKE 36337,ZZ(4): POKE 36338,0: POKE 36340,64: GOTO 10240
10220  POKE 36336,14: POKE 36337,ZZ(5): POKE 36338,1: POKE 36340,64: GOTO 10240
10230  POKE 36336,13: POKE 36337,ZZ(6): POKE 36338,1: POKE 36340,64
10240  CALL 36379: PRINT ZN(ZZ(7),I): RETURN
11300  REM  : LOAD ARRAY
11310  GOSUB 11500
11320  POKE 98,90: POKE 99,ZZ(8): CALL 38152
11330  PRINT  CHR$ (4);"BLOAD"ZD$(0);",A" PEEK (38394) +  PEEK (38395) * 256"
11340 ZN$ = ZD$(0): RETURN
11400  REM : SAVE ARRAY
11410  GOSUB 11500
11420  POKE 98,90: POKE 99,ZZ(8): CALL 38104
11430  PRINT  CHR$ (4);"BSAVE"ZD$(0)",A" PEEK (38394) +  PEEK (38395) * 256",L" PEEK (38396) +  PEEK (38
397) * 256 + PL% * 5 + 12 *  SGN (PL%)"
11435  PRINT  CHR$ (4);"LOCK"ZD$(0)
11440  RETURN
11500  REM ASK SLOT,DRIVE AND VOLUME
11505 ZZ(3) = 2: HOME : VTAB 9: PRINT "ENTER DISK DRIVE NUMBER..";ZZ(3);"..";
11510  HOME : VTAB 5: PRINT "TO ACCESS FLOPPY DISK USE :": PRINT "    S(4),D(1 OR 2),V(0)": VTAB 8: PRINT
"TO ACCESS CORVUS DISK USE :": PRINT "    S(6),D(1 OR 2),V(1 TO 67)
11515  VTAB 12: PRINT "POINTERS CURRENTLY SET AT :": PRINT : PRINT "    SLOT #";S%: PRINT "   DRIVE #";D
```

```
Z: PRINT "  VOLUME #";VZ
11520  VTAB 19: PRINT "CHANGE POINTERS (Y/N) ? ";: GET ZD$(0): IF ZD$(0) = "N" THEN 11550
11530  HOME : VTAB 5:ZZ(3) = SZ:ZZ(4) = 4:ZZ(5) = 6:ZZ(6) = 0: PRINT "    SLOT ";: GOSUB 10120: IF ZEZ(0
) = 1 THEN 11530
11532 SZ =  INT (ZZ(3) + 0.5)
11535  VTAB 10:ZZ(3) = DZ:ZZ(4) = 1:ZZ(5) = 2:ZZ(6) = 0: PRINT "   DRIVE ";: GOSUB 10120: IF ZEZ(0) = 1 THEN
11535
11537 DZ =  INT (ZZ(3) + 0.5): IF SZ <  > 6 THEN VZ = 0: GOTO 11550: REM  FLOPPY
11540  VTAB 15:ZZ(3) = VZ:ZZ(4) = 0:ZZ(5) = 67:ZZ(6) = 0: PRINT "  VOLUME ";: GOSUB 10120: IF ZEZ(0) = 1
 THEN 11540
11542 VZ =  INT (ZZ(3) + 0.5)
11550  PRINT : PRINT "PRESS ANY KEY TO CATALOG ": GET ZD$(0): PRINT : PRINT  CHR$ (4);"CATALOG,S"SZ",D"D
Z",V"VZ
11560  PRINT : PRINT "ANOTHER CATALOG  Y/N ?  ";: GOSUB 10000: IF ZEZ(0) = 1 THEN 11560
11570  IF ZZ(3) = 2 THEN 11500
11580  PRINT : PRINT "FILE NAME WILL BE PRECEDED BY DMS4-": PRINT : INPUT "ENTER FILE NAME = DMS4-";ZD$(
0):ZD$(0) = "DMS4-" + ZD$(0)
11590  RETURN
12000  TEXT : HOME : VTAB 5: PRINT  CHR$ (7): PRINT "GRAPHIC OPTIONS ARE : ": PRINT
12020  PRINT : PRINT "F = FINISH"
12040  PRINT : PRINT "G = GRAPHIC MODE"
12060  PRINT : PRINT "N = NEW PLOT"
12070  PRINT : PRINT "O = OVERLAY PLOT"
12080  PRINT : PRINT "P = DUMP TO EPSON"
12100  PRINT : PRINT "T = TEXT MODE"
12120  PRINT : PRINT "X = CHANGE X MAX/MIN"
12140  PRINT : PRINT "Y = CHANGE Y MAX/MIN"
12200  PRINT : PRINT : GET ZQ$
12220  IF ZQ$ = "F" THEN  GOTO 1000
12240  IF ZQ$ = "G" THEN  GOTO 2400
12260  IF ZQ$ = "N" THEN  GOTO 2080
12280  IF ZQ$ = "P" OR ZQ$ = "D" THEN 18000
12290  IF ZQ$ = "O" THEN  GOTO 18200
12300  IF ZQ$ = "X" THEN II = 0: GOTO 12400
12320  IF ZQ$ = "Y" THEN II = 2: GOTO 12400
12380  GOTO 12000
12400  REM CHANGE MAX/MIN
12420  HOME : VTAB 9: PRINT ZQ$;"-AXIS": VTAB 12: PRINT "","MIN","MAX"
12440  VTAB 14: PRINT "CURRENT";: HTAB 14:ZZ(6) = ZZ(II) / (10 ^ EZ(II)) + .0005: GOSUB 14000: PRINT ZD$
(0) + "E" +  STR$ (EZ(II))
12450  VTAB 14: HTAB 27:ZZ(6) = ZZ(II + 1) / (10 ^ EZ(II)) + .0005: GOSUB 14000: PRINT ZD$(0) + "E" +  STR$
(EZ(II))
12460  VTAB 16: INPUT "NEW VALUES    ";ZZ(II)
12480  VTAB 16: HTAB 27: INPUT "";ZZ(II + 1)
12490  GOTO 12000
12500  REM LABEL AXES
12520  DATA    " ","LOG.","1/","SQ.","SQR.","ISQR","EXP"
12540 ZQ$ = " ":I = 2: GOSUB 12900: REM Y
12560 ZQ$ = ZQ$ + "  VERSUS  ":I = 0: GOSUB 12900: REM X
12580 ZZ(7) = 0: REM  HORIZONTAL
12600 XZ = 10:YZ = 0: GOSUB 13000
12620 ZZ(7) = 0:ZZ(6) = ZZ(0) / (10 ^ EZ(0)): GOSUB 14000:ZQ$ = ZD$(0):XZ = 20:YZ = 175: GOSUB 13000:ZZ(
```

```
6) = ZZ(1) / (10 ^ EZ(0)): GOSUB 14000:ZQ$ = ZD$(0):XZ = 245: GOSUB 13000
12640 ZQ$ = "EXP" +  STR$ (EZ(0)):XZ = 29:YZ = 184: GOSUB 13000:XZ = 245: GOSUB 13000
12660 ZZ(7) = 1:ZZ(6) = ZZ(2) / (10 ^ EZ(2)): GOSUB 14000:ZQ$ = ZD$(0):XZ = 0:YZ = 170: GOSUB 13000:ZZ(6
) = ZZ(3) / (10 ^ EZ(2)): GOSUB 14000:ZQ$ = ZD$(0):YZ = 40: GOSUB 13000
12680 ZQ$ = "EXP" +  STR$ (EZ(2)):XZ = 9:YZ = 170: GOSUB 13000:YZ = 40: GOSUB 13000
12700 ZQ$ = "<<" + ZN$ + ">>":XZ = 273:YZ = 170:ZQ$ =  LEFT$ (ZQ$,22): GOSUB 13000
12899  RETURN
12900  REM HEADING CALCULATION
12920  RESTORE : FOR II = 0 TO BP(I + 1): READ ZD$(0): NEXT II
12940 ZQ$ = ZQ$ + ZD$(0) +  CHR$ (60) + "COLUMN " +  STR$ (BP(I)) +  CHR$ (62)
12960  RETURN
13000  ROT= 0: IF ZZ(7) > 0 THEN  ROT= 48: REM TEXT TO SCREEN
13020  FOR II = 1 TO  LEN (ZQ$):I =  ASC ( MID$ (ZQ$,II,1))
13040  IF I > 127 THEN I = I - 128
13060  IF I = 32 THEN  GOTO 13100
13080  DRAW I - 32 AT XZ,YZ
13100  IF ZZ(7) > 0 THEN YZ = YZ - 7: NEXT II
13120  IF ZZ(7) <  = 0 THEN XZ = XZ + 7: NEXT II
13140  RETURN
14000  REM # FORMAT SUBR
14020 ZD$(0) =  STR$ (ZZ(6)): IF  ABS (ZZ(6)) < .01 THEN ZD$(0) = "0.00"
14040  IF ZZ(6) >  = 0 THEN ZD$(0) = "+" + ZD$(0)
14060 ZD$(0) =  LEFT$ (ZD$(0),5): RETURN
15000  REM CALCULATE EXPONENTS
15020 ZZ(6) =  ABS (ZZ(I + 1) - ZZ(I)):EZ(I) = 0
15040  IF ZZ(6) = 0 THEN  RETURN
15060  IF ZZ(6) < 0.98 THEN ZZ(6) = 10 * ZZ(6):EZ(I) = EZ(I) - 1: GOTO 15060
15080  IF ZZ(6) > 9.8 THEN ZZ(6) = ZZ(6) / 10:EZ(I) = EZ(I) + 1: GOTO 15080
15100  RETURN
16000  REM X&Y INT&SLOPE
16010 :ZZ(7) = 0
16020 ZQ$ =  STR$ (AA(0)):XZ = 100:YZ = 175: GOSUB 13000
16040 ZQ$ =  STR$ (AA(1)):XZ = 100:YZ = 184: GOSUB 13000
16050 ZZ(7) = 1
16060 ZQ$ =  STR$ (AA(2)):XZ = 0:YZ = 122: GOSUB 13000
16080 ZQ$ =  STR$ (AA(3)):XZ = 9:YZ = 122: GOSUB 13000
16100 : RETURN
17000  REM  FILE TRANSFER BLOCK
17010  PRINT : PRINT "CATALOG (Y/N) ? ";: GET ZD$(0): PRINT ZD$(0): IF ZD$(0) = "N" THEN 17040
17020  PRINT  CHR$ (4);"CATALOG,S5,D1,V0"
17030  GOTO 17010
17040  PRINT  CHR$ (4);"OPEN";N$;",L20,S5,D1,V0"
17060  FOR II = ZZ(1) TO ZZ(2)
17080  PRINT  CHR$ (4);"READ ";N$;",R";II
17085 I = I + 1
17090  INPUT ZN(1,I)
17100  INPUT ZN(2,I)
17110  INPUT ZN(0,I)
17130 ZN(3,I) =  SQR (ZN(1,I) * ZN(1,I) + ZN(2,I) * ZN(2,I))
17140 ZN(4,I) =  ATN (ZN(2,I) / ZN(1,I)) * (180 / 3.141592654)
17150 ZN(5,I) =  LOG (ZN(3,I)) / ZT(0): NEXT II
17160  PRINT  CHR$ (4);"CLOSE ";N$
```

```
17180  RETURN
18000  PRINT : PRINT : PRINT "GRAPPLER (G)": PRINT " OR ": PRINT "MICROBUFFER II  ": PRINT "INTERFACE ?
";: GET ZQ$: PRINT ZQ$
18020 ZD$(0) = "GDRS": IF ZQ$ = "G" THEN ZD$(0) = "GDR2"
18100  PRINT : PRINT  CHR$ (4)"PR#1": PRINT  CHR$ (9);ZD$(0)
18120  FOR II = 1 TO 10: PRINT  CHR$ (10): NEXT II
18140  PRINT  CHR$ (4);"PR#0": GOTO 12000
18200  POKE  - 16304,0: POKE  - 16299,0: GOTO 2500
30000  REM AUTO-LIST UTILITY BY ROBERT WEAVER
30020  TEXT : HOME : SPEED= 255
30030  VTAB 5: CALL  - 868: INPUT "ENTER FILE NAME: ";DN$:L =  LEN (DN$)
30040  IF L > 48 THEN  VTAB 20: PRINT "LIMIT TO 48 CHARACTERS": PRINT  CHR$ (7): FOR I = 0 TO 200: NEXT
I: GOTO 30030
30060  PRINT  CHR$ (4);"PR#1": PRINT  CHR$ (15)
30065  PRINT  CHR$ (9);"52P"
30070 L =  INT (24 - L / 2)
30080  PRINT  CHR$ (9);"K"
30090  PRINT  CHR$ (14);
30100  PRINT  TAB( L)DN$:L = L - 1
30120  FOR I = 1 TO  LEN (DN$) + 2:DU$ = DU$ +  CHR$ (95): NEXT I
30150  PRINT  CHR$ (14);
30160  PRINT  TAB( L)DU$
30170  PRINT  CHR$ (9);"122N": PRINT  CHR$ (9);"112R": PRINT  CHR$ (9);"11L"
30180  PRINT  CHR$ (15)
30190  PRINT  CHR$ (9);"A"
30200  LIST : PRINT
30210  PRINT  CHR$ (12)
30220  PRINT  CHR$ (18): PRINT  CHR$ (4);"PR#0": END
```

APPENDIX II

RRDE CALIBRATION

```
1  REM RRDE CALIB 04/AUG/1981
20 PI = 3.14159265
40  ONERR  GOTO 1000
100  DEF  FN F(T) = ( SQR (3) / (4 * PI)) *  LOG ((1 + T ^ (1 / 3)) ^ 3 / (1 + T)) + (3 / (2 * PI)) *  ATN
((2 * T ^ (1 / 3) - 1) /  SQR (3)) + 1 / 4
1000  TEXT : HOME : SPEED= 255: POKE 34,0: VTAB 3: PRINT "ROTATING RING DISK ELECTRODE": VTAB 5: HTAB 3:
 PRINT "COLLECTION EFFICIENCY-": HTAB 3: PRINT "---------- ----------"
1020  VTAB 8: PRINT "USING THE EQUATION DERIVED BY:": VTAB 10: PRINT "ALBERY & BRUCKENSTEIN TFS 62,1920
(1966)": VTAB 11: HTAB 27: PRINT "--"
1040  POKE 34,10: VTAB 14: INPUT "R1 = ";R1: PRINT : INPUT "R2 = ";R2: PRINT : INPUT "R3 = ";R3
1060  IF R3 < R1 THEN N = R3:R3 = R1:R1 = N
1080  IF R2 > R3 OR R2 < R1 THEN  PRINT "": GOTO 1040
1100 A = (R2 / R1) ^ 3 - 1:B = (R3 / R1) ^ 3 - (R2 / R1) ^ 3
1120 N = 1 -  FN F(A / B) + B ^ (2 / 3) * (1 -  FN F(A)) - (1 + A + B) ^ (2 / 3) * (1 -  FN F((A / B) *
(1 + A + B)))
1140  PRINT : PRINT "COLLECTION EFFICIENCY = ";N * 100;" %"
1160  PRINT : PRINT "HIT 'Q' TO QUIT ";: GET A$: PRINT A$
1180  IF A$ <  > "Q" THEN  GOTO 1040
1200  POKE 34,0: END
```

APPENDIX III

_RCR_REGRESSION_

```
1  REM DMS4.RCR FIT 26/APR/1982
10  HIMEM: 36300: PRINT  CHR$ (4)"BRUN B.VMOVE"
20  ONERR  GOTO 9400
30 ZN% = ZN:ZN$ = "NONE": CALL 37312
100  TEXT : HOME : VTAB 7: PRINT "THIS PROGRAM FITS DMS4 FORMATTED DATA": PRINT : PRINT "TO A SERIES/PAR
ALLEL RC CIRCUIT": PRINT : PRINT "USING LARRY ABLOW'S EQUATION": PRINT : PRINT "FIRST IMPLEMENTED JUN/17
/1980"
1000  TEXT : HOME : PRINT
1100  PRINT : PRINT "PROGRAM OPTIONS ARE:"
1120  PRINT : PRINT "  1...DISPLAY FIT"
1140  PRINT : PRINT "  2...PERFORM REGRESSION"
1160  PRINT : PRINT "  3...CHAIN MAIN PROGRAM"
1180  PRINT : PRINT "  4...CHAIN BODE PLOT"
1200  PRINT : PRINT "  5...CHAIN NYQUIST PLOT"
1220  PRINT : PRINT "  6...SAVE DATA ON DISK"
1230  PRINT : PRINT "  7...RETRIEVE DATA FROM DISK"
1240  PRINT : PRINT "  8...CHANGE CONFIGURATION"
1250  PRINT : PRINT "  0...EXIT PROGRAM"
1260 ZZ(3) = 0: VTAB (23):ZZ(4) = 0:ZZ(5) = 8: GOSUB 10100
1280  IF ZE%(0) = 1 THEN 1000
1300  ON ZZ(3) GOTO 1500,2000,3000,4000,5000,6000,7000,8000
1320  HOME : VTAB 9: PRINT "EXIT PROGRAM": PRINT : PRINT "TYPE GOTO 1000 TO RESUME": END
2000  HOME : VTAB 7: PRINT "RCR REGRESSION": PRINT : INVERSE : PRINT "WARNING!!!!!": PRINT : NORMAL : PRINT
"THIS PROGRAM REQUIRES :"
2020  PRINT : PRINT "FREQUENCY (HZ) IN COLUMN 0": PRINT : PRINT "REAL IMPEDANCE IN COLUMN 1": PRINT : PRINT
"IMAGINARY TERM IN COLUMN 2"
2040  PRINT : PRINT : PRINT "THE ARRAY MUST BE": PRINT : PRINT "AT LEAST 5 COLUMNS WIDE,": PRINT : PRINT
"AND COLUMNS 3-5 WILL BE DESTROYED"
2060  PRINT : PRINT : PRINT "HIT 'Q' TO QUIT NOW ": GET ZD$(0): IF ZD$(0) = "Q" THEN 1000
2100  HOME : VTAB 5:ZZ(3) = 1:ZZ(4) = 1:ZZ(5) = ZN(1,0):ZZ(6) = 1: PRINT "FIRST DATA POINT = ";: GOSUB 1
0100: IF ZE%(0) = 1 THEN 2100
2120 E%(0) = ZZ(3)
2140  HOME : VTAB 8:ZZ(3) = ZN:ZZ(4) = AA%(0) + 2:ZZ(5) = ZN:ZZ(6) = 1: PRINT "LAST DATA POINT = ";: GOSUB
10100: IF ZE%(0) = 1 THEN 2140
2160 E%(1) = ZZ(3)
2200  GOSUB 9999
2220  FOR I = 0 TO 9:ZZ(I) = 0: NEXT I
2240  FOR I = E%(0) TO E%(1)
2260 W1 = 6.2831853 * ZN(0,I)
2280 X1 = ZN(1,I)
2300 Y1 =  - ZN(2,J)
2310 ZZ(0) = ZZ(0) + 1
```

```
2320 ZZ(1) = ZZ(1) + Y1
2340 ZZ(2) = ZZ(2) + X1
2360 ZZ(3) = ZZ(3) + W1 * Y1
2380 ZZ(4) = ZZ(4) + Y1 * Y1
2400 ZZ(5) = ZZ(5) + X1 * X1
2420 ZZ(6) = ZZ(6) + W1 * W1
2440 ZZ(7) = ZZ(7) + W1 * W1 * Y1 * Y1
2460 ZZ(8) = ZZ(8) + W1 * W1 * X1
2480 ZZ(9) = ZZ(9) + W1 * W1 * X1 * X1
2600 AA(1) = (ZZ(0) * (ZZ(9) + ZZ(7)) - ZZ(2) * ZZ(8) - ZZ(3) * ZZ(3)) / (ZZ(0) * ZZ(8) - ZZ(2) * ZZ(6))

2620 AA(3) = ZZ(3) / (ZZ(8) - AA(1) * ZZ(6))
2640 AA(2) =  - AA(1) + (ZZ(2) + AA(3) * ZZ(3)) / ZZ(0)
2660 AA(0) = ZZ(5) + ZZ(4) + (ZZ(2) * ZZ(2) + ZZ(1) * ZZ(1)) * (2.0 * ZZ(0) - 1.0) / (ZZ(0) * ZZ(0))
2680 JZN = ZZ(5) + ZZ(4) + ZZ(0) * (AA(1) + AA(2)) * (AA(1) * AA(2)) + AA(3) * AA(3) * ZZ(7) - 2.0 * (AA
(1) + AA(2)) * ZZ(2) - 2.0 * AA(2) * AA(3) * ZZ(3) + AA(3) * AA(3) * (AA(1) * AA(1) * ZZ(6) - 2.0 * AA(1
) * ZZ(8) + ZZ(9))
2700 ZN(3,I) = AA(1)
2720 ZN(4,I) = AA(2)
2740 ZN(5,I) = AA(3) / AA(2)
2760  REM WOT ABOUT P(S0,0) ???
2999  END
3000  HOME : VTAB 9: PRINT "LOADING DMS3.MAIN":NPZ = 4
3010  PRINT  CHR$ (4);"BLOAD CHAIN,A520,S6,D1,V"VBZ
3020  CALL 520"DMS4.MAIN,D1"
4000  HOME : VTAB 9: PRINT "LOADING BODE PLOT PROGRAM":NPZ = 4
4010  PRINT  CHR$ (4);"BLOAD CHAIN,A520,S6,D1,V"VBZ
4020  CALL 520"DMS4.BODE,D1"
5000  HOME : VTAB 9: PRINT "LOADING NYQUIST PROGRAM":NPZ = 4
5010  PRINT  CHR$ (4);"BLOAD CHAIN,A520,S6,D1,V"VBZ
5020  CALL 520"DMS4.NYQUIST,D1"
6000  REM SAVE DATA TO DISK
6020 ZN(0,0) = ZM(25):ZN(1,0) = ZNZ:ZN(2,0) = ZR(1):ZN(3,0) = ZM(20):ZN(4,0) = ZM(9):ZN(5,0) = ZM(24)
6040 ZZ(8) = 78: GOSUB 11400: GOTO 1000
7000  REM  RETRIEVE DATA FROM DISK
7020 ZZ(8) = 78: GOSUB 11300:ZNZ = ZN(1,0): GOTO 1000
8000  REM   MEASUREMENT CONFIGURATION      :RETURN
9400  REM ERR HANDLING ROUTINE
9410  TEXT
9420  PRINT : PRINT : PRINT "ERROR # "; PEEK (222): PRINT : PRINT "IN LINE #"; PEEK (218) +  PEEK (219) *
256
9460  PRINT : PRINT "HIT A KEY TO CONTINUE ";: GET ZQ$
9480  PRINT : GOTO 1000
9999  PRINT : PRINT : INVERSE : PRINT "....CALCULATING....": NORMAL : RETURN
10000  REM  Y/N SUBR
10010 ZEZ(0) = 0: INPUT " ";ZD$(0): IF  LEFT$ (ZD$(0),1) = "Y" THEN ZZ(3) = 2: RETURN
10020  IF  LEFT$ (ZD$(0),1) = "N" OR ZD$(0) = "" THEN ZZ(3) = 1: RETURN
10030 ZEZ(0) = 1: GOSUB 10050: RETURN
10050  REM  ERROR SUBR
10060  PRINT  CHR$ (7):ZEZ(0) = 1: RETURN
10100  REM  I/P SUBR
10110  CALL  - 868
```

```
10120 ZE%(0) = 0: PRINT ZZ(3): INPUT "  ";ZD$(0): IF ZD$(0) = "" THEN ZZ(7) = ZZ(3): GOTO 10170
10130  FOR I = 1 TO  LEN (ZD$(0)):ZQ$ =  MID$ (ZD$(0),I,1)
10140  IF ZQ$ = "+" OR ZQ$ = "-" OR ZQ$ = " " OR ZQ$ = "." OR ZQ$ = "E" THEN 10160
10150  IF ZQ$ < "0" OR ZQ$ > "9" THEN 10050
10160  NEXT I:ZZ(7) =  VAL (ZD$(0))
10170  IF ZZ(7) < ZZ(4) OR ZZ(7) > ZZ(5) THEN 10050
10180 ZZ(3) = ZZ(7): IF ZZ(6) = 1 THEN ZZ(3) =  INT (ZZ(7))
10190  FOR I = 0 TO 200: NEXT I: RETURN
10200  REM  FIXED REAL SUBR
10210  POKE 36336,13: POKE 36337,ZZ(4): POKE 36338,0: POKE 36340,64: GOTO 10240
10220  POKE 36336,14: POKE 36337,ZZ(5): POKE 36338,1: POKE 36340,64: GOTO 10240
10230  POKE 36336,13: POKE 36337,ZZ(6): POKE 36338,1: POKE 36340,64
10240  CALL 36379: PRINT ZN(ZZ(7),I): RETURN
11300  REM  : LOAD ARRAY
11310  GOSUB 11500
11320  POKE 98,90: POKE 99,ZZ(8): CALL 38152
11330  PRINT  CHR$ (4);"BLOAD"ZD$(0);",A" PEEK (38394) +  PEEK (38395) * 256"
11340 ZN$ = ZD$(0): RETURN
11400  REM : SAVE ARRAY
11410  GOSUB 11500
11420  POKE 98,90: POKE 99,ZZ(8): CALL 38104
11430  PRINT  CHR$ (4);"BSAVE"ZD$(0)",A" PEEK (38394) +  PEEK (38395) * 256",L" PEEK (38396) +  PEEK (38
397) * 256 + 12 *  SGN (PL%)"
11435  PRINT  CHR$ (4);"LOCK"ZD$(0)
11440  RETURN
11500  REM ASK SLOT,DRIVE AND VOLUME
11505 ZZ(3) = 2: HOME : VTAB 9: PRINT "ENTER DISK DRIVE NUMBER..";ZZ(3);"..";
11510  HOME : VTAB 5: PRINT "TO ACCESS FLOPPY DISK USE :": PRINT "    S(4),D(1 OR 2),V(0)": VTAB 8: PRINT
"TO ACCESS CORVUS DISK USE :": PRINT "    S(6),D(1 OR 2),V(1 TO 67)
11515  VTAB 12: PRINT "POINTERS CURRENTLY SET AT :": PRINT : PRINT "    SLOT #";S%: PRINT "   DRIVE #";D
%: PRINT "  VOLUME #";V%
11520  VTAB 19: PRINT "CHANGE POINTERS (Y/N) ? ";: GET ZD$(0): IF ZD$(0) = "N" THEN 11550
11530  HOME : VTAB 5:ZZ(3) = S%:ZZ(4) = 4:ZZ(5) = 6:ZZ(6) = 0: PRINT "    SLOT ";: GOSUB 10120: IF ZE%(0
) = 1 THEN 11530
11532 S% =  INT (ZZ(3) + 0.5)
11535  VTAB 10:ZZ(3) = D%:ZZ(4) = 1:ZZ(5) = 2:ZZ(6) = 0: PRINT "   DRIVE ";: GOSUB 10120: IF ZE%(0) = 1 THEN
11535
11537 D% =  INT (ZZ(3) + 0.5): IF S% <  > 6 THEN V% = 0: GOTO 11550: REM  FLOPPY
11540  VTAB 15:ZZ(3) = V%:ZZ(4) = 0:ZZ(5) = 67:ZZ(6) = 0: PRINT "  VOLUME ";: GOSUB 10120: IF ZE%(0) = 1
 THEN 11540
11542 V% =  INT (ZZ(3) + 0.5)
11550  PRINT : PRINT "PRESS ANY KEY TO CATALOG ": GET ZD$(0): PRINT : PRINT  CHR$ (4);"CATALOG S"S%",D"D
%",V"V%
11560  PRINT : PRINT "ANOTHER CATALOG  Y/N ?  ";: GOSUB 10000: IF ZE%(0) = 1 THEN 11560
11570  IF ZZ(3) = 2 THEN 11500
11580  PRINT : PRINT "FILE NAME WILL BE PRECEDED BY DMS4-": PRINT : INPUT "ENTER FILE NAME = DMS4-";ZD$(
0):ZD$(0) = "DMS4-" + ZD$(0)
11590  RETURN
12000  TEXT : HOME : VTAB 5: PRINT "GRAPHIC OPTIONS ARE : ": PRINT
12020  PRINT : PRINT "F = FINISH"
12040  PRINT : PRINT "G = GRAPHIC MODE"
12060  PRINT : PRINT "N = NEW PLOT"
```

```
12080  PRINT : PRINT "P = DUMP TO EPSON"
12100  PRINT : PRINT "T = TEXT MODE"
12120  PRINT : PRINT "X = CHANGE X MAX/MIN"
12140  PRINT : PRINT "Y = CHANGE Y MAX/MIN"
12200  PRINT : PRINT : GET ZQ$
12220  IF ZQ$ = "F" THEN  GOTO 1000
12240  IF ZQ$ = "G" THEN  GOTO 2400
12260  IF ZQ$ = "N" THEN  GOTO 2080
12280  IF ZQ$ = "P" THEN  PRINT : PRINT  CHR$ (4)"PR#1": PRINT  CHR$ (9);"GDR2"
12285  IF ZQ$ = "P" THEN  FOR II = 1 TO 9: PRINT  CHR$ (10): NEXT II
12290  IF ZQ$ = "P" THEN  PRINT  CHR$ (4);"PR#0": GOTO 12000
12300  IF ZQ$ = "X" THEN II = 0: GOTO 12400
12320  IF ZQ$ = "Y" THEN II = 2: GOTO 12400
12380  PRINT  CHR$ (7): GOTO 12000
12400  REM CHANGE MAX/MIN
12420  HOME : VTAB 9: PRINT ZQ$;"-AXIS": VTAB 12: PRINT "","MIN","MAX"
12440  VTAB 14: PRINT "CURRENT";: HTAB 14:ZZ(6) = ZZ(II) / (10 ^ EZ(II)) + .0005: GOSUB 14000: PRINT ZD$
(0) + "E" +  STR$ (EZ(II))
12450  VTAB 14: HTAB 27:ZZ(6) = ZZ(II + 1) / (10 ^ EZ(II)) + .0005: GOSUB 14000: PRINT ZD$(0) + "E" +  STR$
(EZ(II))
12460  VTAB 16: INPUT "NEW VALUES    ";ZZ(II)
12480  VTAB 16: HTAB 27: INPUT "";ZZ(II + 1)
12490  GOTO 2400
12500  REM LABEL AXES
12520  DATA  " ","LOG.","1/","SQ.","SQR."
12540 ZQ$ = " ":I = 2: GOSUB 12900: REM Y
12560 ZQ$ = ZQ$ + "  VERSUS  ";I = 0: GOSUB 12900: REM X
12580 ZZ(7) = 0: REM  HORIZONTAL
12600 X% = 10:Y% = 0: GOSUB 13000
12620 ZZ(7) = 0:ZZ(6) = ZZ(0) / (10 ^ EZ(0)): GOSUB 14000:ZQ$ = ZD$(0):X% = 20:Y% = 175: GOSUB 13000:ZZ(
6) = ZZ(1) / (10 ^ EZ(0)): GOSUB 14000:ZQ$ = ZD$(0):X% = 245: GOSUB 13000
12640 ZQ$ = "EXP" +  STR$ (EZ(0)):X% = 29:Y% = 184: GOSUB 13000:X% = 245: GOSUB 13000
12660 ZZ(7) = 1:ZZ(6) = ZZ(2) / (10 ^ EZ(2)): GOSUB 14000:ZQ$ = ZD$(0):X% = 0:Y% = 170: GOSUB 13000:ZZ(6
) = ZZ(3) / (10 ^ EZ(2)): GOSUB 14000:ZQ$ = ZD$(0):Y% = 40: GOSUB 13000
12680 ZQ$ = "EXP" +  STR$ (EZ(2)):X% = 9:Y% = 170: GOSUB 13000:Y% = 40: GOSUB 13000
12700 ZQ$ = "<<" + ZN$ + ">>":X% = 273:Y% = 170:ZQ$ =  LEFT$ (ZQ$,22): GOSUB 13000
12899  RETURN
12900  REM HEADING CALCULATION
12920  RESTORE : FOR II = 0 TO BP(I + 1): READ ZD$(0): NEXT II
12940 ZQ$ = ZQ$ + ZD$(0) +  CHR$ (60) + "COLUMN " +  STR$ (BP(I)) +  CHR$ (62)
12960  RETURN
13000  ROT= 0: IF ZZ(7) > 0 THEN  ROT= 48: REM TEXT TO SCREEN
13020  FOR II = 1 TO  LEN (ZQ$):I =  ASC ( MID$ (ZQ$,II,1))
13040  IF I > 127 THEN I = I - 128
13060  IF I = 32 THEN  GOTO 13100
13080  DRAW I - 32 AT X%,Y%
13100  IF ZZ(7) > 0 THEN Y% = Y% - 7: NEXT II
13120  IF ZZ(7) <  = 0 THEN X% = X% + 7: NEXT II
13140  RETURN
14000  REM # FORMAT SUBR
14020 ZD$(0) =  STR$ (ZZ(6)): IF  ABS (ZZ(6)) < .01 THEN ZD$(0) = "0.00"
14040  IF ZZ(6) >  = 0 THEN ZD$(0) = "+" + ZD$(0)
```

```
14060 ZD$(0) =  LEFT$ (ZD$(0),5): RETURN
15000  REM CALCULATE EXPONENTS
15020 ZZ(6) =  ABS (ZZ(I + 1) - ZZ(I)):EZ(I) = 0
15040  IF ZZ(6) = 0 THEN  RETURN
15060  IF ZZ(6) < 0.98 THEN ZZ(6) = 10 * ZZ(6):EZ(I) = EZ(I) - 1: GOTO 15060
15080  IF ZZ(6) > 9.8 THEN ZZ(6) = ZZ(6) / 10:EZ(I) = EZ(I) + 1: GOTO 15080
15100  RETURN
16000  REM X&Y INT&SLOPE
16010 :ZZ(7) = 0
16020 ZQ$ =  STR$ (AA(0)):XZ = 100:YZ = 175: GOSUB 13000
16040 ZQ$ =  STR$ (AA(1)):XZ = 100:YZ = 184: GOSUB 13000
16050 ZZ(7) = 1
16060 ZQ$ =  STR$ (AA(2)):XZ = 0:YZ = 122: GOSUB 13000
16080 ZQ$ =  STR$ (AA(3)):XZ = 9:YZ = 122: GOSUB 13000
16100 : RETURN
30000  REM AUTO-LIST UTILITY BY ROBERT WEAVER
30020  TEXT : HOME : SPEED= 255
30030  VTAB 5: CALL  - 868: INPUT "ENTER FILE NAME: ";DN$:L =  LEN (DN$)
30040  IF L > 48 THEN  VTAB 20: PRINT "LIMIT TO 48 CHARACTERS": PRINT  CHR$ (7): FOR I = 0 TO 200: NEXT
I: GOTO 30030
30060  PRINT  CHR$ (4);"PR#1": PRINT  CHR$ (15)
30065  PRINT  CHR$ (9);"52P"
30070 L =  INT (24 - L / 2)
30080  PRINT  CHR$ (9);"K"
30090  PRINT  CHR$ (14);
30100  PRINT  TAB( L)DN$:L = L - 1
30120  FOR I = 1 TO  LEN (DN$) + 2:DU$ = DU$ +  CHR$ (95): NEXT I
30150  PRINT  CHR$ (14);
30160  PRINT  TAB( L)DU$
30170  PRINT  CHR$ (9);"122N": PRINT  CHR$ (9);"112R": PRINT  CHR$ (9);"11L"
30180  PRINT  CHR$ (15)
30190  PRINT  CHR$ (9);"A"
30200  LIST : PRINT
30210  PRINT  CHR$ (12)
30220  PRINT  CHR$ (18): PRINT  CHR$ (4);"PR#0": END
```

This report was done with support from the Department of Energy. Any conclusions or opinions expressed in this report represent solely those of the author(s) and not necessarily those of The Regents of the University of California, the Lawrence Berkeley Laboratory or the Department of Energy.

Reference to a company or product name does not imply approval or recommendation of the product by the University of California or the U.S. Department of Energy to the exclusion of others that may be suitable.

TECHNICAL INFORMATION DEPARTMENT
LAWRENCE BERKELEY LABORATORY
UNIVERSITY OF CALIFORNIA
BERKELEY, CALIFORNIA 94720